ANALYSIS OF THERMOPLASTIC POLYIMIDE + POLYMER LIQUID CRYSTAL BLENDS

DISSERTATION

Presented to the Graduate Council of the

University of North Texas in Partial

Fulfillment of the Requirements

For the Degree of

DOCTOR OF PHILOSOPHY

By

Bhaskar Gopalanarayanan

Denton, Texas

May, 1998

3/30/98

Gopalanarayanan, Bhaskar, Analysis of thermoplastic polyimide + polymer liquid crystal blends. Doctor of Philosophy (Materials Science), May, 1998, 142 pp., 11 tables, 61 illustrations, references, 241 titles.

Thermoplastic polyimides (TPIs) exhibit high glass transition temperatures (T_gs), which make them useful in high performance applications. Amorphous and semicrystalline TPIs show sub-T_g relaxations, which can aid in improving strength characteristics through energy absorption. The α relaxation of both types of TPIs indicates a cooperative nature. The semicrystalline TPI shows thermo-irreversible cold crystallization phenomenon. The polymer liquid crystal (PLC) used in the blends is thermotropic and with longitudinal molecular structure. The small heat capacity change (ΔC_p) associated with the glass transition indicates the PLC to be rigid rod in nature. The PLC shows a small endotherm associated with the melting. The addition of PLC to the semicrystalline TPI does not significantly affect the T_g or the melting point (T_m). The cold crystallization temperature (T_c) increases with the addition of the PLC, indicating *channeling* phenomenon. The addition of PLC also causes a negative deviation of the ΔC_p, which is another evidence for *channeling*. The TPI, PLC and their blends show high thermal stability. The semicrystalline TPI absorbs moisture; this effect decreases with the addition of the PLC. The absorbed moisture does not show any effect on the degradation. The addition of PLC beyond 30 wt.% does not result in an improvement of properties. The amorphous TPI + PLC blends also show the negative deviation of ΔC_p from linearity

with composition. The addition of PLC causes a decrease in the thermal conductivity in the transverse direction to the PLC orientation. The thermomechanical analysis indicates isotropic expansivity for the amorphous TPI and a small anisotropy for the semicrystalline TPI. The PLC shows large anisotropy in expansivity. Even 5 wt. % concentration of PLC in the blend induces considerable anisotropy in the expansivity. Thus, blends show controllable expansivity through PLC concentration. Amorphous TPI + PLC blends also show excellent film formability. The amorphous TPI blends show good potential for applications requiring high thermal stability, controlled expansivity and good film formability.

ANALYSIS OF THERMOPLASTIC POLYIMIDE + POLYMER LIQUID CRYSTAL BLENDS

DISSERTATION

Presented to the Graduate Council of the

University of North Texas in Partial

Fulfillment of the Requirements

For the Degree of

DOCTOR OF PHILOSOPHY

By

Bhaskar Gopalanarayanan

Denton, Texas

May, 1998

ACKNOWLEDGEMENT

I would like to thank Prof. Witold Brostow, who gave me the opportunity to learn more, beyond just research. I am thankful for his guidance throughout my research. I am grateful to Dr. Nandika Anne D'Souza for providing constant encouragement and advice, on and off the research. I would like to thank the Departments of Materials Science and Chemistry, for admission to the University of North Texas. I would like to thank my committee members for their valuable critique of this dissertation.

I am thankful to Dr. Kevin Menard for allowing me the use of his equipment, especially the Pyris-1, and for his advice and suggestions. I would like to thank Texas Instruments Inc., Checkmate Engineering and Retractable Technologies for their financial support. I am thankful to the Interlibrary Loan system of the UNT libraries for providing me with the many articles and books I requested. I also would like to thank Bryan Bilyeu for the discussions and suggestions. I would like to thank my colleagues in the Laboratory of Polymers and Composites for their cooperation throughout my research.

I would like to thank the Department of Polymer Science of the University of Madras and the faculty there for introducing me to the interesting field of polymers. I am grateful to my friends, especially Subramanian, Karthik, Rajesh, Sid and Ashutosh for their constant encouragement and friendship.

Most importantly, this dream of mine would not have become possible without the constant support of my family, especially my parents and brothers.

TABLE OF CONTENTS

LIST OF TABLES

LIST OF ILLUSTRATIONS

CHAPTER 1

POLYIMIDES AND POLYMER LIQUID CRYSTALS

1.1 Introduction

Polyimides have been in existence for nearly a century. The first mention of polyimides dates back to 1908 when Bogert and Renshaw [1] reported the characteristics of 4-aminophthalic anhydride, which evolved water upon reaction with 4-nitrophthalic anhydride at high temperatures to yield oligomers of 8 to 10 units. Polyimides started appearing in the literature more consistently from the late 1960s onward. The high temperature stability and high performance imparted by the imide linkage make them useful in a variety of high performance applications. Polyimides can be prepared by either condensation or addition polymerization routes. The advantage of addition polyimides being the ease of preparation of the composites and the minimal void formation during curing.

NASA's Langley Research Center developed the new class of addition polyimides, "Polymerized from Monomer Reactants" (PMR) which combines the advantage of low viscosity of reactants with the voidless cure typical of addition polyimides. The difficulty in processing for the condensation polyimides limited their applications. Developments in the monomer architecture led to condensation polyimides being processed in the poly(amic acid) stage, which is usually a soluble precursor. Some of these precursors, for both addition and condensation polyimides, were called

thermoplastic polyimides and were commercially available. Although they were not truly thermoplastic, the ease of their processing through conventional means made them an interim solution.

The progress in terms of truly thermoplastic polyimides was made through the modification of molecular architecture by introducing keto and ether groups to impart flexibility and lower the melting point of the polyimide. One of the first commercial truly thermoplastic polyimides (TPI), Ultem (an amorphous polyetherimide), is produced by GE Plastics. Developments made by NASA led to commercialization of new TPIs, amorphous as well as semicrystalline. A variety of synthetic routes is being published for thermoplastic polyimides.

Properties of the polyimide can be significantly modified by varying the diamine and dianhydride segments. Despite such attempts, one often finds copolymerization and blending with other polymers as viable routes for the improvement and achievement of desired properties. One of the blending processes of interest is the blending with polymer liquid crystals (PLCs). PLC blends with *engineering plastics* (EPs) have been known since 1985. They are added to EPs for various reasons - the most significant being ease of processing as a result of melt viscosity reduction and their reinforcement at the molecular level. Some of the basic information about polyimides and PLCs are presented in subsequent sections followed by a discussion of PLC blends.

1.2 Classification and Synthesis of Polyimides

Polyimides are polymers with imide linkage in their main chain [2] as shown in Figure 1. Depending on the type of chemical moieties attached to the imide links, polyimides can be classified as aliphatic or aromatic and as linear or three-dimensional.

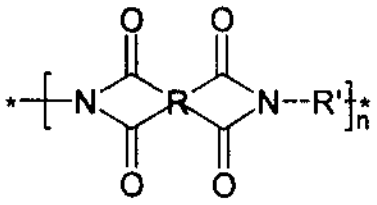

Figure 1. Structure of a polyimide

Typically, all the three-dimensional and many of the linear polyimides tend to be thermosetting in nature because their degradation temperature is higher than their melting temperature. To reduce the melting point, research was directed towards introducing aliphatic or alicyclic groups instead of the aromatic moieties. These groups reduced not only the melting temperature but also the degradation temperature, reducing the thermal stability of the polyimide.

The schematic structure above (Fig. 1) shows the polyimide linkage. Depending on the type of functional group present in R and R', the polyimide can be classified. The classification of copolyimides is based on their other functional groups such as ether, ester or amide as respectively, etherimide, esterimide or amideimide. The research on copolyimides was motivated by the fact that introduction of various flexible links such as

ester, amide or ether groups would reduce the melting point of the polymer below its degradation temperature.

Polyimides can be further classified into addition [2, 3] and condensation polyimides [2, 4], based on their synthetic route. Addition polyimides are usually low molecular weight, at least difunctional monomers, prepolymers or mixtures thereof, with reactive functional terminations and imide functionality on their backbone. A schematic structure of the addition polyimide is shown. Ar and Ar' are the dianhydride and diamine moieties and 1, 2 and 3 respectively represent maleimide, nadimide and acetylene terminated precursors.

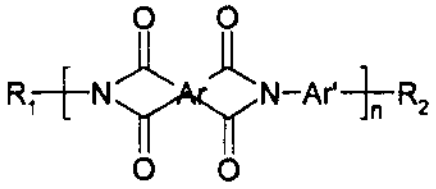

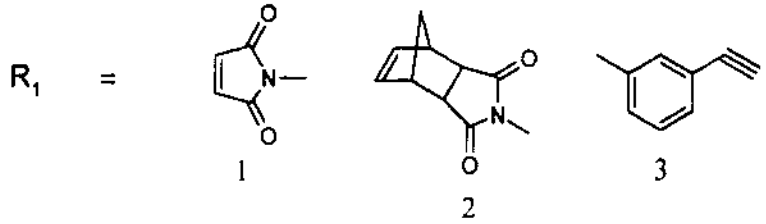

Figure 2. Structure of addition polyimides

The molecular weight build up occurs as a result of polymerization through the unsaturation. Consequently, addition polyimides are usually thermosetting. Their properties are manipulated through the proper choice of dianhydride and diamine segments. Their properties can also be modified through the incorporation of thermoplastics or rubbers.

Condensation polyimides, conversely, do not contain any reactive functional end groups for molecular weight development. Their molecular weight is built up through the condensation reaction. They can be made by either one or two step process. The two step process, shown in Fig. 3, involves the poly(amic acid) intermediate.

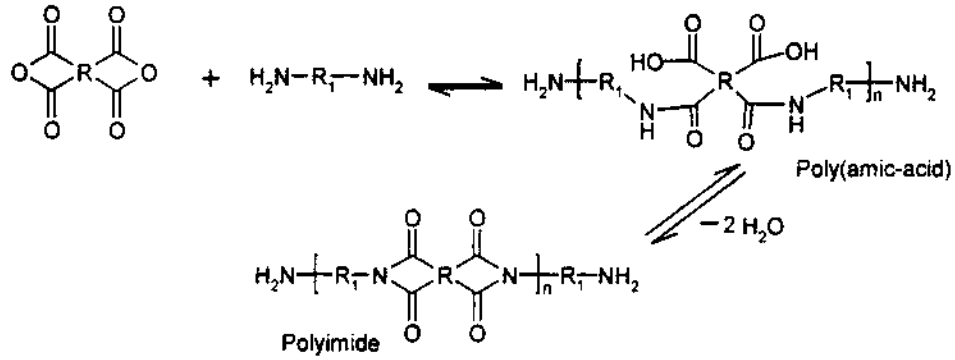

Figure 3. Preparation of condensation polyimides

The anhydride can be substituted with tetracarboxylic acids or their esters. The poly(amic acid) is usually soluble in many polar aprotic solvents such as N-methyl pyrrolidone (NMP), dimethyl formamide (DMF) and dimethyl acetamide (DMAc). The conversion of this poly(amic acid) can be performed either by thermal or chemical imidization procedures. Thermal conversion is usually performed at high temperature, where the temperature depends on the monomers and solvent system used. By contrast, the use of dehydrating agents in the chemical imidization procedure eliminates the need for high temperatures. Chemical conversion invariably is carried out in solution. If the polyimide is insoluble in the solvent, it precipitates out subsequent to cyclization. If it is a soluble polyimide, the use of either a non-solvent or drying procedure follows.

The one step process [5, 6] involves the synthesis in phenolic solvents at elevated temperatures in the presence of tertiary amines or polyphosporic acid. This process works for most monomers, which could be used under two step synthesis and for monomers unsuitable for the two step process. The two step process is highly sensitive to the acid/base balance and steric factors. Some monomers with high steric hindrance cannot be used under a two step process. Other routes conducted at lower temperatures involving chemically modified monomers are also available [7, 8, 9].

Demands of the electronic industry for a solventless process for producing polyimide films resulted in the vapor deposition process [10, 11] as an alternative to the spin coating method. Polyimide coatings or thin films are prepared in this method by impinging the substrate with the heated monomer mixture. This process is extensively used for the production of uniform thin films or coatings of ODA-PMDA [12, 13], PPD-PMDA and fluorinated polyimides [14].

Polyimides can also be synthesized by nucleophilic displacement polymerization [15, 16, 17, 18]. This method is especially useful for the polymerization of sterically hindered monomers. Similar to the synthesis of polyesters, transimidization is another viable method. In this method, the imide of the tetracarboxylic acid is reacted with the appropriate diamine to yield the polyimide [19, 20, 21]. Many other synthetic procedures via ether exchange reaction [18, 22], cycloaddition reaction [23, 24] and from diisocyanates and dianhydrides [25, 26] are also used in the synthesis of polyimides.

Some of the common monomers used for the synthesis of condensation polyimides are given in Fig. 4.

Pyromellitic dianhydride (PMDA)

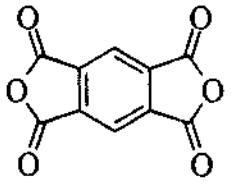

3,3',4,4'-biphenyltetracarboxylic dianhydride(BPDA)

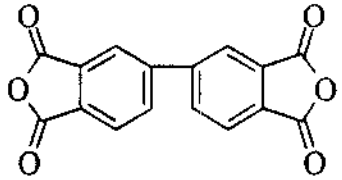

3,3',4,4'-benzophenonetetracarboxylic dianhydride(BTDA)

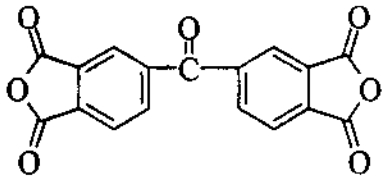

p-phenylene diamine (PPD)

m-phenylene diamine (MPD)

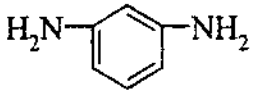

4,4'-diaminodiphenyl ether (ODA)

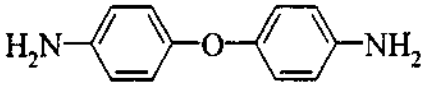

4,4'-diaminobezophenone (4,4'-DABP)

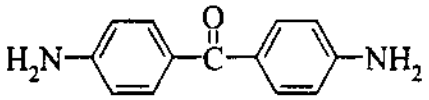

2,2-dimethyl-1,3-(4-aminophenoxy)propane (DMDA)

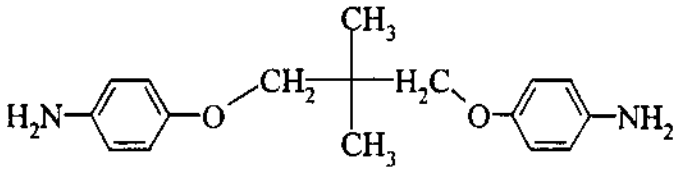

4,4' bis(3-aminophenoxy)) biphenyl

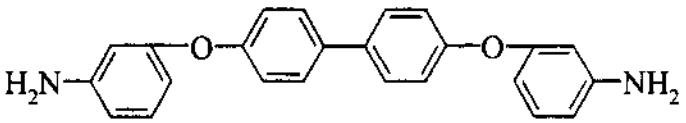

Figure 4. Common monomers used for condensation polyimides

1.3 Thermoplastic Polyimides

Most of the early polyimides were thermosetting in nature due to their network structure. Many linear polymers made from PMDA with ODA, PPD and MPD also resulted in polymers which could not be melt processed. To overcome the processing difficulties, two methods were developed. The first method involved the improvement of solubility of polyimides while the second method embraces the idea of reducing the melting and glass transition temperatures.

The improvement of solubility could be achieved through the incorporation of bulky groups in the backbone. This method produced a variety of polyimides soluble in organic solvents [27, 28, 29, 30]. In these polyimides, the introduction of such bulky groups as methyl, ethyl and phenyl improved their solubility while preserving their linearity and chain rigidity.

The research on melt processable polyimides took an alternative approach to modify the linearity and chain rigidity. It should be noted that the PMR type polyimides and poly(amic acid) type materials were often included under this thermoplastic polyimide category, as a result of their prepolymer nature. Since they can be molten in their prepolymer stage, to form the composite, this observation seems justified. These materials once formed into a composite usually forms a network structure, deeming them not suitable for further processability by thermal means. In this discussion they will not be considered thermoplastic or melt processable polyimides. The introduction of flexible linkages and groups such as aliphatic, ether, ketone or sulfone, in the backbone reduces

the T_g and melting temperature. This modification can be performed on the diamine fragment or the dianhydride. The introduction of such flexible groups also reduced their high temperature stability.

One of the first truly thermoplastic polyimides was a polyetherimide, under the name ULTEM 1000, manufactured by General Electric Corporation [31]. This polyetherimide incorporates aliphatic and ether linkages in the backbone. This aliphatic linkage reduces thermal stability as well. To maintain high thermal stability and improve flexibility, the introduction of *meta-* and *ortho-* linkages in combination with ether and ketone links became popular. The incorporation of such meta and ortho links reduces the close packing of the polymer chains by steric effects. These linkages, in combination with the ether and keto groups, impart higher flexibility without the compromising thermal stability. A Substantial number of review articles which deal with the structure-property relations in such materials are available [2, 32, 33, 34, 35, 36, 37, 38].

The work of St. Clair e. a. [39, 40, 41, 42] led to the introduction of different polyimides. These are semicrystalline in nature, in contrast to most of the amorphous TPIs with *meta* and *ortho* links. Such semicrystalline TPIs can be modified morphologically through heat treatment to change their *degree of crystallinity*. This fact has an important consequence, namely it provides the capability to control adhesion to metal substrates [43, 44]. Ishida and Huang have defined a molecular mechanism of crystallization process using Fourier transform infrared spectroscopy (FTIR) [45, 46]. There are a number of papers on effects of chemical structure of diamine and dianhydride

segments on the crystallinity [47, 48, 49]. Further, Tamai e. a. [50] also evaluated the number of benzene rings, ether links and position of attachment (*meta and para*) on the melt processability of the polyimides. A similar account was given by Hsiao e. a. [51] for the ortho linkage. This flexibility and semicrystallinity does not compromise the oxidative aging resistance [52, 53]. Detailed accounts on the thermal stability of polyimides in relation to their structure [54] can be found in the references listed for the structure-property relations.

Despite their disadvantages, polyimides always found their unique place in electronic applications. This is mainly due to their high temperature stability, low dielectric constant and their mechanical strength. They have found applications in electronic packaging, flexible circuitry base sheets, planarization coatings, interlayer dielectrics and circuit boards. They have many advantages such as, high temperature stability, chemical resistance, ease of microfabrication, low dielectric constant, good step coverage, good elasticity and damping characteristics. The important properties required of polyimides for interlayer or the back film for flexible circuits are low expansivity, high thermal stability, reworkability and chemical inertness towards cleaning fluids.

1.4 Polymer Liquid Crystals

Liquid crystals have been known for more than a century. Their discovery dates back to 1888 [55, 56, 57, 58, 59]. The liquid crystalline phase refers to a mesophase where a liquid phase exhibits orientational order. This orientational order results from the rigid mesogens, which can be in the form of discs or rods. Apart from the orientational order,

some liquid crystals exhibit some positional order as well. Depending on the type of order observed, they can be classified as nematic, cholesteric and smectic phases following Friedel [60] and Kast [61]; for a more recent discussion see the book, "Science of Materials" [62].The name nematic is of Greek origin meaning thread like. As the name suggests, nematic phase is observed when these mesogens are aligned in a general direction and do not show any positional order. This orientation is long range in nature. The cholesteric phase, named after the esters of cholesterol, was the first liquid crystal phase discovered. On a very local scale, this phase resembles the nematic phase. This phase consists of layers of nematic structures. The orientation direction of each layer follows a helical path. In other words, each layer of a nematic is at some angle with respect to the orientation of the previous layer. This twist is related to the temperature in a thermotropic liquid crystal and concentration of the solution in lyotropic liquid crystals. Usually the cholesteric phase exhibits more positional order than the nematic by virtue of the layered structure. The smectic phase resembles the cholesteric phase since it represents a layered structure. The difference is in the long axis, which is parallel to the plane of the layer in cholesteric phase, while in the smectic phase it is normal to the plane of the layers. The positional order in a smectic phase within the layers is more significant than that in a cholesteric phase. A smectic phase in many respects is closer to a crystalline solid. Smectic phases can further be subdivided into many categories based on the extent and type of positional order and the angle between the director and the plane of the layer.

Some materials show liquid crystalline behavior when they are dissolved in a solvent. They are classified as *lyotropic* liquid crystals. If the behavior is caused by an increase in temperature, in the melt stage, they are thermotropic liquid crystals. Following Brostow's [56] suggestion, barotropic liquid crystals are the ones, which show liquid crystalline behavior, as a result of pressure changes [63].

There are two types of liquid crystals. In the first, each mesogen comes from an individual molecule and the mesogens are not linked together by direct or indirect chemical bonds. This type of liquid crystal is called monomeric liquid crystal (MLC). If many mesogens come from a single molecule, the liquid crystal is called polymeric liquid crystal (PLC). In this case, some or many of the mesogens are chemically bonded directly or indirectly. This classification was suggested by Samulski [64]. As can be imagined, the difference in properties of MLCs and PLCs are significant. This can be further emphasized, when we look at the hierarchy of structures and the rules pertaining to it [65], especially rules 4 and 5, which related to the complexity and the arrangement of the mesogens.

PLCs, as indicated in the previous paragraph, are comprised of many mesogens. Depending on whether the mesogens are connected to each other directly or indirectly, PLCs can be called rigid or semiflexible. In rigid PLCs, the rigid rod mesogens are connected to each other leaving the whole polymer rigid in nature. As mentioned in Sections 1.2 and 1.3, the rigidity of the polyimides limits their application through limitations in processing. Rigid PLCs face similar difficulties. The strength of PLCs

residing in their LC phase is inaccessible unless they are lyotropic liquid crystals. Just as in polyimides, the deliberate addition of flexible spacers succeeded in reducing their melting temperature below the degradation point. These flexible spacers also impart the ability to form a variety of liquid crystalline phases while limiting the upper use temperature. A comprehensive list of such liquid crystalline phases was provided by Brostow e. a. [56]. Unlike the semiflexible PLCs, rigid PLCs usually show only the nematic phase due to their chain rigidity. Another main distinction between the semiflexible and rigid PLCs arises from the crystallinity development as a result of flexible spacers. Unlike semiflexible PLCs, the rigid PLCs usually show very weak melting and broad glass transition. The melting point of poly(4-hydroxybenzoate) (PHB) was thought to be over 600°C [66,57], but was later found to be about 350°C [67](weak endotherm). Several rigid PLCs are available from various companies, including Amoco, du Pont and Hoechst Celanese. Some of the common repeat units and monomers for these rigid PLCs are shown in Fig. 5.

PLCs, due to their rigid rod nature and high anisotropy, exhibit unique properties. Some of the important properties [56, 68] relevant to the thermotropic longitudinal PLCs are summarized. Polymers with LC segments in their backbone and the long axis of the LC segments in the chain direction are called thermotropic longitudinal PLCs. Compared to usual EPs, PLCs show greater chemical stability and flame retardance. They posses low isothermal compressibility due to the efficient packing of mesogens. They show low expansivities, sometimes even negative depending on the direction. Thermotropic

longitudinal PLCs usually show low melt viscosity under processing conditions allowing more efficient processing and resulting in cost reduction. Their orientation in most cases can be controlled and modified by the application of various fields, such as electric, magnetic and mechanical. Rigid rod PLCs, in addition to all the above stated properties, exhibit LC phase with relative ease [57, 58].

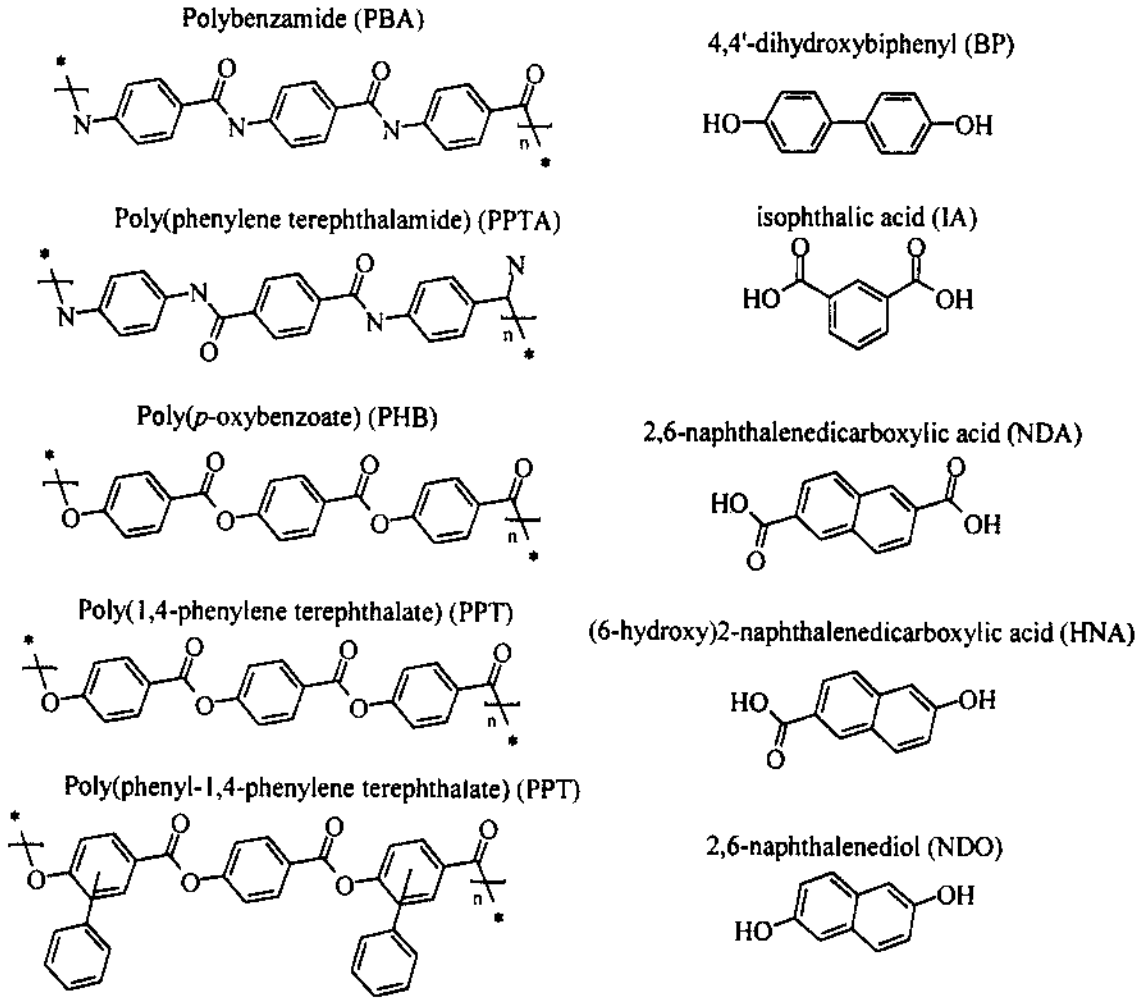

Figure 5. Monomers and repeat units for PLCs

1.5 Polymer Liquid Crystal Blends

Polymers are finding more and more applications due their flexibility in the property modification. Their properties can modified through proper choice of monomer, control of molecular weight and its distribution, controlled development of morphology and proper additives. Despite the diverse possibilities, it is not always possible to achieve the required set of properties. This difficulty can be overcome by copolymerization and/or blending. The ease of preparation and the variety of blends, make them an attractive alternative. An interesting avenue in blending is the addition of PLCs. Two important characteristics of PLC blending are reduction in viscosity and composite morphology. From an economic point of view adding a PLC, potentially improves the efficiency of processing [69, 70, 71], and leads to reduction in processing costs. From the performance perspective, addition of rigid rod PLC potentially simulates fiber-reinforced composites. This reinforcement is at the molecular level making the blends act as molecular composites. PLCs are also useful in inducing potential anisotropy in blends. Specifically, the expansivity of the blend can be controlled by the addition of the PLC [72, 73]. This control of expansivity can be a tool in expanding the applications of polymers. Many electronic applications demand precise expansivity characteristics for the material, which seriously limits the material selection. Polyimides by virtue of their high performance are suitable for many applications in electronics, but an inappropriate expansivity prohibits their usefulness. The control of expansivity through PLC blending opens new electronic applications for many polyimides.

1.6 References

1. Bogert, T. M., Renshaw, R. R., *J. Am. Chem. Soc.*, **30**, 1135 (1908).
2. C. E. Sroog, *Prog. Polymer Sci.*, **16**, 561 (1991).
3. H. D. Stenzenberger, *Adv. Polymer Sci.*, **117**, 165 (1994).
4. W. Volksen, *Adv. Polymer Sci.*, **117**, 111 (1994).
5. T. Takekoshi, *Polyimides Fundamentals and Applications*, Eds.: M. K. Ghosh and K. L. Mittal, Mercel Decker Inc., New York, Chap. 2 (1996).
6. A. V. Gerashchenko, Ya. S. Vygodskii, G. L. Slonimskii, A. A. Klimova, F. B. Sherman and V. V. Korshak, *Polymer Sci. USSR*, **15,** 1927 (1973).
7. N. Yamazaki, F. Higashi and J. Kawabata, *J. Polymer Sci. Chem.*, **12**, 2149 (1974).
8. N. Yamazaki, M. Matsumoto and F. Higashi, *J. Polymer Sci. Chem.*, **13**, 1373 (1974).
9. J-H. Kim and J. A. Moore, *Macromol.*, **26**, 3510 (1993).
10. M. Iijima, Y. Takahashi, K. Inagawa and A. Itoh, *J. Vac. Soc. Jpn.*, **28**, 437 (1985).
11. J. R. Salem, F. O. Sequeda, J. Duran, W. Y. Lee and Y. M. Yang, *J. Vac. Sci. Technol. A*, **4,** 369 (1986).
12. M. Grunze and R. N. Lamb, *Surface Sci.*, **204**, 183 (1988).
13. M. Iijima and Y. Takahashi, *Macromol.*, **29**, 2944 (1989).
14. Y. Y. Maruo, Y. Andoh and S. Sasaki, *Vac. Sci. Technol. A*, **11**, 2590 (1993).
15. J. G. Wirth and D. R. Heath, U. S. Patent 3,787,364 (1974).
16. F. J. Williams, U. S. Patent 3,847,869 (1974).

17. T. Takekoshi, J. G. Wirth, D. R. Heath, J. E. Kochanowski, J. S. Manello and M. J. Webber, *J. Polymer Sci., Chem.*, **18**, 3069 (1980).

18. F. J. Williams and P. E. Donahue, *J. Organic Chem.*, **42**, 3414 (1977).

19. F. S. Spring and J. C. Woods, *Nature*, **158**, 754 (1946).

20. H. J. Barber and W. R. Wragg, *Nature*, **158**, 514 (1946).

21. Y. Imai, *J. Polymer Sci. B*, **8**, 555 (1970).

22. T. Takekoshi, U. S. Patent 4,024,110 (1977).

23. J. K. Stille, F. W. Harris, H. Mukamal, R. O. Rakutis, C. L. Schilling, G. K. Noren and J. A. Reeds, *Adv. Chem. Series*, **91**, 628 (1969).

24. F. W. Harris, S. O. Norris, *J. Polymer Sci. Chem.*, **11**, 2143 (1973).

25. W. M. Alvino and L. E. Edelman, *J. Appl. Polymer Sci.*, **19**, 2961 (1975).

26. M. Kakimoto, R. Akiyama, S. Negi and Y. Imai, *J. Polymer Sci. Chem.*, **26**, 99 (1988).

27. F. W. Harris and L. H. Lenier, *Structure - Solubility Relationships in Polymers*, Eds.: F. W. Harris and R. B. Seymour, Academic Press, New York (1977).

28. D. Kumar, *J. Polymer Sci. Chem.*, **22**, 3439 (1984).

29. F. W. Harris, S. L. C. Hsu and C. C. Tso, *High Perf. Polymers*, **1**, 1 (1989).

30. S. Z. D. Cheng, F. E. Arnold Jr., A. Zhang, S. L. C. Hsu and F. W. Harris, *Macromol.*, **24**, 5856 (1991).

31. J. G. Wirth, *High Performance Polymers: Their Origin and Development*, Eds.: R. B. Seymour and G. S. Krishenbaum, Elsevier, Amsterdam (1986).

32. M. I. Bessonov, M. M. Koton, V. V. Kudryavtsev and L. A. Laius, Polyimides - Thermally Stable Polymers, Plenum, New York (1987).

33. T. L. St. Clair, Polyimides, Eds.: D. Wilson, H. D. Stenzenberger and P. M. Hergenrother, Chapman and Hall, New York (1985).

34. M. Ree, K. Kim, S.H. Woo and H. Chang, *J. Appl. Phys.*, **81,** 698 (1997).

35. N. Bicak and G. Koza, *Angew. Makromol. Chemie,* **217,** 71 (1994).

36. G. Rabilloud and B. Sillion, *J. de Physique IV,* **3,** 1493 (1993).

37. N. A. Adrova, M. I. Bessonov, L. A. Laius and A. P. Ruakov, *Polyimides - New Class of Thermally Stable Polymers*, Technomic Publishing Company Inc., Lancaster, PA (1970).

38. P. E. Cassidy, *Thermally Stable Polymers*, Mercel Decker, New York (1980).

39. D. M. Stoakley, A. K. St. Clair and R. M. Baucom, *SAMPE Quart.*, **20,** 3 (1989).

40. T. H. Hou and R. M. Reddy, *SAMPE Quart.*, **22,** 38 (1991).

41. T. L. St. Clair, K. S. Whitney and J. R. Pratt, *NASA Tech Briefs*, **Feb.**, 58 (1994).

42. A. K. St. Clair, D. M. Stoaldey and B. R. Emerson, *NASA Tech Briefs*, **Feb.**, 59 (1994).

43. H. Ishida and K. Kelley, *Polymer,* **32,** 1585 (1991).

44. W. H. Tsai, F. J. Boerio and K. M. Jackson, *Langmuir,* **8,** 1443 (1992).

45. H. Ishida and M. T. Huang, *Spectrochim. Acta*, **51**, 319 (1995).

46. H. Ishida and M. T. Huang, *J. Polymer Sci. Phys.*, **32**, 2271 (1994).

47. J. B. Friler and P. Cebe, *Polym. Eng. & Sci.*, **33**, 587 (1993).

48. B. S. Hsiao, B. B. Sauer and A. Biswas, *J. Polymer Sci. Phys.*, **32**, 737 (1994).

49. C. R. Gautreaux, J. R. Pratt and T. L. St. Clair, *J. Polymer Sci. Phys.*, **30**, 71 (1992).

50. S. Tamai, A. Yamaguchi and M. Ohta, *Polymer*, **37**, 3683 (1996).

51. S. H. Hsiao, C. P. Yang and K. Y. Chu, *Macromol.*, **30**, 165 (1997).

52. J. A. Hinkely and J. J. Yeu, *J. Appl. Polymer Sci.*, **57**, 1539 (1995).

53. Mitsui Toatsu Chemicals Inc., Product Datasheet for Aurum Thermoplastic Polyimides .

54. J. A. Cella, *Polyimides Fundamentals and Applications*, Eds.: M. K. Ghosh and K. L. Mittal, Mercel Decker Inc., New York, Chap. 13 (1996).

55. P. J. Collings, *Liquid Crystals: Nature`s Delicate State of Matter*, University Press, Princeton, NJ (1990).

56. W. Brostow, *Polymer*, **31**, 979 (1990).

57. F. P. La Mantia, (Ed.) *Thermotropic Liquid Crystal Polymer Blends*, Technomic Publishing Company Inc., Lancaster, PA (1993).

58. A. M. Donald and A. H. Windle, *Liquid Crystalline Polymers*, University Press, Cambridge, UK (1992).

59. S. Kobayashi, *Mol. Cryst. Liq. Cryst.*, **165**, 1 (1988).

60. M.G. Friedel, *Ann. Physique*, **18**, 273 (1922).

61. W. Kast, *Angew. Chemie*, **67**, 592 (1955).

62. W. Brostow, *Science of Materials*, Robert E. Krieger Publishing Company Inc., Malabar, FL. (1979).

63. B. S. Hsiao, M. T. Shaw and E. T. Samulski, *Macromol.*, **21**, 543 (1988).

64. E. T. Samulski, *Faraday Disc.*, **79**, 7 (1985).

65. W. Brostow and M. Hess, *Mater. Res. Soc. Symp. Proc.*, **255**, 57 (1992).

66. W. J. Jackson Jr., *Brit. Polymer J.*, **12**, 154 (1980).

67. J. Economy, W. Volksen, C. Viney, R. Geiss, R. Seimens and T. Karis, *Macromol.*, **21**, 2777 (1988).

68. W. Brostow, *Liquid Crystal Polymers: From Structures to Applications*, Ed.: A. A. Collyer, Elsevier Applied Science, London and New York, Chapter 1 (1992).

69. F. N. Cogswell, B. P. Griffin and J. B. Rose, U. S. Patent 4,386,174 (1983).

70. M. F. Froix, U. S. Patent 4,460,735 (1984).

71. F. N. Cogswell, B. P. Griffin and J. B. Rose, U. S. Patent 4,460,735 (1984).

72. R. W. Lusignea, W. S. Stevenson J. F. McCoy, III, U. S. Patent 4,966,806 (1990).

73. L. S. Rubin and K. G. Blizard, U. S. Patent 5,529,741 (1996).

CHAPTER 2

EXPERIMENTAL TECHNIQUES AND INSTRUMENTATION

2.1 Overview

This chapter discusses the various experimental techniques used in this dissertation. In this work, the specific characterization techniques used are: differential scanning calorimetry (DSC), temperature modulated differential scanning calorimetry (TMDSC), thermal conductivity measurement, thermogravimetric analysis (TGA), thermomechanical analysis (TMA) and thermally stimulated depolarization (TSD). A brief introduction to each technique followed by apparatus description and calculation methods will be presented. Information on materials and sample preparation will be presented in each chapter, due to individual differences in the material and sample information pertaining to each chapter.

2.2 Differential Scanning Calorimetry

The primary thermal characterization of polymers involves differential scanning calorimetry. This technique has established itself as the standard method for evaluation of transition temperatures, heat capacity measurements, crystallization and curing kinetic evaluations and many other characteristics in polymers.

Historically, the first reported instance of differential temperature measurement of a sample, with respect to a reference material, appeared in 1889 [1, 2]. This instrument gave a readout of the temperature difference and the temperature of the furnace in which the sample and reference were placed. An apparatus for low temperature thermal analysis using liquid N_2 was reported by Jenson e. a. [3] in 1938. The introduction of a controlled atmosphere within the furnace using a gas or vapor was reported by Stone [4]. The next innovation was the differential thermal analyzer (DTA) design by Boersma [5] in 1955. The DSC based on power compensation technique, with a furnace each for the sample and reference, was developed by Watson e. a. in 1963 [6]. Unlike the predecessors (DTAs), DSC instruments provide quantitative calorimetric information in addition to the temperature measurements. The power compensated DSC and many heat-flux DSCs introduced in the market in mid to late 60's were considered true innovations due to the very small sample size, as little as 10 mg, and the heating rates as fast as 40 K/min. A recent advancement in DSC is the introduction of TMDSCs [7] by Reading e. a. The concept of an oscillatory heating method has been in existence from 1968 [8], but the introduction of TMDSC did not occur until 1993 [9].

The Perkin-Elmer DSC-7, on a UNIX platform, apparatus used in this dissertation is based on the power compensation principle. This DSC contains two furnaces one for the sample and another for the reference. The reference is an inert material that does not undergo any transition in the temperature range of interest. The temperature difference between the sample and reference with the use of Platinum resistance thermometers is

monitored. Any deviation from the null difference (± 0.01K) is used to drive the heaters. The energy spent in maintaining this null difference is the energy associated with the phase change of the sample. During an exothermic transition, the energy is sent to the reference heaters indicating a negative sign on the output and vice versa for an endothermic process. This representation is a major difference between the power compensation DSC and the DTAs. This representation is also in conformity with the thermodynamic convention. The direct measurement of the energy also results in quantitative measurements without the need for hardware and software corrections, which distinguishes power compensation DSC from heat flux DSCs. A detailed description of the two types of DSCs and DTA is given by Hatakeyama e. a. [10] and others [1,11, 12, 13]. Calibration of the DSCs and the quantitative DTAs involves baseline (slope and curvature), temperature and energy. Unlike quantitative DTAs and heat flux DSCs, power compensation DSC requires only a single point energy compensation by virtue of not requiring hardware and software corrections. Since the type of DSC used in this work is based on power compensation technique, the term DSC from here onwards will correspond to the power compensation DSC.

Experimental variables such as gas flow rate, type of gas, type of coolant and laboratory atmosphere, such as humidity and room temperature, can often affect the performance of any instrument. These effects can be minimized by periodic calibration measures. The baseline correction in DSC involves verification and correction of the slope and curvature of the baseline. The slope and curvature are factors related to the

linearity of operation in the temperature range of interest. The baseline correction is performed on a run with references on both sides using slope and curvature adjustments. Temperature calibration is performed with the use of standards certified by International Confederation of Thermal Analysis and Calorimetry (ICTAC) and available through the National Institute of Standards and Testing (NIST) and the instrument manufacturers. Some of the standards covering the normal temperature of DSC-7 are shown in Table 1 [1]. The DSC apparatus requires only a single point calibration of energy. For this DSC, two-point temperature calibration and single point energy calibration were performed at regular intervals of 15 days to a month using indium and zinc.

Table 1.

Standard	Melting Point (°C)	Enthalpy (J/g)
Indium	156.5985	28.42
Zinc	419.527	112.0

In this work, N_2 purge gas was used for all experiments and a constant pressure of 40 psi was maintained from the cylinder. A water and ice mixture at 0°C was used as the coolant. The sample was heated from 30°C to 410 °C, annealed for 20 minutes, subsequently cooled at 10 K/min to 30°C and then heated to 400 °C at 10 K/min. This temperature program was used for all samples unless indicated otherwise.

The calculation of transition temperatures was performed from the heat capacity rather than the heat flow as a function of temperature. The heat capacity is calculated

using the algorithm provided with the instrument, [13] from the run with the sample, baseline and the stored values of heat capacity of sapphire. The heat absorbed or evolved by the sample in unit time is dH/dt and the scanning rate is dT/dt. The heat flow dH/dT corresponds to the heat capacity, C_p, through the mass of the sample *m*

$$dH/dT = m.C_p \quad (1)$$

$$dH/dt = K_c \cdot m \cdot C_p \cdot dT/dt \quad (2)$$

where the correlation coefficient, K_c is calculated from the sapphire heat capacity using Eq. 2.

The glass transition temperature T_g, from DSC, can be calculated by three methods. The first is the half C_p height method, in which the temperature pertaining to the half height of the C_p step associated with the glass transition is taken as the T_g. In the second method, half C_p width method, the temperature at the half width of the C_p step is taken as the T_g. The third method, onset method, is usually used for thermosetting materials and assigns the onset temperature of the glass transition C_p step as the T_g. Usually the T_g from the first two methods does not differ significantly. The T_g from the third method is often close to the heat distortion temperature (HDT) (ASTM D-648). The first method is widely used as the standard method for T_g calculation. The peak area for the melting and crystallization were calculated using the software provided with the DSC. Other relevant methods of calculations and evaluations are presented in the individual chapters. The sensitivity of the DSC is 35μW. Due to the high reproducibility of the DSC, the experiments were performed once, unless necessary.

2.3 Temperature Modulated Differential Scanning Calorimetry

Temperature modulated techniques involve the perturbation of the linear temperature program normally used in the DSCs. This perturbation can be applied in various forms such as sinusoidal or square waveforms. The TMDSC version from TA instruments uses the sinusoidal function. The Perkin-Elmer TMDSC uses the square wave method thereby the temperature changes in a saw tooth manner. In essence, both methods offer adjustable amplitude (ΔT) and period (Δt) of modulation. Theoretical developments in understanding and using this technique have been reported by Reading[14,15,16], Schawe [17,18,19,20,21,22,23,24] and Wunderlich[25,26]. A comprehensive treatment of the different types of TMDSC and a single parameter model for the same is reported by Hutchinson e. a. [27].

The Pyris-1 DSC, operating on a Windows NT platform, from Perkin-Elmer Corporation, Norwalk, CT, was used in this work. This TMDSC offers two modes, namely the iso-scan and heat-cool modes. In the iso-scan mode, a heating ramp is followed by an isothermal segment to provide the modulation of the temperature program. In the heat-cool mode, heating and subsequent cooling provides the oscillation of temperature around the linear heating rate. In both modes, the duration of heating, cooling or the isothermal step is half of the total duration of the cycle. In addition, the cooling rate is half the heating rate in the heat-cool mode.

The temperature T(t) is:

$$T(t) = T_0 + \beta_0 t + \frac{4}{\pi} T_a \left(\frac{\sin(\omega_0 t)}{1^2} - \frac{\sin(3\omega_0 t)}{3^2} + \frac{\sin(5\omega_0 t)}{5^2} - \ldots \right) \quad (3)$$

where T_0 is the initial temperature, β_0 is the underlying linear scanning rate, T_a is the temperature amplitude of the periodic modulation, $\omega_0 = 2\pi/t_p$ is the angular frequency and t_p is the period time. The T_a can be calculated from the heating rates and the period (e.g., in the iso-scan procedure, T_a = heating rate of the initial heating ramp • $t_p/4$). Under the conditions of the first harmonic dominating the series, temperature modulation can be represented by a sine wave.

Assuming a normal sinusoidal perturbation, the heat flow rate, $\Phi(T(t))$ given by Schawe [17] is:

$$\Phi(T(t)) = C_\beta(T)\beta_0 + \omega_0 T_a \left| C(T,\omega_0) \right| \cos(\omega_0 t - \varphi) \quad (4)$$

where the first term corresponds to the underlying linear heating rate, C_β is heat capacity at a constant heating rate of β_0, the $|C| = \sqrt{C'^2 + C''^2}$, where C' and C" respectively represent the real and imaginary portions of the heat capacity.

The underlying linear heat flow is separated from the oscillating part Φ_a. The modulus of complex heat capacity can be calculated as,

$$\left| C(T,\omega_0) \right| = \frac{\Phi_a(T,\omega_0)}{T_a \omega_0} \quad (5)$$

and the real and imaginary parts of the heat capacity can be calculated from the knowledge of the phase lag angle φ using the equation:

$$C'(\omega_0) = |C(\omega_0)| \cos \varphi \quad (6)$$

$$C''(\omega_0) = |C(\omega_0)| \sin \varphi \quad (7)$$

In the case of a time dependent process, the underlying heat capacity C_β is different from the oscillating signal of $|C(\omega_0)|$, but in a time independent thermal event, they are the same as $C'(\omega_0)$ and the imaginary part $C''(\omega_0)$ being zero. The imaginary part is interpreted to be due to the dissipative processes, in other words, C" is the loss heat capacity and C' is the storage heat capacity. This method of evaluation also shows the importance of phase lag in the calculation and interpretation of TMDSC results. In this work, the iso-scan procedure is used, with the heating rate of 10 K/min for the initial heating ramp for 30 seconds followed by an isothermal segment for 30 seconds. A sample mass in the order of 3 - 5 mg was used.

2.4 Thermal Conductivity

Thermal conductivity is a measure of the transmission of thermal energy. Typically, at temperatures between 100 K and their T_g, the thermal conductivity of amorphous polymers gradually increases, similar to the heat capacity trace [28]. At the Tg, the slope of the thermal conductivity changes from positive to negative. Similar behavior is observed for semicrystalline polymers but the magnitude of thermal conductivity is significantly higher for the later as compared to amorphous polymers. Various models have been developed for thermal conductivity of composites and copolymers [28, 29, 30]. Thermal conductivity measurements on PLCs are also available [28, 31], although the heat

conduction mechanisms are not very well understood.

Thermal conductivity evaluation is important in determining the applicability and processing optimization of the material. As a specific example, during the operation of microelectronic devices, heat is generated which must be dissipated to ensure optimal performance of the device. The knowledge of thermal conductivity of a material will aid in the potential design modification to accommodate for low or high thermal conductivity of the material.

There are various methods of measuring thermal conductivity. They are classified as steady state and non-steady state measurements. Steady state measurements determine equilibrium thermal conductivity. Despite the usefulness of steady state measurements, they are usually cumbersome and slow. In addition to the speed of non-steady state thermal conductivity measurements, many do not require dedicated instruments. Among non-steady state methods, the impulse method [32, 28] and flash radiometry [33, 34, 35] are quite useful. DSCs can be used for thermal conductivity measurements.

Four methods of thermal conductivity measurements using DSC are available from the literature. The first method uses two identical cylinders. In the steady state, using the DSC output and temperature difference across each cylinder, thermal conductivity is determined [36]. The second method involves the use of a sample sandwiched between the sample holder and a copper rod. A thermocouple is embedded in the copper rod, which allows the measurement of the top surface temperature. The unit is equilibrated at various temperatures and thermal conductivity is calculated from the DSC

output and top surface temperatures [37]. The third method involves the use of a TMDSC [38]. In this method, an oscillating temperature program is applied to one side of the sample. Thermal conductivity is obtained from the output signal. The fourth method involves no change to the conventional DSC instrument. Two identical circular samples are placed in the sample and reference pans and a thin coating of indium or similar standard metal is applied to the sample in the sample pan. Thermal conductivity is calculated from the front slope of indium melting peak [13, 39, 40]. The accuracy of this method is reported to be ± 10% of the thermal conductivity measured using steady state methods. In the fourth method, standards such as Wood's alloy and gallium can also be used [1]. Other standards are reported by Flynn e. a. [41]. In this work, the fourth method is employed. Details regarding sample arrangements and thickness are provided in Section 5.5.

2.5 Thermogravimetric Analysis

Thermobalances were known as early as 1903 [1, 42]. The first commercial version, based on the design of Chevenard e. a., was introduced in 1954 [43]. The derivatograph, a simultaneous TG/DTA, was developed by Erdey e. a. [44]. Controlled atmosphere was introduced in a TG during 1962 by Garn e. a. [45]. The modern thermogravimetry began with the electrobalance of Chan and Schultz in 1963 [46]. Detailed accounts of the history of design in thermogravimetry has been presented by many authors with two are listed here [1, 11].

The most important aspect of a thermogravimetric analyzer is the balance. The designs of the balance and furnace have gone through many generations of developments.

A variety of designs for the balance and its mode of measurement are available [10]. Typical types include beam, cantilever, spring and torsion wire. Sensitivity and range depend on the balance design. Size and shape of crucibles for balances are abundant. A comprehensive review of such information is presented by Wendlandt [11]and Hatakeyama e. a. [10]. One of the interesting extensions of TGA is evolved gas analysis, in which TGA is coupled with many other analytical techniques such as DTA, Gas Chromatography (GC), Mass Spectrometry (MS) and Fourier Transform Infrared spectroscopy (FTIR). TGA can be used in polymers for such studies as degradation phenomena [47], compositional analysis [48], curing reactions [49], gas absorption, additives and total ash content.

Temperature calibration procedure can be performed in many ways. Two of them, the curie point calibration and fusible link procedure are prominent. Due to the ease of calibration, the curie point method is generally preferred over the fusible link method. In the fusible link method, a weight is suspended with a link of a metal of known melting point. During the heating ramp, at the melting point, the weight drops as a result of the metal link melting and the sudden loss of weight is realized in the output. The curie point calculation requires a magnetic material of known curie temperature (T_c). A permanent magnet is used to increase the apparent weight of the standard. Upon heating, when the curie point is reached, the standard is no longer affected by the permanent magnet and the loss of weight is characterized. Multiple standards can be sandwiched to obtain a comprehensive multipoint calibration.

The TGA used in this work is a Perkin-Elmer TGA-7. With this TGA, curie point calibration was performed at regular intervals using the standard Perkalloy (T_c=596°C). Nitrogen purge gas was used with an inlet pressure of 25 psi for all the experiments unless stated otherwise. The movement of the TGA furnace was pneumatically controlled with dry compressed air at an inlet pressure of 30 psi. The furnace was cleaned periodically, once in 10 to 20 runs depending on the carbon buildup from the degradation of the polymer, using a built-in procedure of heating in air at 900°C. The platinum sample crucibles were cleaned at a very high temperature (about 1100°C) after each run. Individual sample information and experimental specifications are provided in the pertinent chapters.

2.6 Thermomechanical Analysis

Thermal expansivity measurements have been performed on polymers as early as 1942 [50]. In 1944 Boyer e. a. [51, 52, 53] reported the difference in the thermal expansivity of polystyrene below and above the T_g. A Pyrex dilatometer, sealed with a glass plug and filled with mercury, was placed in a water bath to measure the volume change as a function of temperature. The level of mercury was used to measure volume change. Directional expansivity measurements are believed to have been developed from the hardness test methods. This type of expansivity measurement and the term "thermomechanical" was introduced by Kargin e. a., in 1948 [54, 55]. The first commercial TMA apparatus was introduced by du Pont in the 1960s.

There are various ways of measuring the change in length of a sample. A linear

voltage differential transformer (LVDT) is commonly used in TMA for the measurement of height. Laser interferometry and capacitance are some of other methods [1] used in TMA. The use of an LVDT is popular due to the ease and accuracy of operation. In an LVDT, a magnetic core rod is inserted through three circular electromagnets. The movement of the core rod results in a potential, whose sign depends on the direction of movement and whose magnitude is related to amplitude of the motion. The output voltage is often calibrated with mechanical gauge blocks, to maintain and verify the linearity of operation. LVDTs are capable of measuring changes in the order of 0.1μm. LVDTs are often isolated from the furnace and kept in a thermostat. This isolation is to eliminate and minimize the effect of temperature variations on the performance of the LVDT. TMAs are also equipped with force motors, to control the force applied to the sample.

TMA calibration procedure involves height, temperature and furnace calibrations. Height calibration is performed using the gauge blocks mentioned above. Temperature calibration is performed with high purity standards such as indium or zinc. This calibration is usually performed in the penetration mode and as the standard reaches the transition temperature, the probe penetrates the standard. The temperature corresponding to this drop in height is calibrated against the expected transition temperature. ASTM E-831 [55] describes this calibration method in detail. Furnace calibration verifies the operation of the furnace with the calibrated temperature.

A Perkin-Elmer TMA-7 operating on a UNIX platform is used for the expansivity

measurements. No purge gas was used in the TMA evaluation. All the samples were evaluated in the temperature range between 30°C - 220°C at a heating rate of 5 K/min, unless stated otherwise. All experiments were conducted in compression mode. Sample preparation is provided in Section 5.2. TMA evaluation was performed on all three directions of the sample to determine the anisotropy. Other experimental details are provided in relevant chapters.

2.7 Thermally Stimulated Depolarization

Electrets were first reported by Eguchi in the 1920s [56, 57]. Electrets are materials, which retain the charge induced as a result of exposure to the polarizing field. Similar to the magnets, various strengths of electrets are possible. Despite many studies on the nonisothermal discharge of these electrets, only in 1966 was the theoretical model proposed by Bucci e. a. [58, 59] based on the one proposed by Frey e. a. [60,61]. This model was further developed by many authors [62, 63, 64]. Much of the historical information is available from reviews [65, 66, 67, 68, 69].

The principle of TSD involves the study of electrical discharge. Usually this discharge is a result of the relaxation of orientation of dipoles by the electric field. Typical experiments are thermally stimulated polarization current (TSPC), thermally stimulated discharge current (TSDC) and thermal window polarization methods (TW). Other variations of the experiments are also possible, the details of which can be found in reviews by D'Souza [69] and Lavergne e. a. [70].

In a TSPC experiment, the sample is heated at a set rate under a preset electric

field. The current is monitored as a function of temperature. The dipolar orientation at a specific temperature results in an electrical current. The temperature dependence of the mobility of the dipoles can thus be characterized. The advantage of this technique is the ability to study the stress, orientation and other phenomena which disappear upon or are altered by heat treatments.

The TSDC experiment is also called global TSD experiment or complex TSD. This will be referred to as global TSD or global experiment. The sample is polarized at a specific electric field (E_p), at a temperature, T_p for a polarization time of t_p. The sample is then cooled to a temperature T_0 at a preset heating rate and the electric field is removed. The orientation of the dipoles induced by the polarization step is frozen. The sample is heated at a preset heating rate to a temperature T_f and electrical current resulting from the relaxation of the orientation of the dipoles is monitored. The choice of temperatures T_p, T_0 and T_f are determined by the polymer and the relaxation being studied. For experiments described in this dissertation, the sample was annealed for 60 minutes at 250°C before the polarization step and the sample was polarized at 250°C (T_p) under 250 V/mm (E_p), for 2 minutes (t_p). The sample was cooled at 2 K/min to 30°C (T_0) and kept at that temperature for 2 minutes. The sample was heated to 250°C (T_p) at 5 K/min. The global TSD was also performed at the polarizing fields of 100, 200, 300 and 500 V/mm.

The TWs generally are performed similar to the global TSD experiment. However subsequent to the polarization step, during cooling at the temperature (T_p - x)°C, the electric field is removed and further cooling takes place under short circuit

condition. Thus the dipoles that are mobile, in the x K window, are polarized. The value of x (here it is 2 K) is the width of the polarization thermal window. This method was first described by Lacabanne [71].The rest of the experiment is identical to the global TSD experiment. For the TW experiments in this work, the T_p was varied from 120 - 230°C at 5 K intervals. In the TW experiments described in this work the cooling rate was 2 K/min, T_0 was T_p - 40 K, the isotherm at T_0 was 5 minutes, the heating rate was 5 K/min and the T_f was T_p + 80 K. The polarizing field of 250 V/mm was used for all TW experiments.

2.8 References

1. P. K. Gallagher, *Thermal Characterization of Polymeric Materials*: Vol. 1, Ed.: E. A. Turi, Academic Press, New York, Chapter 1 (1997).
2. W. C. Roberts-Austin, *Metallographist*, **2**, 186 (1889).
3. E. T. Jensen and C. A. Beevers, *Trans. Faraday Soc.*, **34**, 1478 (1938).
4. R. L. Stone, *Bull.-Ohio State Univ. Eng. Exp. Stn.*, **146**, 1 (1951).
5. S. L. Boersma, *J. Am. Ceramic Soc.*, **38**, 281 (1955).
6. E. S. Watson, M. J. O'Neill, J. Justin and N. Brenner, *Anal. Chem.*, **36**, 1233 (1964).
7. M. Reading, D. Elliott and V. Hill, *Proc. 21st North Am. Thermal Anal. Soc. Conf.*, 145 (1992).
8. P. Sullivan and G. Seidel, *Phys. Rev.*, **173**, 679 (1968).
9. M. Reading, B. K. Hahn and G. S. Crowe, U. S. Patent 5224775 (1993).
10. T. Hatakeyama and F. X. Quinn, *Thermal Analysis: Fundamentals and Applications to Polymer Science*, John Wiley & Sons, New York (1994).
11. W. W. Wendlandt, *Thermal Analysis*, Wiley, New York (1986).
12. B. Wunderlich, *Thermal Analysis*, Academic Press, San Diego, CA (1990).
13. V. A. Bershtein and V. M. Egorov, *Differential Scanning Calorimetry of Polymers: Physics, Chemistry, Analysis, Technology*, Ellis Horwood, New York City (1994).
14. M. Reading, D. Elliott and V. Hill, *J. Thermal Anal.*, **40**, 949 (1993).

15. P. S. Gill, S. R. Sauerbrunn and M. Reading, *J. Thermal Anal.*, **40**, 931 (1993).

16. M. Reading, A. Luget and R. Wilson, *Thermochim. Acta.*, **238**, 295 (1994).

17. J. E. K. Schawe, *Thermochim. Acta,* **260**, 1 (1995).

18. J. E. K. Schawe, *Thermochim. Acta,* **261**, 183 (1995).

19. J. E. K. Schawe, *Thermochim. Acta,* **271**, 127 (1996).

20. J. E. K. Schawe and G. W. H. Höhne, *Thermochim. Acta,* **287**, 213 (1996).

21. A. Hensel, J. Dobbertin, J. E. K. Schawe, A. Boller and C. Schick, *J. Thermal Anal.*, **46**, 935 (1996).

22. J. E. K. Schawe and G. W. H. Höhne, *J. Thermal Anal.*, **46**, 893 (1996).

23. J. E. K. Schawe and E. Bergmann, *Thermochim. Acta,* **304-305**, 179 (1997).

24. J. E. K. Schawe and M. Margulies, U. S. Patent 5549387 (1996).

25. A. Boller, Y. Jin and B. Wunderlich, *J. Thermal Anal.*, **42**, 307 (1994).

26. B. Wunderlich, Y. Jin and A. Boller, *Thermochim. Acta*, **238**, 277 (1994).

27. J. M. Hutchinson and S. Montserrat, *Thermochim. Acta*, **286**, 263 (1996).

28. Y. Godovsky, *Thermophysical Properties of polymers*, Springer-Verlag Berlin, New York (1994).

29. V. P. Privalko and V. V. Novilov, *The Science of Heterogeneous Polymers: Structure and thermophysical properties*, John Wiley and Sons Ltd., West Sussex (1995).

30. D. M. Bigg, *Adv. Polymer Sci.*, 119, 1 (1995).

31. C. L. Choy, Y. W. Wong, K. W. E. Lau, Guangwu Yang and A. F. Lee, *J. Appl. Polymer Sci.*, 33, 2055 (1995).

32. R. C. Steere, *J. Appl. Phys.*, **37**, 3338 (1966).

33. W. J. Parker, R. J. Jenkins, C. P. Butler and G. L. Abbot, *J. Appl. Phys.*, **32**, 1679 (1961).

34. F. C. Chen, Y. M. Poon and C. L. Choy, *Polymer*, **18**, 129 (1977).

35. C. L. Choy, W. P. Leung and Y. K. Ng, *J. Polymer Sci. Phys.*, **25**, 1779 (1987).

36. J. E. S. D. Ladbury, B. R. Currell, J. R. Horder, J. R. Parsonage and E. A. Vidgeon, *Thermochim. Acta*, **169**, 39 (1990).

37. A. B. Buhri and R. P. Singh, *J. Food Sci.*, **58**, 1145 (1993).

38. S. M. Marcus and R. L. Blaine, *Thermochim. Acta*, **243**, 231 (1994).

39. G. Hakvroot and L. L. van Reijen, *Thermochim. Acta*, **93**, 317 (1985).

40. W. Brostow, N. A. D'Souza and B. Gopalanarayanan, *Proc. Annual Tech. Conf. Soc. Plast. Eng.*, **55**, 1499 (1997).

41. J. H. Flynn and D. M. Levin, *Thermochim. Acta*, **126**, 93 (1988).

42. W. Nernst and E. H. Riesenfeld, *Ber. Dtsch. Chem. Ges.*, **36**, 2086 (1903).

43. P. Chevenard, X. Wache and R. De La Tullaye, *Bull. Soc. Chem. Fr.*, **11**, 41 (1954).

44. L. Erdey, F. Paulik and J. Paulik, *Acta Chim. Acad. Hung.*, **10**, 61 (1956).

45. P. D. Garn, C. R. Geith and S. De Balla, *Rev. Sci. Instru.*, **33**, 293 (1962).

46. L. Cahn and H. Schultz, *Anal. Chem.*, **35**, 1729 (1963).

47. I. C. McNeill and S. Basan, *Polymer Degradat. Stabil.*, **39**, 145 (1993).

48. S. Nakatsuka and A. L. Andrady, *J. Appl. Polymer Sci.*, **45**, 1881 (1992).

49. S. Numata, K. Fujisaka and N. Kinjo, *Polyimides: Synthesis, Characterization and Applications*, Ed.: K. L. Mittal, Plenum Press, New York, Vol. 1, 259 (1984).

50. F. E. Wiley, *Ind. Eng. Chem.*, **34**, 1052 (1942).

51. R. F. Boyer and R. S. Spencer, *J. Appl. Phys.*, **15**, 398 (1944).

52. R. F. Boyer and R. S. Spencer, *J. Appl. Phys.*, **16**, 594 (1945).

53. R. S. Spencer and R. F. Boyer, *J. Appl. Phys.*, **17**, 398 (1946).

54. V. A. Kargin and G. V. Slonimskii, *Dokl. Akad. Nauk SSSR*, **62**, 239 (1948).

[55] C. M. Neag, *Thermomechanical Analysis in Materials Science: Materials Characterization by Thermomechanical Analysis*, Eds.: A. T. Riga and C. M. Neag, American Society for Testing and Materials, Philadelphia, p. 3 (1991).

56. M. Eguchi, *Phil. Mag.*, **49**, 178 (1925).

57. M. Eguchi, *Jap. J. Phys.*, **1**, 10 (1922).

58. C. Bucci and R. Fieschi,. *Phys. Rev. Lett.*, **12**, 16 (1964).

59. C. Bucci, R. Fieschi and Guidi, *Phys. Rev.*, **148**, 816 (1966).

60. H. Frei and G. Groetzinger, *Physik Z.*, **37**, 720 (1936).

61. J. Bayard, J. Grenet, C. Cabot and E. Dargent, *IEE Proc. Sci. Measur. Technol.*, **144**, 168 (1997).

62. B. Gross, *J. Electrochem. Soc.*, **115**, 376 (1968).

63. R. Chen, *J. Appl. Phys.*, **40**, 570 (1969).

64. J. van Turnout, *Polymer J.*, **2**, 173 (1971).

65. J. van Turnhout, *Thermally Stimulated Discharge of Polymer Electrets*, Elsevier, Amsterdam (1975).

66. J. Vanderschueren and J. Gasiot, *Thermally Stimulated Relaxation in Solids*, Ed.: P. Bräunlich, Springer-Verlag, New York, Chapter 4 (1979).

67. B. Chowdhury, *New Characterization Techniques for Thin Polymer Films*, Eds.: H. Tong and L. T. Nguyen, Wiley, New York, Chapter 10 (1990).

68. S. Chen, *J. Mater. Sci.*, **28**, 3823 (1993).

69. N. A. D'souza, *PLC book series*, Ed.: W. Brostow, Thomson Science, London, Vol. 4, Chapter 4 (1998).

70. C. Lavergne and C. Lacabanne, *IEEE Electr. Insul. Mag.*, **9**, 5 (1993).

71. C. Lacabanne, Ph. D. Thesis, University of Toulouse, France (1974).

CHAPTER 3

EVALUATION OF THE THERMOPLASTIC POLYIMIDES

3.1 Introduction and Overview

Aromatic polyimides are known to be useful for high temperature applications due to their high thermal stability and good mechanical properties. Typically, polyimides had always been thermosetting in nature, with obvious limits to their applications. In recent years, due to breakthroughs in their resin chemistry, thermoplastic polyimides (TPIs) have become commercially available [1, 2, 3, 4, 5, 6].

TPIs are available in both completely amorphous and semicrystalline grades. The TPIs used in this work are made from pyromellitic dianhydride (PMDA) and (4,4' bis(3-aminophenoxy))biphenyl. The diamine contains meta linkages, which lower the glass transition temperature (Tg), and two ether groups, which impart additional flexibility to the backbone structure while lowering the T_g. Due to their complex chemical structures, TPIs exhibit various relaxations below and above their T_g. The T_g values were obtained by differential scanning calorimetry (DSC) for both the amorphous and semicrystalline TPIs. However, in order to probe the potential sub-T_g relaxations in the amorphous region, thermally stimulated depolarization (TSD) was employed. Due to its low experimental frequency range, the TSD technique has been successfully used in the evaluation of these relaxations [7, 8, 9, 10, 11, 12, 13, 14, 15, 16, 17, 18]. Global TSD experiments

were conducted with a polarizing temperature (T_p) of 250°C, which is above the T_g. Parameters for the window polarization were obtained from the global experiments. Window polarization experiments were conducted individually on unaged films for temperatures between 75°C and 250°C with a thermal window of 2 K. An annealing at 250°C for 60 minutes was performed for all thermal window experiments to give consistent thermal history for all samples.

3.2 Sample Preparation

TPI samples obtained from MTC America, Regulus – g and – u, semicrystalline and amorphous TPIs respectively, were used in this study. Both TPIs are based on pyromellitic dianhydride (PMDA) and (4,4' bis(3-aminophenoxy))biphenyl. Samples for DSC characterization were made from the Regulus films using a hole punch to obtain circular samples of uniform shape and size. Square sections cut from the Regulus films were provided with gold coating using a Kapton® mask film with 0.38 cm diameter hole, which is the diameter of the electrode used in the TSD. Gold deposition was necessary to avoid homo-charging of the samples. The deposition was performed under a low-pressure argon atmosphere. Samples for the dynamic mechanical evaluation were obtained by cutting rectangular specimens from the films.

3.3 Differential Scanning Calorimetry

The description of the DSC used is discussed in Section 2.1. Figures 1 and 2 show the heat capacity as a function of temperature obtained from the first and second

heating ramps respectively. The distinct increase in heat capacity around 250°C is assigned to the α relaxation, that is T_g, of the polymer chains or portions of chains. The glass transition temperature is calculated to be the temperature at half-height of the heat capacity increase associated with the glass transition. The T_gs of the amorphous and semicrystalline TPIs are 240 and 249°C. The T_gs from the first and second runs are identical for both TPIs.

The semicrystalline TPI exhibits an exothermic cold crystallization followed by an endothermic melting peak in the first heating ramp. Only an endothermic melting is observed in the second run. This indicates the thermo-irreversible nature of this cold crystallization, which is consistent with the literature [19, 20, 21, 22, 23, 24]. Returning to the heat capacity traces for the amorphous TPI for the first runs, (Figure 1) the exothermic curvature following the glass transition is indicative of reorientation of the molecular chains. This process is similar to the cold crystallization observed in the semicrystalline TPI. Such a process is not observed for the second run (Figure 2) in the amorphous TPI indicating thermo-irreversibility. It can be seen from both figures, that the amorphous TPI does not show any melting in either heating ramp as expected.

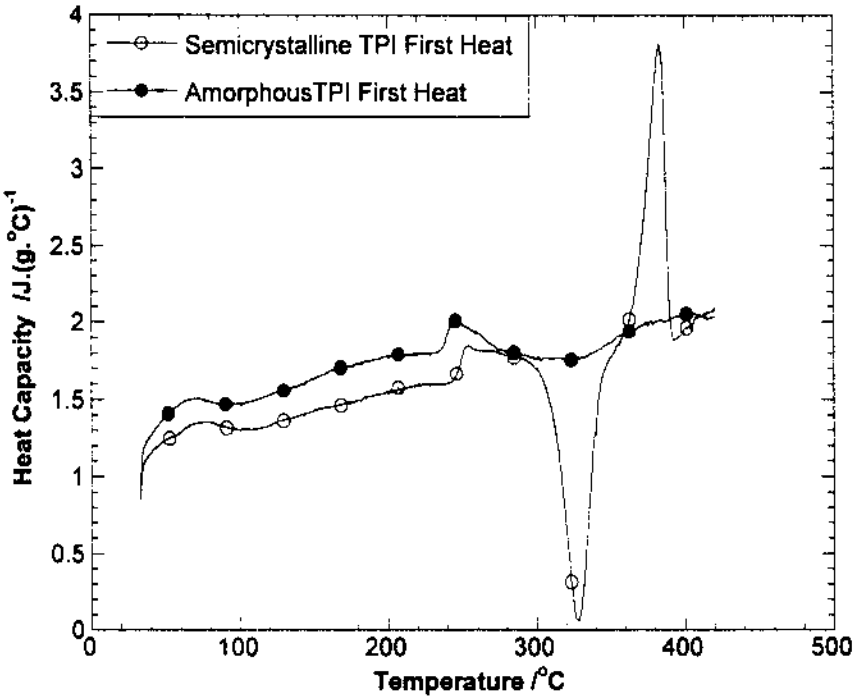

Figure 1. Heat capacity of thermoplastic polyimides, from the first heating ramps

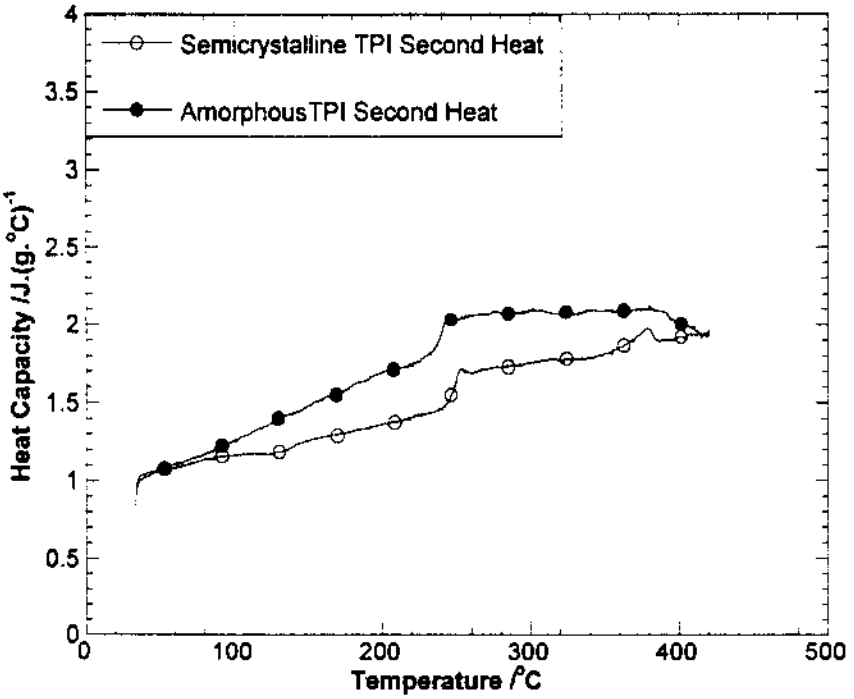

Figure 2. Heat capacity of thermoplastic polyimides, from the second heating ramp.

The amorphous TPI shows an increase of 0.238 and 0.223 $J(g^{\cdot}°C)^{-1}$ in heat capacity associated with the glass transition in the first and second heating runs, respectively, while the semicrystalline TPI shows an increase of 0.207 $J(g^{\cdot}°C)^{-1}$ in both heating runs. The larger magnitude of the heat capacity step at glass transition is clearly due to the lack of long range order in the amorphous TPI. The decrease from 0.238 to 0.223 $J(g^{\cdot}°C)^{-1}$ in the case of amorphous TPI is possibly due to local order set by the reorganization seen from Figure 1.

We can see that both TPIs show similar heat capacity traces until the glass transition. A closer look reveals that both TPIs show a gradual increase in heat capacity between 100 and 200°C indicating possible broad relaxation in that temperature region.

3.4 Temperature Modulated DSC (TMDSC)

Pyris-1 DSC from Perkin-Elmer was used for TMDSC measurements. An isotherm followed by a heating ramp is used for this evaluation as described in Section 2.1. In a TMDSC run, the thermodynamic and kinetic effects are separated into storage and loss heat capacities. Figures 3 and 4 show the storage and loss heat capacities as a function of temperature for the amorphous and semicrystalline TPIs. The storage heat capacity indicates the thermodynamically reversible part of the heat capacity while the loss part is indicative of the thermodynamically irreversible heat capacity originating from kinetic effects. Similar to the DSC results for the first and second runs, Figure 3 also shows a melting endotherm for the semicrystalline TPI and none for the amorphous TPI.

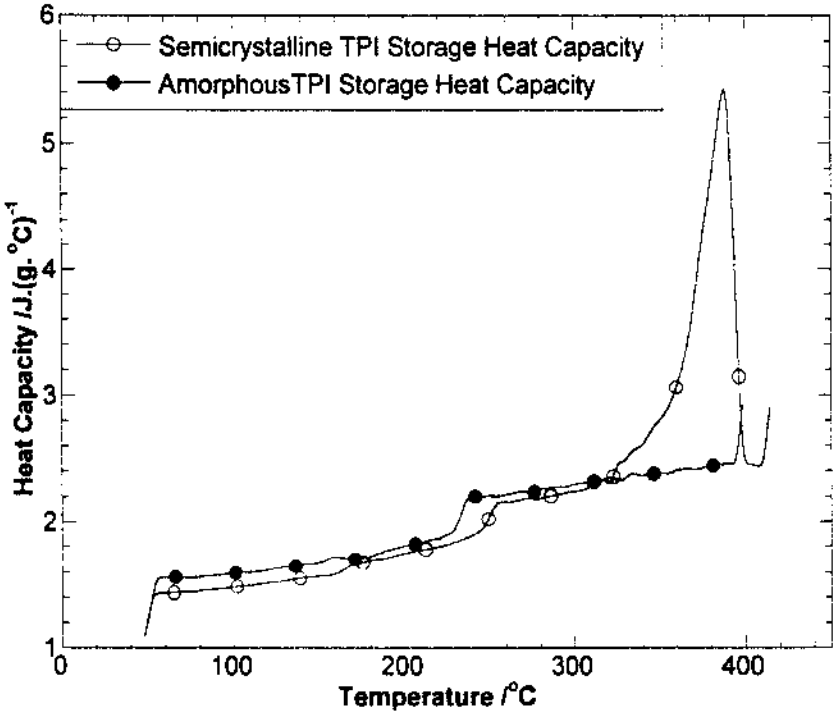

Figure 3. Storage heat capacity of thermoplastic polyimides, from TMDSC.

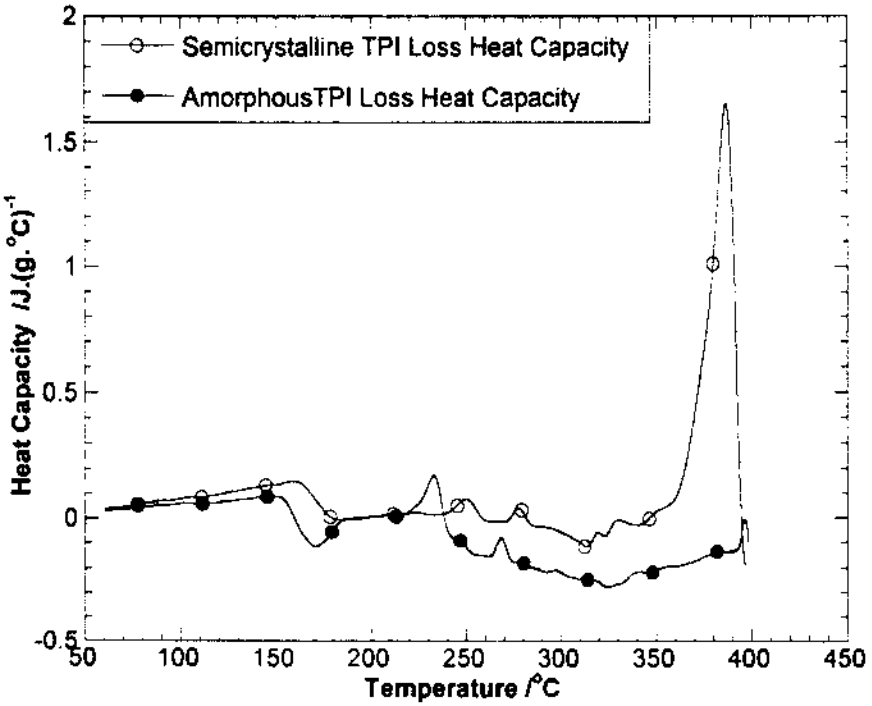

Figure 4. Loss heat capacity of thermoplastic polyimides, from TMDSC.

It can be seen from Figure 4 that the loss heat capacity indicates the presence of a sub-T_g relaxation in the temperature of 120 – 190°C for both TPIs. The loss peak associated with the glass transition is larger in the amorphous TPI. This is an indication of the presence of larger kinetic factors involved in the glass transition. Huo e. a. [25] suggested that a small portion of amorphous material bound between the crystallites, relaxes within a narrow temperature range above the T_g. This can be seen from the loss heat capacity in Figure 4 as the second peak in the temperature range of 265 - 275°C for the amorphous and 270 - 280°C for the semicrystalline TPI. As suggested by Hou e. a., this peak is expected for the semicrystalline TPI. The presence of this peak in the amorphous TPI indicates the existence of local order.

The exothermic valley observed between 280 and 340°C in the semicrystalline TPI corresponds to the cold crystallization seen in the conventional DSC result in Figure 1. The occurrence of the valley between 280 and 390°C in the amorphous TPI is also consistent with the DSC result. This valley shows that the reorientation occurs over a wider temperature range for the amorphous TPI. This reorganization phenomenon can be explained by as follows: the amorphous TPI does not develop any long-range order and more chain fragments (of varying length) are available for this reorientation process. Amorphous TPI does not show any loss C_p associated with the melting process, which indicates the absence of any transition in this temperature range. This absence also confirms the amorphous nature of this TPI, since the presence of any long range order should show an irreversible kinetic process associated with melting. The semicrystalline

TPI on the other hand does show a melting endotherm and the kinetic loss process indicating the presence of long range order, in other words, crystallinity.

3.5 Thermally Stimulated Depolarization

A TSC/RMA 9000 apparatus manufactured by Thermold L. P., Stamford, CT, was used for the TSD evaluation of the two TPIs. The experimental procedure is outlined in Section 2.6. Global TSD experiments were conducted with the polarizing temperature (T_p) = 250°C, which is above the T_g. Prior to each global TSD experiment, the sample was annealed at 250°C for 60 minutes in order to eliminate any affects of thermal history. Figure 5 shows the results from global TSD runs on the semicrystalline and amorphous TPIs. The T_g values obtained from the global experiments were lower than that from the DSC. The lower value is attributed to the lower experimental frequency of the TSD technique. Both the TPIs show sub glass transition relaxations between 120 and 200°C. The loss heat capacity from the MTDSC also indicates relaxations in this temperature range. The global TSD experiments were conducted at different polarizing fields. As the strength of the polarizing electric field is increased, Figures 6 and 7, the peak heights increase linearly, which is an indication of a true dipolar relaxation. Amorphous TPI shows additional relaxations between 50 and 100°C at higher polarizing fields. Slight movement of the peak with increasing fields was observed. A similar effect was reported for a PET/xPHB copolymer [7] - possibly a result of development of a different conduction mechanism at higher fields. It is also possible that this peak arises from non-dipolar relaxations such as the space charge effect or the electrode effect.

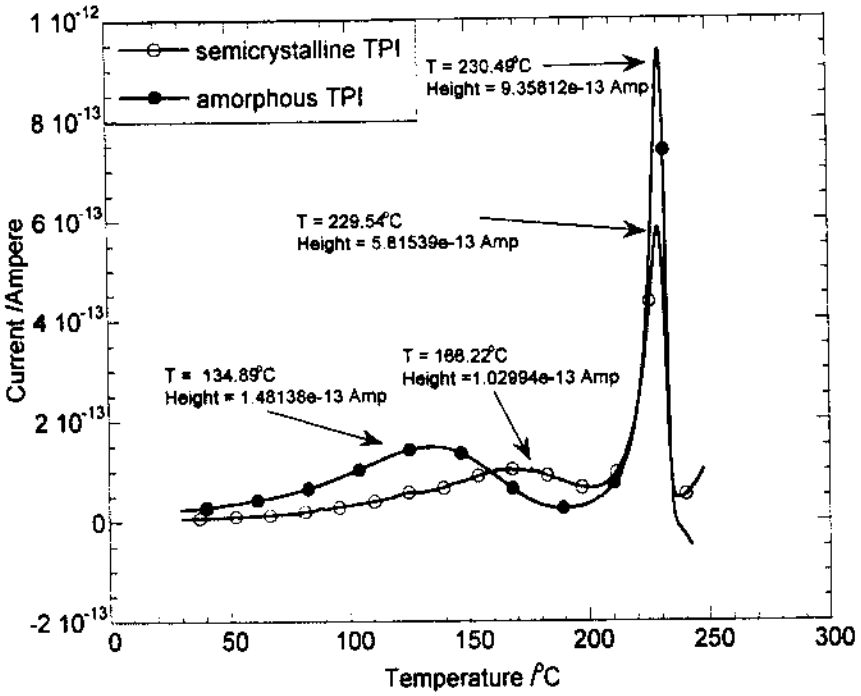

Figure 5. Global TSD spectra of amorphous and semicrystalline TPIs.

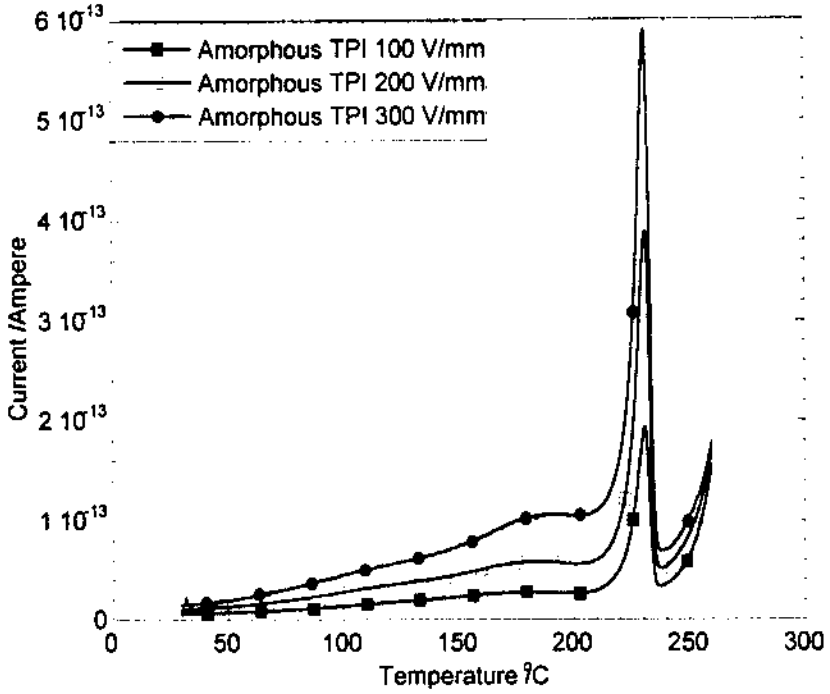

Figure 6. Global TSD spectra of amorphous TPI at different polling fields.

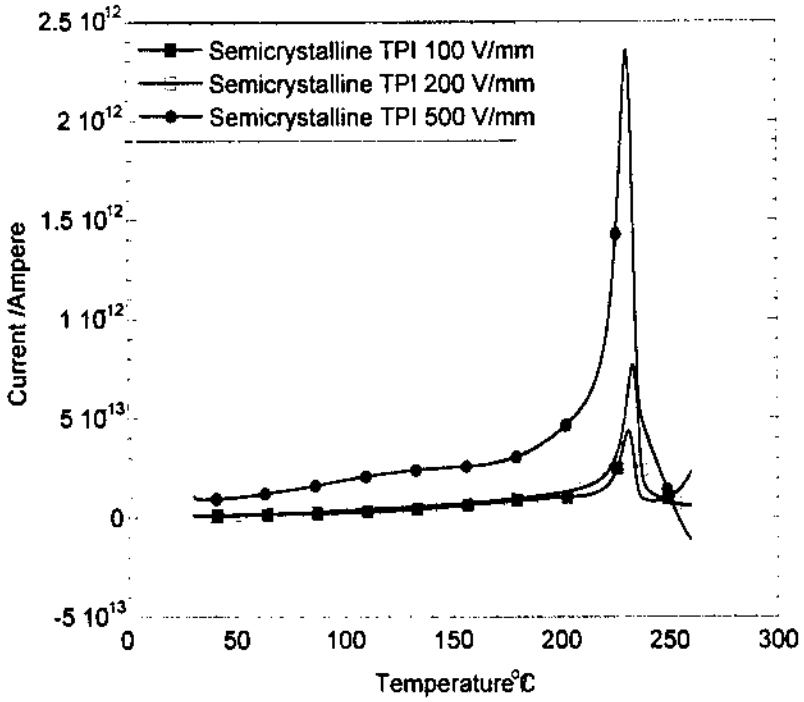

Figure 7. Global TSD spectra of semicrystalline TPI at different polling fields.

In order to investigate these relaxations, the window polarization method is employed. The window parameters are obtained from the global TSD runs. As mentioned above, the global TSD indicates the presence of two relaxation phenomena for both TPIs, the glass transition relaxation in the temperature range of 200 – 240°C and the sub-T_g relaxation between 120 and 190°C. The window experiments were performed for the temperature range of 75 – 250°C in order to evaluate both these relaxations. Window polarization experiments were conducted on annealed films with a thermal window of 2 K for 2 minutes. Under such a small thermal window, only the dipoles responding with a specific relaxation time are polarized. Subsequent heating causes their depolarization. Measurement of the resultant current enables the calculation of the temperature dependent

relaxation time for the specific fraction of dipoles as described below. The relaxation times were calculated using the Bucci equation

$$\tau(T) = \frac{P(T)}{J(T)} \tag{1}$$

where J(T) is the measured current as a function temperature and P(T) is the total polarization, that is the area under the J(T) curve. Lacabanne e. a. have shown that, under Debye relaxation conditions, the peak area on the left side of the peak equals $^2/_3$ of the total peak area pertaining to the relaxation. Even though polymers do not follow Debye relaxation in its entirety, under a narrow thermal window, this is a valid approximation. Therefore, the P(T) is calculated as:

$$P(T) = \int_{T}^{T_{max}} J(T)dT + \frac{1}{2}\int_{T_0}^{T_{max}} J(T)dT \tag{2}$$

The use of Eq. 2 also eliminates any possible contribution from other higher temperature relaxational modes by this calculation of the peak area only from the initial half of the peak. This acts as an additional correction for the non-Debye character of the relaxation of polymers. Following this, assuming a single relaxation time, $\tau_i(T)$, for the specific relaxation mode, the temperature dependent relaxation times can be described by the Arrhenius equation:

$$\tau_i(T) = \tau_{0i} * \exp\left(\frac{E_a}{kT}\right) \tag{3}$$

where k is the Boltzmann constant, E_a is the activation energy and τ_{0i} is the pre-exponential factor.

Table 1 shows the values of the temperature at peak maximum of the thermal window experiments for the amorphous and semicrystalline TPIs. Figures 8 – 11 show results for the thermal window experiments for the sub T_g relaxation and glass transition relaxation for both TPIs. Figure 12 shows the variation of the peak maxima as a function of the polarizing temperature.

Table 1

Polarization Temperature T_p and Peak Maxima T_m

T_p K	T_m K	
	Amorphous TPI	Semicrystalline TPI
393	-	418
398	414	418
403	417	427
408	-	434
413	423	431
418	-	432
423	429	-
428	-	435
463	483	485
468	490	488
473	494	496
478	498	499
483	499	500
488	501	501
493	503	503
498	505	505
503	507	507

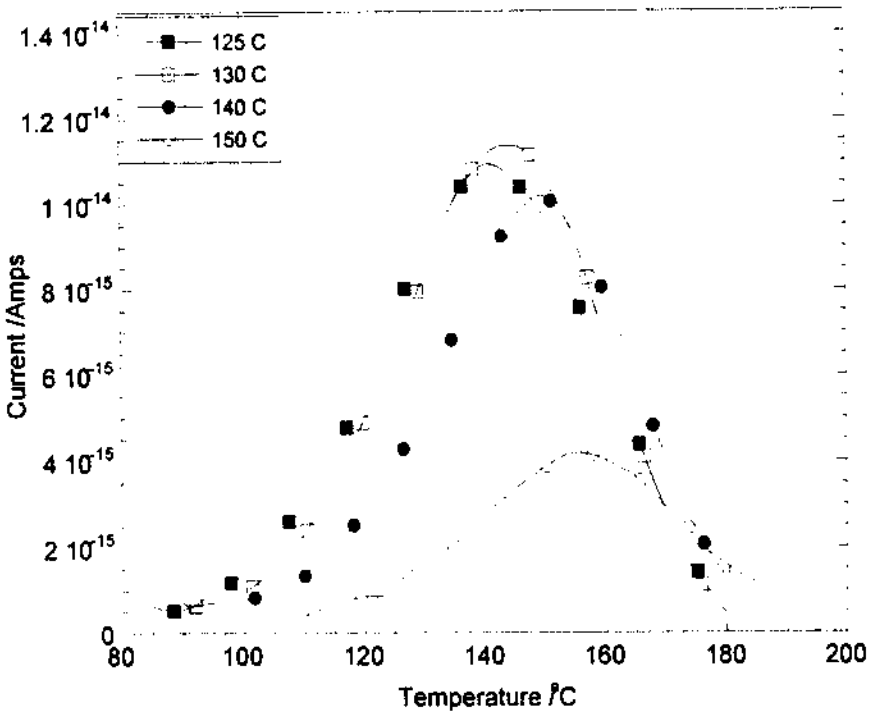

Figure 8. Window polarization spectra of amorphous TPI sub-Tg relaxations.

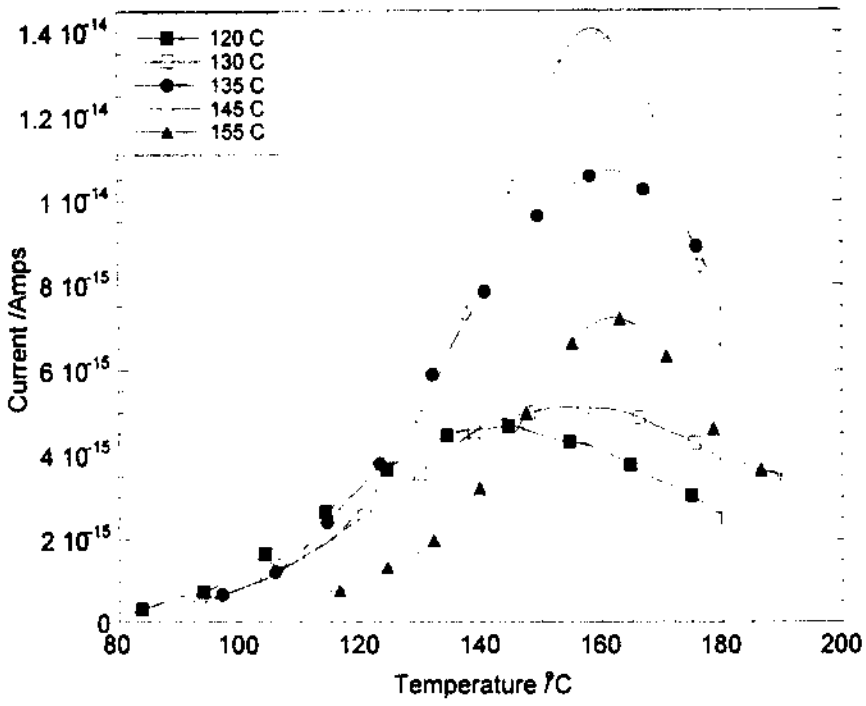

Figure 9. Window polarization spectra of semicrystalline TPI sub-Tg relaxations.

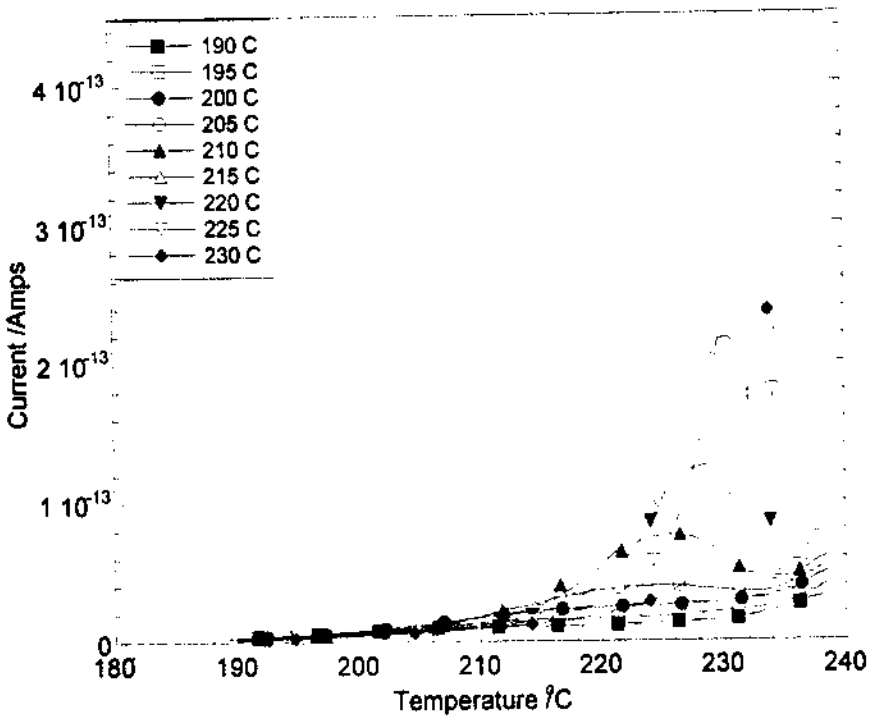

Figure 10. Window polarization spectra of amorphous TPI Tg relaxations.

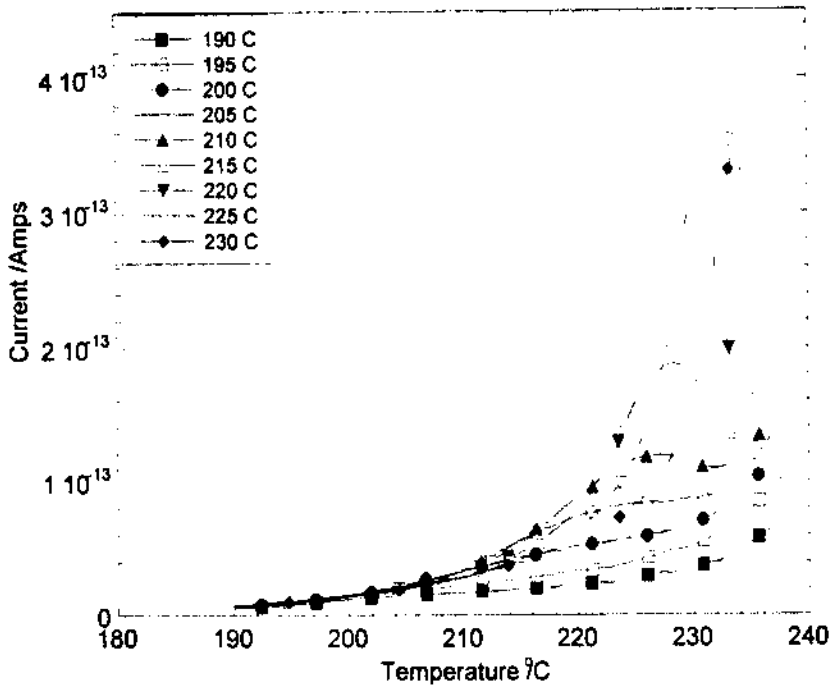

Figure 11. Window polarization spectra of semicrystalline TPI Tg relaxations.

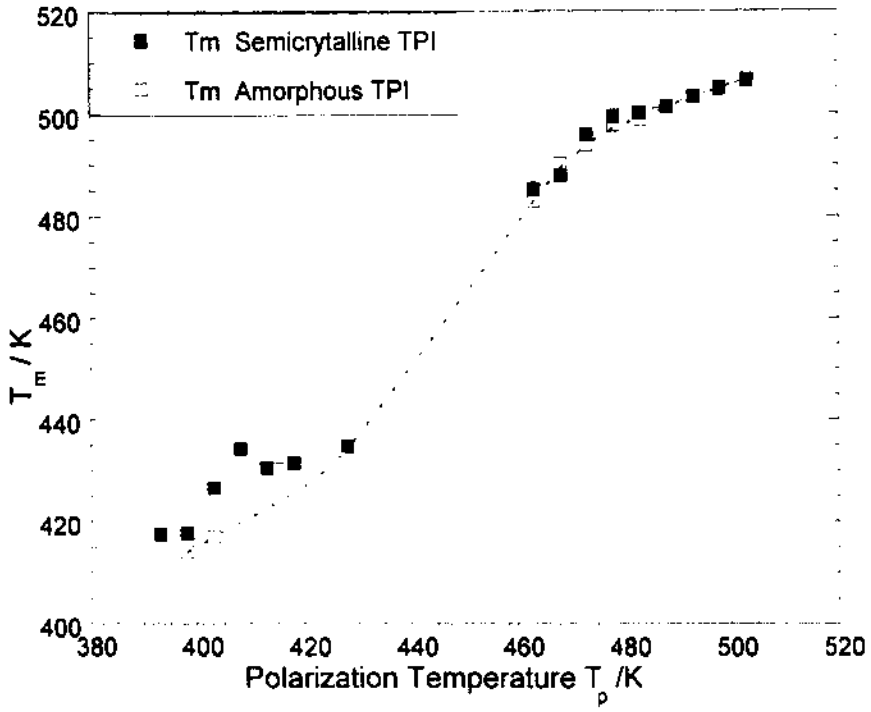

Figure 12. Peak temperatures of thermal windows as a function of polarization temperature.

According to Eyring [26] the pre-exponential factor τ_0 is:

$$\tau_0 = \left(\frac{h}{kT}\right)\exp\left(-\frac{S}{k}\right) \tag{4}$$

using Eq. 3 yields

$$\tau_i = \left(\frac{h}{kT}\right)\exp\left(-\frac{S}{k}\right)\exp\left(\frac{H}{kT}\right) \tag{5}$$

where h is the Planck constant and k is the Boltzmann constant, while S and H are respectively the activation entropy and enthalpy. Entropy and enthalpy are calculated from the intercept and slope of the plot of $\log([\tau_i/(h/kT)]$ vs. $1/T$. The Gibbs function is:

$$G = H + T_p S \tag{6}$$

where T_p is the polarization temperature in Kelvin. The thermodynamic quantities so obtained are given in Tables 2 – 7.

Table 2

The parameters obtained by fitting Arrhenius Eq. (3) for amorphous TPI

T_p K	log(τ) sec	E_a eV	r^2
398	-10.9842	1.076	0.9961
403	-12.2635	1.187	0.9995
413	-14.9181	1.418	0.9963
423	-18.8278	1.761	0.9942
463	-22.5121	2.346	0.9951
468	-23.2003	2.443	0.9775
473	-29.2666	3.053	0.9592
478	-33.7094	3.508	0.9631
483	-42.3390	4.361	0.9789
488	-52.9929	5.434	0.9864
493	-66.4771	6.794	0.9902
498	-71.4705	7.321	0.9963
503	-134.474	13.648	0.9890

Table 3

The parameters obtained by fitting Vogel equation for amorphous TPI

T_p K	T_{inf} K	α_f 1/K	$\log(\tau_{ov})$	r^2
398	156	2.13E-04	-5.7791	0.8609
403	101	1.28E-04	-8.6191	0.8513
413	113	1.15E-04	-10.2209	0.7777
423	166	1.33E-04	-10.5722	0.6629
463	185	1.01E-04	-12.4465	0.9667
468	187	9.66E-05	-12.8718	0.9669
473	191	7.73E-05	-16.6454	0.9869
478	192	6.72E-05	-19.3091	0.9903
483	191	5.37E-05	-24.5690	0.9948
488	193	4.31E-05	-31.0643	0.9954
493	196	3.48E-05	-39.0313	0.9958
498	194	3.18E-05	-42.3666	0.9942
503	199	1.74E-05	-80.1155	0.9965

Table 4

The parameters obtained by fitting Eyring Eqs. (5 and 6) for amorphous TPI

T_p	H	S	G	H/T_m
K	kJ/mol	kJ/K	kJ/mol	kJ/mol.K
398	115.76	-0.05	118.57	0.24
403	127.88	-0.02	119.60	0.27
413	153.59	0.03	121.11	0.32
423	191.65	0.10	122.27	0.39
463	255.56	0.17	141.83	0.46
468	265.64	0.19	144.16	0.47
473	332.60	0.30	147.15	0.59
478	382.95	0.38	148.90	0.67
483	477.87	0.55	149.44	0.83
488	597.19	0.75	150.59	1.04
493	748.54	1.01	150.73	1.29
498	808.48	1.11	148.91	1.39
503	1509.37	2.32	146.88	2.59

Table 5

The parameters obtained by fitting Arrhenius Eq. (3) for semicrystalline TPI

T_p	log(τ)	E_a	r^2
K	sec	eV	
393	-6.146	0.701	0.9998
398	-7.560	0.814	0.9988
403	-7.004	0.786	0.9994
408	-7.218	0.820	0.9983
413	-9.985	1.040	0.9997
418	-12.122	1.220	0.9992
428	-14.549	1.430	0.9990
463	-20.822	2.196	0.9950
468	-25.932	2.695	0.9890
473	-24.391	2.588	0.9912
478	-26.343	2.799	0.9955
483	-29.580	3.124	0.9991
488	-36.064	3.770	0.9988
493	-54.253	5.585	0.9907
498	-59.700	6.148	0.9912
503	-92.939	9.490	0.9809

Table 6

The parameters obtained by fitting Vogel equation for semicrystalline TPI

T_p	T_{inf}	α_f	$\log(\tau_{ov})$	r^2
K	K	1/K	sec	
393	153	3.27E-04	-2.6947	0.7216
398	115	2.08E-04	-4.6183	0.8147
403	211	4.76E-04	-1.9211	0.7645
408	266	8.48E-04	-0.6976	0.7527
413	84	1.30E-04	-7.4385	0.8836
418	-	6.07E-05	-13.2791	0.9112
428	96	1.00E-04	-10.7391	0.8331
463	387	1.41E-03	-1.0096	0.9529
468	415	2.33E-03	-0.4376	0.9712
473	187	9.01E-05	-13.6451	0.9656
478	188	8.31E-05	-14.8649	0.9719
483	320	2.38E-04	-8.1872	0.9816
488	81	3.29E-05	-29.6002	0.9881
493	195	4.21E-05	-31.7466	0.9939
498	193	3.76E-05	-35.3628	0.9899
503	198	2.49E-05	-55.1220	0.9945

Table 7

The parameters obtained by fitting Eyring Eqs. (5 and 6) for semicrystalline TPI

T_p K	H kJ/mol	S kJ/K	G kJ/mol	H/T_m kJ/mol.K
393	64.28	-0.14	118.53	0.15
398	75.18	-0.11	119.35	0.18
403	72.42	-0.12	121.54	0.17
408	75.59	-0.12	123.71	0.17
413	96.91	-0.06	123.68	0.23
418	114.28	-0.02	124.24	0.26
428	134.53	0.02	124.90	0.31
463	207.63	0.14	142.42	0.43
468	255.42	0.24	144.05	0.52
473	245.19	0.21	146.50	0.49
478	265.55	0.25	147.86	0.53
483	297.22	0.31	148.13	0.59
488	359.94	0.43	148.31	0.72
493	534.29	0.78	149.46	1.06
498	589.88	0.89	147.98	1.17
503	910.92	1.52	145.75	1.80

From the slope and intercept of the plot of temperature dependent relaxation time for each thermal window on semi-logarithmic scale against inverse of temperature, the activation energy and the pre-exponential factor for the Arrhenius Eq. (2) are calculated. Figures 13 and 14 show the Arrhenius plots of the relaxation times for semicrystalline and amorphous TPIs. The reason for the convergence of the lines is said to be the compensation effect.

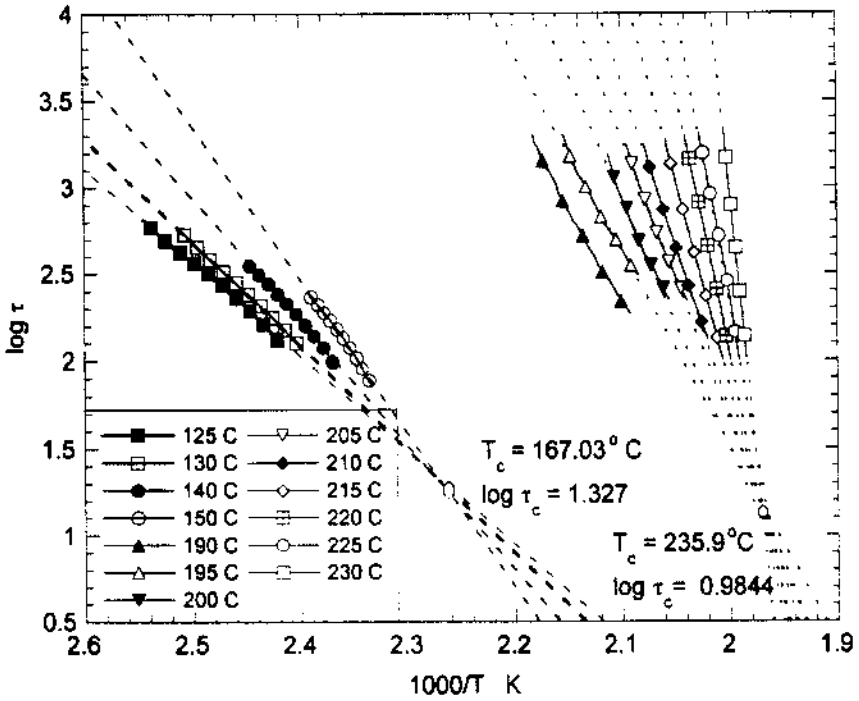

Figure 13. Arrhenius Plots of relaxation time for the amorphous TPI.

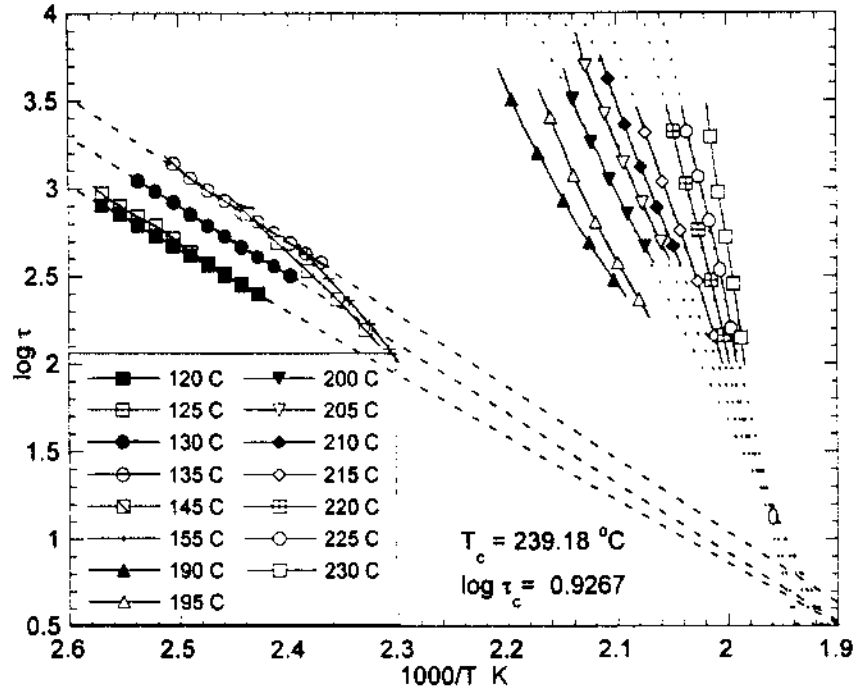

Figure 14. Arrhenius Plots of relaxation time for the semicrystalline TPI.

A plot of slope vs. intercept, Figure 15, yields the compensation points for the pertinent relaxation. The compensation coordinates τ_c and T_c obey the compensation law expressed as:

$$\tau(T) = \tau_c \exp\left(\frac{E}{k}\left[\frac{1}{T} - \frac{1}{T_c}\right]\right) \tag{7}$$

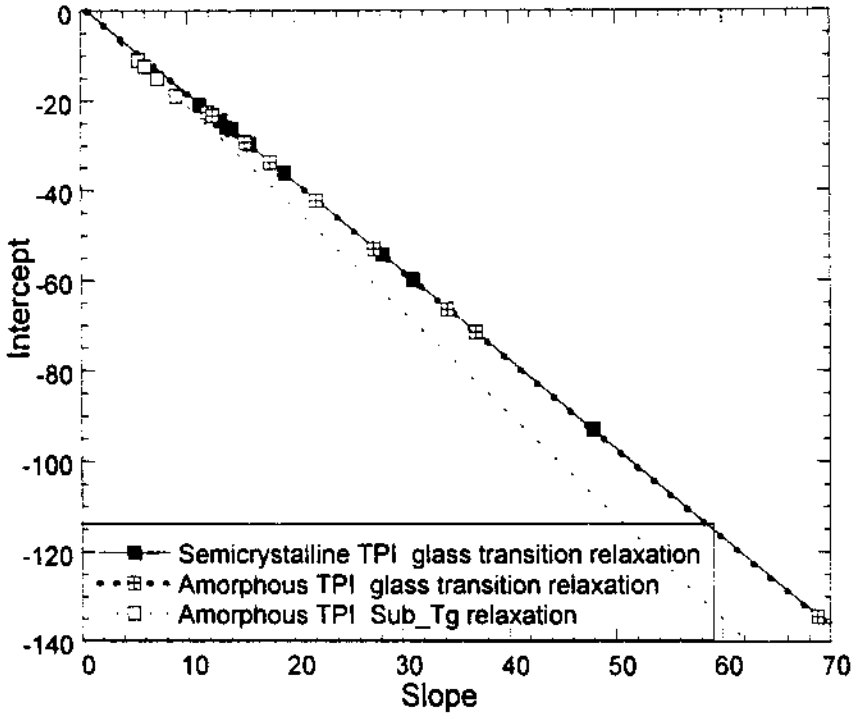

Figure 15. Compensation diagram for amorphous and semicrystalline TPIs.

The coordinates of the compensation point, namely the relaxation time (τ_c) and temperature (T_c) are the compensation time and temperature. According to the compensation law, the relaxational processes pertaining to the lines converging to the compensation point, in Figures 13 and 14, have a unique relaxation time of τ_c at T_c. The compensation temperatures (T_c) obtained for the amorphous TPI are 165 and 236°C for the sub-T_g relaxation and the α relaxation respectively. The T_c for the semicrystalline

TPI is 239°C for the α relaxation. The semicrystalline TPI does not show any compensation phenomenon for the sub-T_g relaxation. A TSD study performed by Cebe e. a. [27], on this semicrystalline TPI, before (as amorphous) and after (semicrystalline) the cold crystallization, reports two peaks below the glass transition temperature (at 159 and −13°C). Cebe e. a. attributed the −13°C peak to the electrode effects and the 159°C peak to space charge effects. From the TMDSC, and global TSD results we see a sub-T_g relaxation for both semicrystalline and amorphous TPI.

Critics of the compensation law have attributed the phenomenon to be the result of statistical propagation of error [28] rather than a material property. Tetsseydre e. a. [29, 30], therefore, used statistical analysis to determine the validity of compensation phenomena. The compensation temperature is related to the measurement temperature via its harmonic mean as:

$$T_{hm} = < T_{mi}^{-1} >^{-1} \tag{8}$$

for 95% confidence in T_c

$$T_c \cong T_c \pm \bar{t}_{N-2,0.975}\sqrt{V(T_c)} \tag{9}$$

$$V = \frac{\sum_i \left[G_i^*(T_c) - G_e^*(T_c)\right]^2}{(N-2)\sum_i \left[S_i^* - < S^* >\right]^2} \tag{10}$$

where N is the number of [H, τ_{oi}] pairs (number of windows); $\bar{t}$ is the statistical dispersion limit, V is the variance of the estimated T_c and G_e^* is the estimated value of G

at T_c. G_i^* is calculated from H and S which are given by

$$H^* = H_i - kT_{mi} \tag{11}$$

$$S^* = -k\ln(\tau_{oi}) + kT_{mi} \tag{12}$$

Table 8

Statistical Error Analysis of the Compensation Temperature for the TPIs

	G_e^* kJ/mol·K	T_{hm} Eq. (8) °C	T_c Eq. (9) °C
Amorphous TPI Sub-T_g relaxation	120.4	136	167 ± 58
Amorphous TPI T_g relaxation	141.0	210	236 ± 13
Semicrystalline TPI T_g relaxation	136.8	210	239 ± 8

The difference, $T_c - T_g$, can be viewed as the extent of restriction imposed on the relaxing species. The higher the difference, the greater the restriction. Considering the complete absence of the melting endotherm from the DSC results for amorphous TPI and the development of cold crystallization in the semicrystalline TPI, the $T_c - T_g$ difference between the two TPIs is expected to be large. The T_c - T_g values of 5.4 and 9.2 K for the amorphous and semicrystalline TPIs are significantly smaller than expected. A survey [31] of T_c - T_g values for various polymers indicates generally higher T_c - T_g for semicrystalline polymers and polymers with rigid chain structure. Some polymers have the T_c - T_g values exceeding 50 K. This is evidence for the high flexibility of the TPI chains, due to the presence of ether linkages.

Lacabanne e. a. [12, 32] reported that the slopes of the compensation diagrams for amorphous and semicrystalline PET were the same, which shows that the compensation points were unaffected by the development of crystallinity. Similar results were also reported for PEEK. Based on the model for dielectric relaxation of paraffins, by Hoffman e. a. [33], Lacabanne e. a. [12, 32] suggest that the presence of crystallites hinders the propagation of the cooperative relaxational movements resulting in smaller mobile sequences. A similar situation is observed for the α relaxation of semicrystalline TPI. The width of the distribution of enthalpy and entropy are relatively narrower for the semicrystalline TPI as compared to the amorphous TPI.

Generally β and γ relaxations involve motions of a side chain or a small portion of the main chain, usually a few carbon atoms long, and do not require cooperativity over the neighboring chains or portions of the chains, resulting in the absence of compensation phenomena for these sub-T_g relaxations. There are some cases where β and γ relaxations, exhibiting localized cooperativity, do show compensation behavior. In the amorphous TPI, the sub-T_g relaxation does show compensation phenomenon, indicating the presence of a cooperative relaxation. The width of the distribution of enthalpy and entropy for this lower temperature relaxation is greatly reduced in comparison to the α relaxation transition of both the TPIs. This is consistent with the fact that the sub-T_g relaxation involves smaller clusters than the α relaxation. The compensation coordinates for this sub-T_g relaxation are different from the α relaxation, indicating that the origins of this relaxation are different.

Using the Eyring transform from Eq. (5), the enthalpy and entropy are calculated. The Gibbs function G is subsequently calculated using Eq. (6). The enthalpy as a function of the polarization temperature is shown in Figure 16. The variation of entropy with the function H/T_m is shown in Figure 17. The variation of G as a function of the polarizing temperatures is displayed in Figure 18. It has been stated by Moura Ramos e. a. [34] that representation of the Gibbs function for activation as a function of temperature could be misleading since the variation of that function for activation does not depend on the type of chemical structure or the relaxational mechanism and the same is said to be true for the enthalpy - entropy relationships.

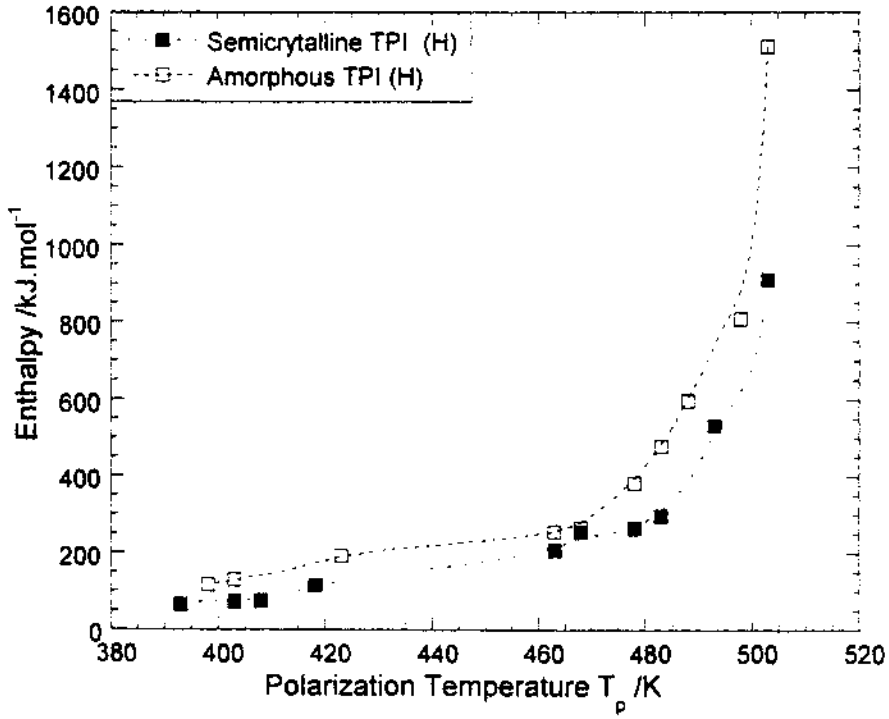

Figure 16. Enthalpy as a function of the polarization temperature calculated from the TSD analysis.

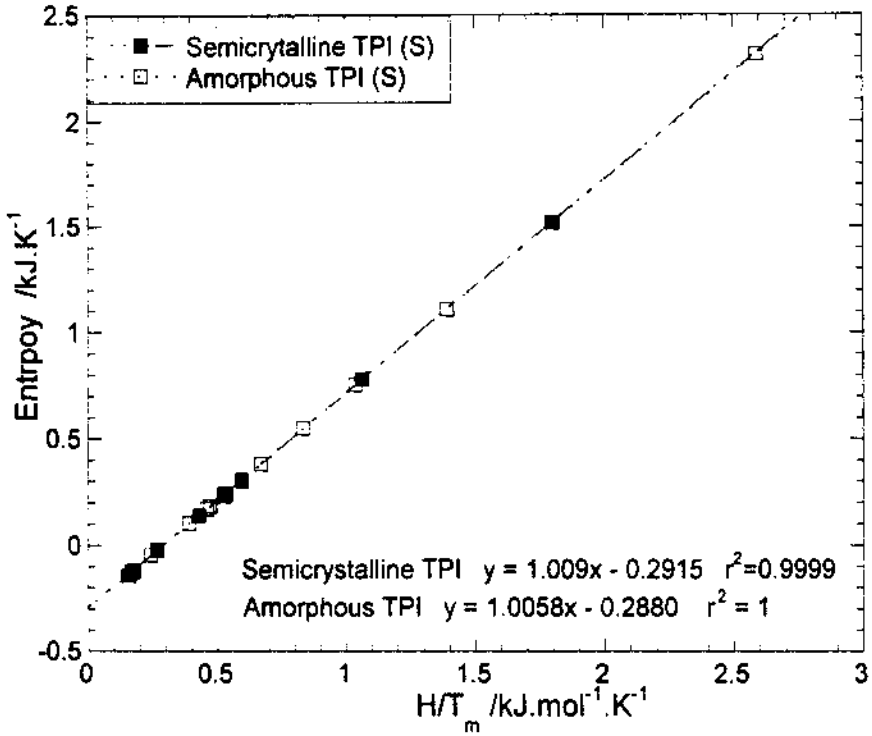

Figure 17. Enthalpy as a function of entropy for the amorphous and semicrystalline TPIs.

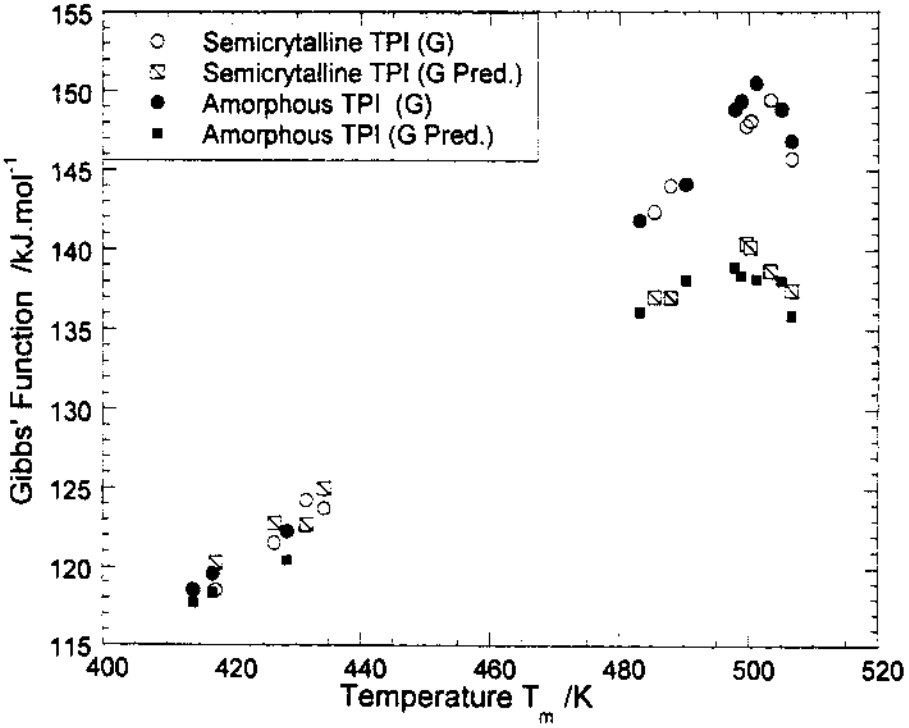

Figure 18. Gibbs function for activation for amorphous and semicrystalline TPIs.

Each thermal window experiment isolates the process corresponding to a certain relaxation time. Thus, the activation energy obtained for a thermal window experiment corresponds to the relaxation process pertaining to that window. The variation of the activation energy as a function of the polarizing temperature is shown in Figure 15. Using this function, obtained using the Arrhenius Eq. (6), from the thermal window experiments and the T_m values, the maximum frequency equivalent of the T_m is calculated as:

$$f_m = \frac{E_a r}{2\pi R T_m^2} \tag{13}$$

The $G^{\ddagger}$ is calculated as follows:

$$G_m^{\ddagger} = RT_m\left(21.922\_\ln\left[\frac{T_m}{f_m}\right]\right) \tag{14}$$

Figure 15 shows the calculated $G^{\ddagger}$ as predicted values. Tables 8 and 9 show the activation energy, and the Gibbs function obtained from the Eyring transform and the $G^{\ddagger}$ from Eq. 14 for the amorphous and semicrystalline TPIs. The magnitude of the difference between the activation energy and the $G^{\ddagger}$ shows the significance of activation entropy for the relaxational process. The magnitude of entropy indicates the extent of cooperative nature in the relaxation. As can be seen from Tables 8 and 9, the entropic effects are larger at higher temperatures. Isoentropic processes usually involve local relaxations requiring very little or no cooperation from the neighboring molecular clusters. Typically some of the β and many of the γ relaxations exhibit such relaxational

phenomena. The presence of compensation phenomenon for the amorphous TPI is evidence for the cooperativity of the sub-T_g relaxation in amorphous TPI. The narrow distribution function width and the low entropic effect show that the level of cooperativity is far less significant than observed in the α relaxation for the same TPI. In the case of semicrystalline TPI, both the TMDSC and the global TSD results show the presence of a sub-T_g relaxation in the same temperature region as in amorphous TPI. The absence of any compensation behavior suggests the lack of cooperativity. In the presence of crystallites, the propagation of any cooperative motion will be obstructed and such relaxation will be localized by the surrounding crystalline region resulting in the absence of compensation behavior.

The activation energies listed in Tables 8 and 9 show that the sub-T_g relaxation is in the range of 67 to 126 kJ/mol for the semicrystalline TPI and 100 to 168 kJ/mol for the amorphous TPI. The activation energies of the α relaxation for the TPIs are in the range of 628 to 837 kJ/mol with the amorphous TPI on the higher side of the range. Cheng and co-workers [35] showed that the thermoplastic aliphatic-aromatic polyimide PI-2 based on the monomers 3,3',4,4'-benzophenonetetracarboxylic dianhydride (BDTA) and 2,2'-dimethyl -1,3-bis(4-aminophenoxy)propane (DMDA), exhibit α, β and γ relaxations at 270, 100-170 and -80°C respectively. Their respective activation energies are reported as 420, 180 and 42 kJ/mol. Considering the all-aromatic nature of TPIs (amorphous and semicrystalline), the activation energies are expected to be higher. Many polymers including bisphenol-A polycarbonate have been reported [36, 37, 38, 39] to exhibit phenyl ring

flip with and without some degree of main chain motion. David e. a. [40] has indicated crankshaft type motions as possible β and γ relaxational mechanisms for *para* linked polyaryls. They also report activation energies in the order of 105 kJ/mol for the β-relaxation in PEEK.

The lower activation energy associated with the sub-T_g relaxation for the semicrystalline TPI is probably due to the relatively *smaller* size of the relaxing unit as compared to amorphous TPI. The absence of compensation phenomena also indicates that there is no cooperativity in the sub-T_g relaxation of semicrystalline TPI. A smaller relaxing unit such as a *para* linked phenyl ring or a pyromellitimide unit does not necessarily need cooperative neighboring units for the relaxation if the free volume available for the unit is more than the activation volume. This is the possible situation for the semicrystalline TPI. The presence of compensation phenomena and the higher activation energy suggests a relatively larger relaxing unit for the amorphous TPI.

3.6 Compensation and Cooperativity

The cooperative theory proposed by Kubát [41, 42, 43, 44, 45] has been shown to well describe the stress relaxation behavior of metals, polymers and molecular compounds. According to the theory, the relaxing unit could occupy one of the two states (relaxed and unrelaxed). When the unit is strained, it occupies the upper level of the two level system, namely the unrelaxed state. The relaxation of this unit releases phonons, which subsequently induce transition in other unrelaxed units. Such phonons clustering together will increase the probability of relaxation with increasing cluster size. Brostow e. a. [46, 47,

[48, 49] verified the assumptions and the validity of this theory through stress relaxation computer simulations. Their results, as expected, show very different stress-strain behavior for metals and polymers, but the stress relaxation between the initial and terminal plateau was found to be similar for both materials as explained by the cooperative relaxation theory of Kubát. They also validated, through their simulations, the assumption that relaxing units do consist of several particles, corresponding to molecular units or chain fragments of polymer. This is also cited as the reason for the similarity in the stress relaxation of materials of varied chemical and physical nature.

The purpose of the above discussion is to emphasize the common feature present in stress relaxation behavior and the compensation phenomena observed in biology [50], chemistry [51, 52, 53, 54], physics [55, 56, 57, 58] and in polymers [59, 60, 61, 62, 63, 64, 65, 66, 67, 68]. A compensation phenomenon is essentially the linear relationship between the entropy and enthalpy of activation for a process. For TSD, it is the linear relation between the slope and the intercept of the Arrhenius plot of log τ against the inverse of absolute temperature. A similar result is obtained for the slope vs. intercept for the plot of $\log([\tau_i/(h/kT)]$ vs. $1/T$ from Eq. (5). The lines from individual thermal window experiments converge to a point with coordinates τ_c and T_c such that they obey the compensation law, Eq. (7). The reason for the convergence is the fact that the intercept varies linearly with the slope. Thermal window experiments isolate the processes pertaining to a unique relaxation time, in terms of the cooperative theory mentioned in the previous paragraph, of a specific cluster size. The achievement of a specific cluster size

is dependent on the polarization temperature, which determines the activation energy or the enthalpy of the formation of the specific cluster size.

Hoffmann e. a. [33] assigned the compensation phenomena in paraffins to the size of the relaxing unit. Lacabanne e. a. [12, 32] suggested a similar explanation for the narrower distribution of the enthalpy and entropy for the semicrystalline PET as compared to the amorphous PET and for PEEKs of higher to lower crystallinities. The same inverse relation is observed for TPIs. The reason for the narrower distribution in all these cases is attributed to the increasing size of the relaxing unit with decreasing crystallinity. It is clear from the results of Lacabanne e. a. [12, 32], Hoffmann e. a. [33] and us, that the distribution is absent only at the higher activation energies, which is consistent with the fact that with increasing crystallinity formation of larger clusters becomes difficult.

Moura Ramos e. a. [34] reported that the Gibbs function varies linearly with temperature and is independent of the chemical nature of the polymer or the type of the relaxation studied. Interesting to notice is the fact that this is true for relaxations, which show compensation phenomena. This is not a coincidence. The cooperative relaxation theory predicts such universality for the middle slope of the relaxation, between the initial and terminal plateau regions, to follow:

(15)

where, is the initial effective stress and c is a constant reported to be 0.1. This relation has been shown to be true for metals, polymers and many other solids [69]. The

common aspect of these two universal relations is the cooperative nature of the relaxation. Despite the very different chemical nature of the species or the type of relaxation phenomena, the mechanism of the relaxation is governed by the cluster formation.

3.7 References

1. W. M. Alvino, *Plastics for Electronics: Materials, Properties and Design Applications*, McGraw-Hill, New York (1995).
2. J. Maxwell, *Plastics in High Temperature Applications*, Pergamon Press, Oxford-New York (1992).
3. D. M. Stoakley, A. K. St. Clair and R. M. Baucom, *SAMPE Quart.*, **20**, 3 (1989).
4. T. H. Hou and R. M. Reddy, *SAMPE Quart.*, **22**, 38 (1991).
5. T. L. St. Clair, K. S. Whitney and J. R. Pratt, *NASA Tech Briefs*, **Feb.**, 58 (1994).
6. A. K. St. Clair, D. M. Stoaldey and B. R. Emerson, *NASA Tech Briefs*, **Feb.**, 59 (1994).
7. W. Brostow, B. K. Kaushik, S. B. Mall and I. M. Talwar, *Polymer*, 33, 4687 (1992).
8 D. Ronarc'h, P. Audren and J. L. Moura, *J. Appl. Phys.*, **58,** 466 (1985).
9 D. Ronarc'h, P. Audren and J. L. Moura, *J. Appl. Phys.*, **58,** 474 (1985).
10. J. J. del Val, J. Colmenero and C. Lacabanne, *Solid State Commun.*, **69,** 707 (1989).
11. J. P. Ibar, *Polymer Eng. & Sci.*, **31,** 1467 (1991).
12. A. Bernes, D. Chatain and C. Lacabanne, *IEEE Trans. Electrical Insul.*, **27,** 464 (1992).
13. J. P. Ibar, A. Matthiesen, R. McIntyre and J. R. Saffell, *6th Nat. Conf. Rheol.*, Clayton (1992).

14. M. Mourgues-Martin, A. Bernes, C. Lacabanne, O. Nouvel and G. Seytre, *IEEE Trans. Electrical Insul.*, **27,** 795 (!992).

15. F. McIntyre, C. Hasson, A. Matthiesen, and J. P. Ibar, *Thermochim. Acta,* **226,** 133 (1993).

16. G. Collins and B. Long, *J. Appl. Polymer Sci.*, **53**, 587 (1994).

17. H. Shimizu, T. Kitano and K. Nakayama, *Jpn. J. Appl. Phys.*, **35,** L231 (1996).

18. N. A. D`souza, *PLC book series*, Ed.: W. Brostow, Thomson Science, London, Vol. 4, Chapter 4 (1998).

19. K. Engberg, M. Ekblad, P-E. Werner and U. W. Gedde, *Polymer Eng. and Sci.* **34,** 1346 (1994).

20. W. Brostow, T. Sterzynski and S. Triouleyre, *Polymer,* **37**, 1561 (1996).

21. L. Torre, A. Maffezzoli and J. M. Kenny *J. Appl. Polymer Sci.*, **56**, 985 (1995).

22. T. H. Hou and R. M. Reddy *SAMPE Quart.*, **22**, 38 (1991).

23. P. P. Huo, J. B. Friler and P. Cebe, *Polymer,* **34**, 4387 (1993).

24. J. B. Friler and P. Cebe, *Polymer Eng. and Sci.* **33**, 587 (1993).

25. P. Huo, P. Cebe, *Polymer*, **34**, 696 (1993).

26. S. Glasstone, K. J. Laidler and H. Eyring, *The Theory of Rate Processes*, McGraw Hill, New York (1941).

27. S. X. Lu, P. Cebe, and M. Capel, *J. Appl. Polymer Sci,* 57, 1359 (1995).

28. R. R. Krug, W. G. Hunter and R. A. Grieger, *J. Phys. Chem* **80**, 2341 (1976).

29. G. Tessèdre and C. Lacabanne, *J. Phys.D. Appl. Phys.*, **28**, 1478 (1995).

30. G. Tessèdre, P. Demont and C. Lacabanne, *J. Appl. Phys.D,* **79**, 9261 (1996).

31. C. Lacabanne, A. Lamure, G. Teyssedre, A. Bernes, M. Mourgues, *J. Non-Cryst. Solids*, **172-174**, 884 (1994).

32. A. Bernes, D. Chatain and C. Lacabanne, *Thermochim. Acta,* **204,** 69 (1992).

33. J. D. Hoffman, G. Williams and E. Passaglia, *J. Polymer Sci. C,* **14,** 173 (1966).

34. J. J. Moura Ramos, J. F. Mano and B. B. Sauer, *Polymer*, **38**, 1081 (1997).

35. S. Z. D. Cheng, T. M. Chalmers, Y. Gu. Y. Yoon, F. W. Haris, *Macromol. Chem. and Phys.*, **196**, 1439 (1995).

36. U. Natarajan and W. L. Mattice, *Macromol. Theory and Simul.*, **6**, 949 (1997).

37. M. Hutnik, A. S. Argon and U. W. Suter, *Macromol.*, **24**, 5970 (1991).

38. A. C. Lunn and I. V. Yannas, *J. Polymer Sci. Phys.*, **10**, 2189 (1972).

39. J. Schaefer, E. O. Stejskal, D. Perchak, J. Skolnick and R. Yaris, *Macromol.*, **18,** 368 (1985).

40. L. David, C.. Girard, R. Dolmazon, M. Albrand and S. Etienne, *Macromol.*, **29**, 8343 (1996).

41. L. Bohlin and J. Kubát, *J. Solid State Commun,* **20,** 211 (1976).

42. Ch. Hogfors, J. Kubát and M. Rigdahl, *Phys. Status Solidi B*, **107**, 147 (1981).

43. J. Kubat, L. A. Nilsson and W. Rychwalski, *Res Mechanica*, **5,** 309 (1982).

44. J. Kubat, *Phys. Status Solidi,* **111,** 599 (1982).

45. J. Kubat and M. Rigdahl, *Failure of Plastics*, Eds.: W. Brostow and R. D. Corneliussen, Hanser Publishers, New York, Chap. 4 (1986).

46. S. Blonski, W. Brostow and J. Kubat, *Makromol. Chem, Macromol. Symp.*, **65,** 109 (1993).

47. S. Blonski, W. Brostow and J. Kubat, *Phys. Rev. B,* **49,** 6494 (1994).

48. W. Brostow, J. Kubat and M. J. Kubat, *Mat. Res. Soc. Symp. Proc.*, **321,** 99 (1994).

49. W. Brostow, J. Kubat and M. J. Kubat, *Mechanics of Compo. Mater.*, **321,** 99 (1994).

50. G. Kemeny and B. Rosenberg, *Nature*, **243**, 400 (1973).

51. Z. Adonyl and G. Korosi, *Thermochim. Acta,* **60,** 23 (1983).

52. E. Sommer and H. J. Keuzer, *Phys. Rev. Lett.*, **49,** 61 (1982).

53. E. Sommer and H. J. Keuzer, *Surface Sci.*, **119,** L331 (1982).

54. L. Horvath, *Thermochim. Acta.* **85,** 193 (1985).

55. D. D. Eley, *J. Polymer Sci. C*, **17,** 73 (1967).

56. B. Rosenberg, B. B. Bhowmik, H. C. Harder and E. Postow, *J. Chem. Phys.*, **49,** 4108 (1968).

57. G. G. Roberts, *J. Phys. C.* **4,** 3167 (1971).

58. T. J. Coutts and N. M. Pearsall, *Appl. Phys. Lett.*, **44,** 134 (1984).

59. G. Sawa, K. Kitagawa, and M. Ieda, *Jap. J. Appl. Phys.*, **11,** 416 (1972).

60. M. Masui, H. Nagasaka and K. Yahagi, *Jap. J. Appl. Phys.*, **16,** 177 (1977).

61. J. Barandiarán, J. J. Del Val, C. Lacabanne, D. Chatain, J. Millán and G. Martínez, *J. Macromol. Sci. Phys.*, **B22**, 645 (1983).

62. J. J. del Val, A. Alegría, J. Colmenero and C. Lacabanne, *J. Appl. Phys.*, **59**, 3829 (1986).

63. J. C. Monpagens, D. Chatain and C. Lacabanne, *Electrostatics*, **3**, 87 (1977).

64. C Lacabanne, D. Chatain and J. C. Monpagens, *J. Macromol. Sci. Phys.*, **B13**, 537 (1977).

65. J. Colmenero. Alegria. J. M. Alberdi, J. J. del Val and G. Ucar, *Phys. Rev. B*, **35**, 3995 (1987).

66. J. J. del Val, A. Alegría, J. Colmenero and J. M. Barandiarán, *Polymer*, **27**, 1771 (1986).

67. C. Lacabanne, D. Chatain, J. C. Mopagens, A. Hiltner and E. Baer, *Solid State Commun.*, **27**, 1055 (1978).

68. A. Dufresne, C. Lavergne and C. Lacabanne, *Solid State Commun.*, **88**, 753 (1993).

69. J. Kubát, *Nature*, **204**, 378 (1965).

CHAPTER 4

ANALYSIS OF SEMICRYSTALLINE THERMOPLASTIC POLYIMIDE + POLYMER LIQUID CRYSTAL BLENDS

4.1 Introduction

In the previous Chapter, we characterized the differences between the semicrystalline and amorphous TPIs. Thermal stability of polyimides is better than that of typical engineering polymers (EPs). Low density, resistance to radiation and low conductivity are some of the features of the thermoplastic polyimides (TPIs) used in this analysis. Their glass transitions extend up to 250°C. Radiation resistance is supported by 100 % tensile strength retention at dosages up to 12,000 Mrads of β radiation and up to 10,000 Mrads of γ radiation. Low out-gassing in vacuum conditions, between $130 \cdot 10^{-8}$ and $130 \cdot 10^{-9}$ Torr, makes TPIs applicable for manufacturing semiconductor equipment components [1].

Semicrystalline TPIs can be modified morphologically through heat treatment to change their *degree of crystallinity*. This fact has an important consequence; namely, it provides us with the capability to control adhesion to metal substrates [2, 3]. Ishida and Huang [4, 5] have defined a molecular mechanism of the crystallization process using the Fourier transform infrared spectroscopy (FTIR). There are a number of papers on the effects of chemical structure of PI components on the crystallinity [6, 7, 8].

Similar to the development of crystallinity, blending provides another interesting avenue for the modification of properties or achieving desired properties. An interesting category of blend components is polymer liquid crystals (PLCs). Compared to *engineering plastics* (EPs), PLCs have greater mechanical strength and thermal stability, frequently lower melt viscosity, flammability and thermal expansivity. They are more stable in vacuum and resist chemical and radiational degradation [9, 10, 11]. In spite of their higher cost, numerous researchers have successfully demonstrated PLCs propensity for blending with various EPs to obtain specific end-use properties [12, 13, 14, 15, 16, 17]. Addition of a PLC to several EPs results in viscosity lowering even for 5 wt. % PLC concentration [18]. This lowering of viscosity in many instances is desirable for the reduction in processing costs.

Blends of TPIs with PLCs are also currently being reviewed for printed wiring board applications [19, 20, 21]. Tamai e. a. [22] co-reacted polyimide precursors with monomer liquid crystals (MLCs) to make PLCs with polyimide segments in their chains. Aihara and Cebe [23] investigated blends of a commercial PLC called Xydar® with a TPI by zone drawing. A large number of papers report the thermo-irreversibility of the cold crystallization of TPIs [5, 7, 8, 24, 25, 26]. In this chapter the effect of PLC on the cold crystallization of the semicrystalline TPI + PLC blends using DSC and TGA is evaluated [27]. Oxidative aging resistance of TPIs has been studied by Hinkely and Yeu [28].

4.2 Sample Preparation

The semicrystalline thermoplastic polyimide was Aurum PD 450 obtained from

Mitsui Toatsu Chemical Co./ MTC America, New York City. The semicrystalline TPI is based on pyromellitic dianhydride (PMDA) and (4,4' bis(3-aminophenoxy))biphenyl [6, 7, 23]. The polymer liquid crystal was a Zenite 7130, from E. I. du Pont de Nemours & Co., Wilmington, DE, containing 30 % glass by weight. Zenite 7130 is described by the manufacturer as a "wholly aromatic polyester". We presume it is a longitudinal PLC [9, 10, 11], that is with the LC sequences in the main chain and oriented along the chain backbone.

The semicrystalline TPI was obtained in powder form. Pellets of the dry blended TPI powder with the PLC were prepared using a Leitstritz Twin Screw Extruder with 9 temperature zones. Prior to extrusion compounding, dry blending was performed to ensure physical mixing. For the extrusion compounding the processing temperatures were as follows: the feed zone was maintained at 390 °C, the compression region at 400° C and the metering region at 410°C. The sample compositions investigated are listed in Table 1. Thin slices were cut from the pellets obtained from the extruder and used for the DSC and TGA investigations.

4.3 Differential Scanning Calorimetry (DSC)

The DSC was performed using a Perkin-Elmer DSC-7 calorimeter. A description of the DSC apparatus is provided in Section 2.1. The extruded pellets were dried for 24 hours at 100°C before testing. All the samples were heated to 410°C, which is above the melting point. Following the heating, samples were annealed for 20 minutes, subsequently cooled at 10 K/min to 30°C and then slowly heated to 400 °C at 10 K/min. Data from the first and second heating runs were analyzed.

Figures 1 and 2 show the DSC thermograms for pure components as well as blends. Figure 1 shows the first heating of the sample where as Figure 2 shows the second heat. The first heat followed by the annealing, above the melting point, removes the thermal history. The values of the glass transition, crystallization and melting temperatures so obtained are shown in Table 2. The TPI has the T_g = 240°C, while the PLC exhibits the T_g = 220°C. The results together with the absence of a melting point depression indicate that there is no thermodynamic miscibility between these two materials. Figure 3 shows the enthalpies of fusion and crystallization as a function of TPI weight fraction. The relationship is almost linear with composition, indicating that the crystalline structure is *not* affected by the presence of the PLC.

Table 1. Composition of samples examined

Name	Wt. % PLC	Wt. % PI	Wt. % Glass
0/100	0.00	100.00	0.00
10/90	7.00	90.00	3.00
20/80	17.15	77.38	5.47
30/70	22.07	68.47	9.46
40/60	29.22	58.26	12.52
50/50	35.00	50.00	15.00
70/30	50.04	28.51	21.45
80/20	56.79	18.87	24.34
90/10	63.43	9.39	27.18
100/0	70.00	0.00	30.00

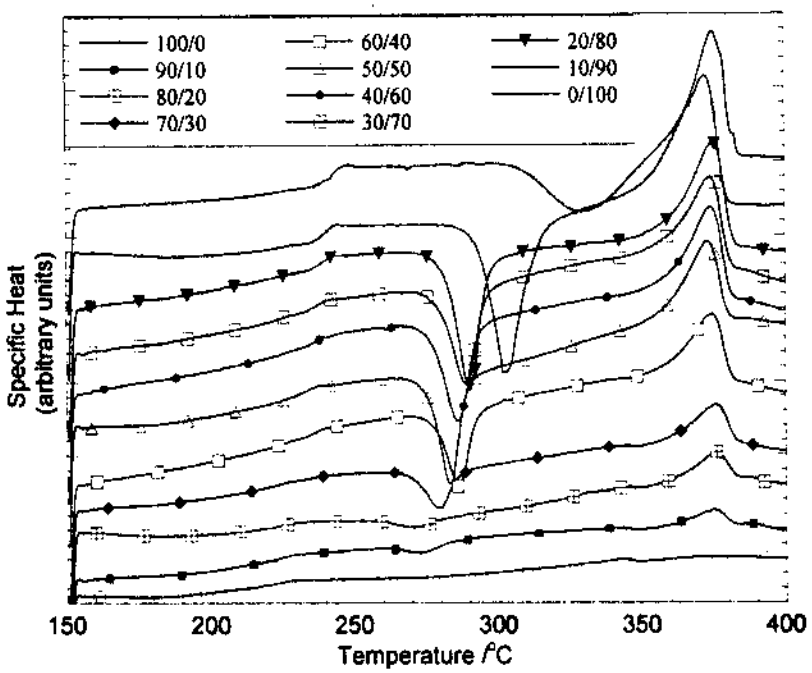

Figure 1. Heat capacities of semicrystalline thermoplastic polyimide + y polymer liquid crystal blends, from the first heating ramp.

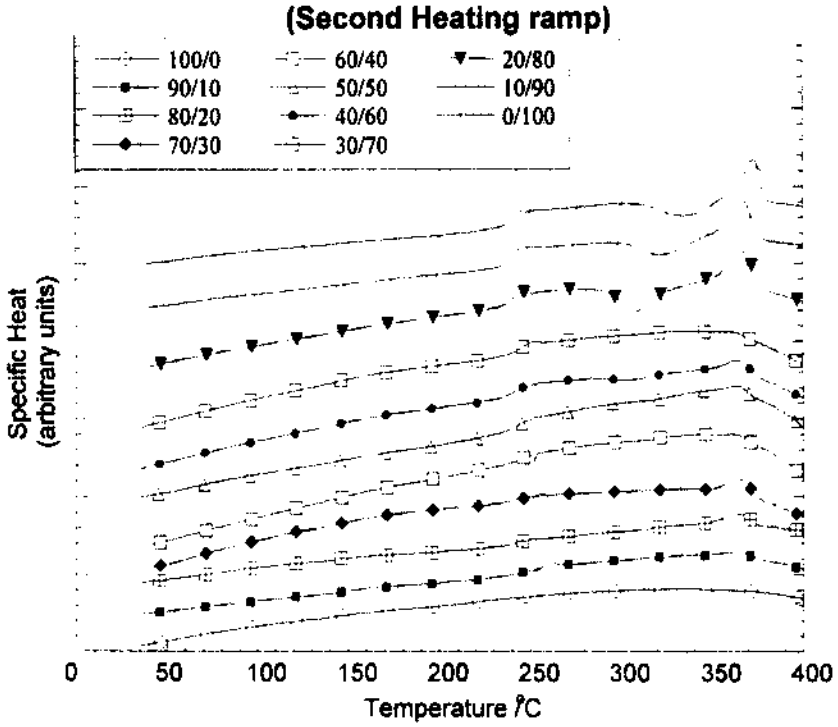

Figure 2. Heat capacities of semicrystalline thermoplastic polyimide + y polymer liquid crystal blends, from the second heating ramp.

Table 2.

Transition Temperatures of Samples Examined

Name	T_g1	T_g2	T_c1	T_c2	T_m1	T_m2
0/100	243	240	331	334	375	373
10/90	240	241	303	325	372	368
20/80	240	240	290	308	375	367
30/70	237	244	289	-	374	365
40/60	242	241	286	306	374	364
50/50	233	241	283	329	373	365
70/30	227	242	280	291	376	366
80/20	222	242	271	298	376	365
90/10	218	248	273	-	375	364
100/0	220	-	-	-	343	338

T_g1 = Glass transition from the first heat; T_g2 = Glass transition from the second heat; T_c1 = Crystallization temperature from the first heat; T_c2 = Crystallization temperature from the second heat; T_m1 = Melting point from the first heat; T_m2 = Melting point from the second heat.

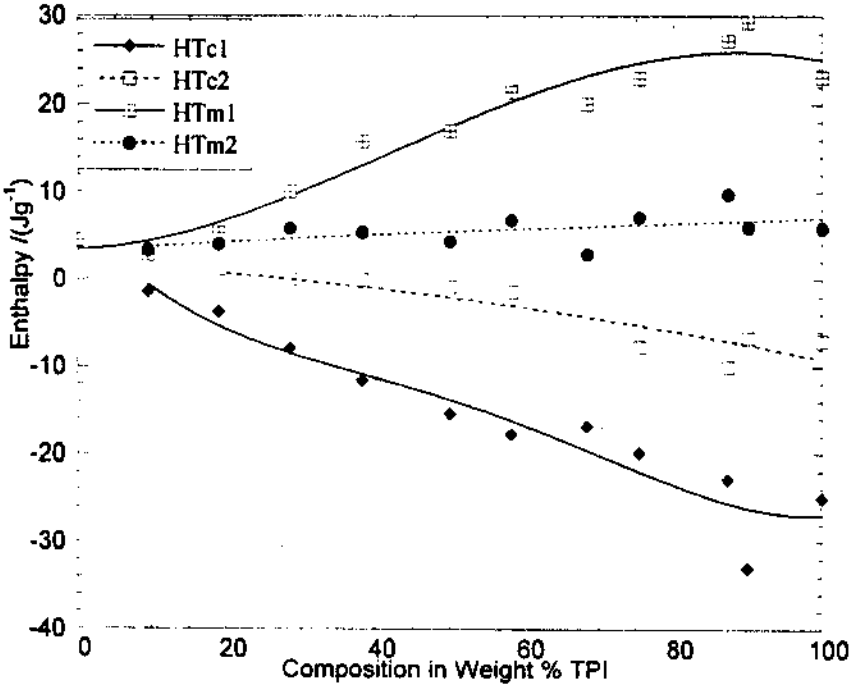

Figure 3. Enthalpies of fusion and crystallization for the semicrystalline thermoplastic polyimide + y PLC blends, HTc1 and HTc2 are respectively enthalpies of cold crystallization for the first and second heating ramps; HTm1 and HTm2 are respectively enthalpies of melting for the first and second heating ramp.

Returning to Table 2, the drop in the crystallization temperature with increased PLC presence is explained by the formation of structures with a higher degree of orientation. This explanation is based on statistical-mechanical theory of Flory [29, 30]. In a work involving an extension of this theory, Brostow e. a. [31] have found high values of the LC order parameter at fairly low PLC concentrations for ternary systems containing a solvent, a PLC and a flexible polymer. This high order parameter was explained by the orientation of the non-LC material or flexible sequences by the rigid LC sequences. In other words, the LC sequences channel the non-LC sequences into orienting between the former. This effect has been called *channeling* and also found experimentally for a different EP + PLC blend earlier [14]. The channeling occurs even at relatively low LC sequence concentrations in the aliphatic-aromatic PLC copolymers. For the present fully aromatic PLC, one expects *even more* that the rigid rods of the PLC draw the flexible sequences into alignment. This alignment should facilitate the crystal nucleation and cause a decrease in the crystallization temperature - as indeed is observed. This effect is similar to the "rigid amorphous phase" observed in semicrystalline polymers. We see in Figures 1 and 2 that the breadth of the crystallization peaks does not change significantly, indicating that for PLC concentrations greater than 20 - 30% the number of nucleating sites is *not* the determining factor.

Figure 4 shows the increase in the heat capacity, ΔC_p, at the T_g as a function of the composition of blends. This ΔC_p can be viewed as the change in restrictions imposed on the mobility of the chain [32]. The lower ΔC_p for the PLC indicates the lack of mobility and

a very broad glass transition region indicative of highly restricted mobility. This small ΔC_p is evidence for the rigid rod structure of the PLC. The ΔC_p vs. composition for the second heating ramp is smaller than that prior to the annealing. This decrease shows the additional restrictions imposed on the mobile chains as a result of the annealing.

Miscible polymer blends can be described by the Fox equation [33, 34, 35]:

$$\frac{1}{T_g} = \frac{w_1}{T_{g1}} + \frac{w_2}{T_{g2}} \quad \text{.....(1)}$$

where w and T_g are the weight fractions and glass transition temperature and the subscripts 1 and 2 correspond to the of the blend components 1 and 2 respectively.

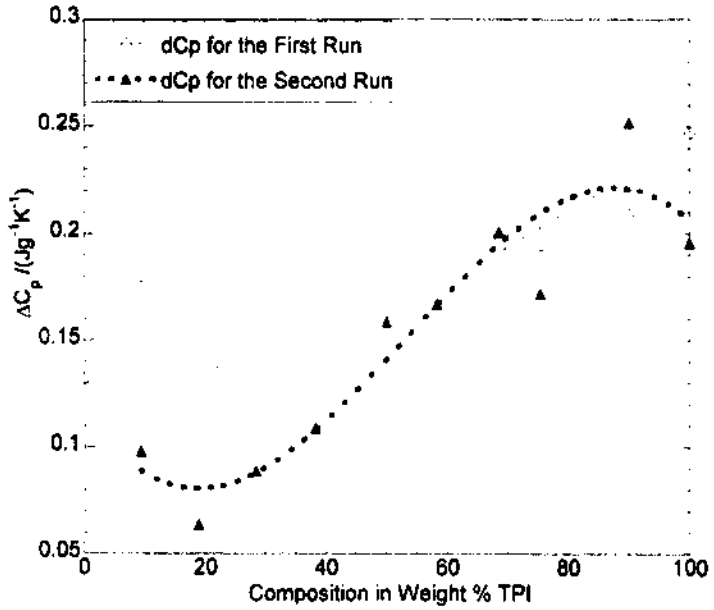

Figure 4. The increase in heat capacity at the glass transition as a function of composition for semicrystalline TPI + y PLC blends.

Eq. 1 has been effective for many miscible polymer blends where the component polymers have comparable ΔC_p at the glass transition. Couchman's equation [36]:

$$\ln(T_g) = \frac{w_1 \Delta C_{p1} \ln(T_{g1}) + w_2 \Delta C_{p2} \ln(T_{g2})}{w_1 \Delta C_{p1} + w_2 \Delta C_{p2}} \quad \text{.....(2)}$$

where w, T_g and ΔC_p are the weight fractions, glass transition temperature and the change in heat capacity at the glass transition and the subscripts 1 and 2 correspond to the blend components 1 and 2 respectively. In Eq. 2, the entropic contribution is included via ΔC_p. Evaluation of both equations and the T_g values for the blends are shown in Figure 5. Eq. 2 provides a better fit for the T_g of the blends. The T_g of the blends remains relatively unaffected up to about 50 % TPI. At higher PLC concentrations, a reduction in T_g similar to miscible blends is observed. An opposite T_g composition relation is observed upon annealing. Figure 6 shows the T_g for the second heating ramp. The T_gs remain relatively unaffected through the whole composition range. The small increase in the T_g as the PLC concentration along with the reduction in ΔC_p for the second heating ramp, is consistent with the same *channeling* phenomenon predicted [31].

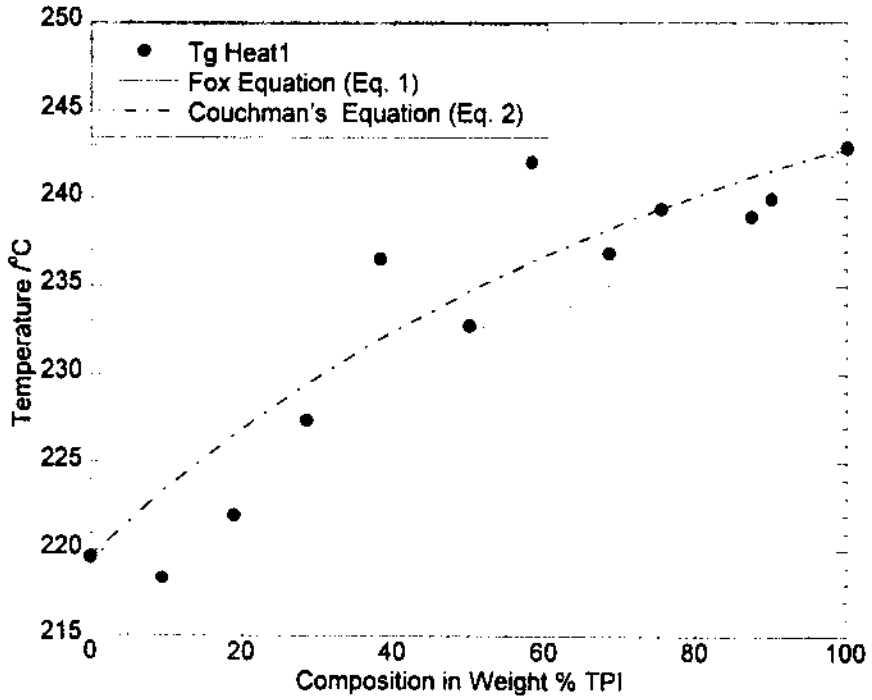

Figure 5. Glass transition temperatures from the first heating ramp as a function of composition for the semicrystalline thermoplastic polyimide blends.

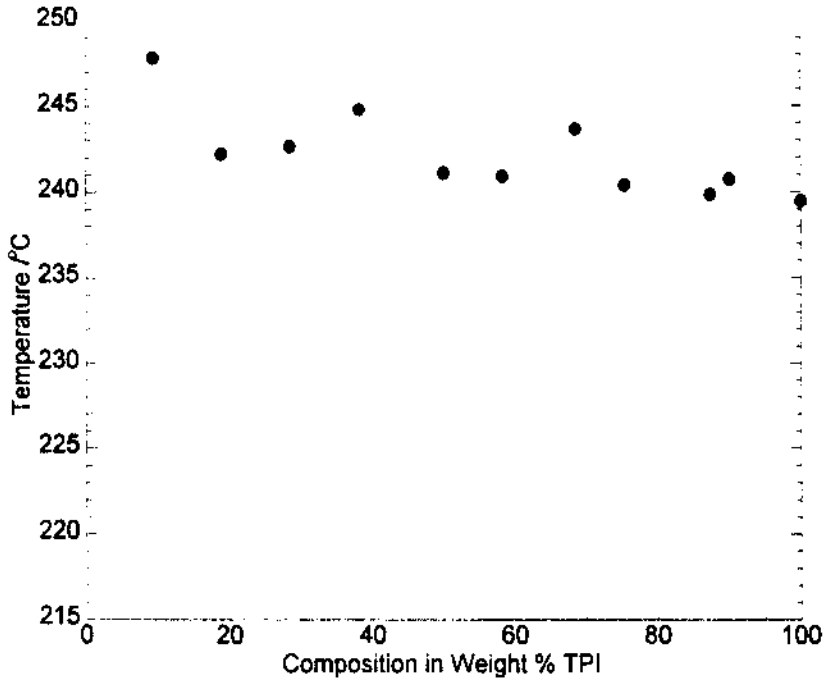

Figure 6. Glass transition temperatures from the second heating ramp as a function of composition for the semicrystalline thermoplastic polyimide blends.

4.4 Thermogravimetry

A Perkin-Elmer TGA-7 apparatus operating on a UNIX platform was used for the non-isothermal thermogravimetry of the samples under a N_2 atmosphere. A heating rate of 10 K/min was employed for all samples. Sample weight was in the range of 7.5 - 8.5 mg. Moisture effects were examined by conducting the thermogravimetry on both undried and dried samples.

Thermogravimetry (TG) curves for the blends are shown in Figures 7 and 8, respectively for the undried and dried samples. Figures 9 and 10 show the differential thermograms, of the TG curves (DTG), of the undried and dried samples. Figure 11 shows the degradation onset temperature and temperature at maximum rate of weight loss (T_{max}) of the blends. Figure 12 shows the amount of moisture loss vs. the concentration

of polyimide in the blend. Figures 7 and 8 show the residual weight fraction as a function of temperature for the blends. None of the samples degraded completely in the investigated temperature range. There was no appreciable weight loss until the onset temperature, which consistently was above 520°C for all samples. Since evaluation of the degradation process based solely on the weight loss vs. temperature curves could be misleading, the DTGs of the undried and dried samples are shown (Figures 9 and 10). The multiple peaks observed for all samples in the DTGs suggest multi-step degradation processes. The peak heights in Figures 6 and 7 also show higher rates of degradation for the PLCs than the TPI. This can be explained by better thermal stability of the imide linkages present in TPIs. The absorbed moisture did not affect the degradation process of the system; this is evident from the insignificant differences observed between the undried and dried samples.

All the samples absorbed moisture. This is reflected in the small initial weight loss in the thermograms between 50 - 300°C. This is shown in Figures 11 - 14. The amount of moisture absorbed *decreases* as the concentration of the PLC in the blend increases. This can also be explained by the presence of the ester linkages in the PLC as contrasted to the imide linkages in the TPI. The moisture *retained* in the sample was estimated by predrying all samples at 56°C for at least 48 hours under vacuum (0.8 Torr). As a result of drying, there was a decrease in the moisture weight loss, except for the 50/50 blend. The amount of *retained* moisture increased parabolically with the concentration of the PLC.

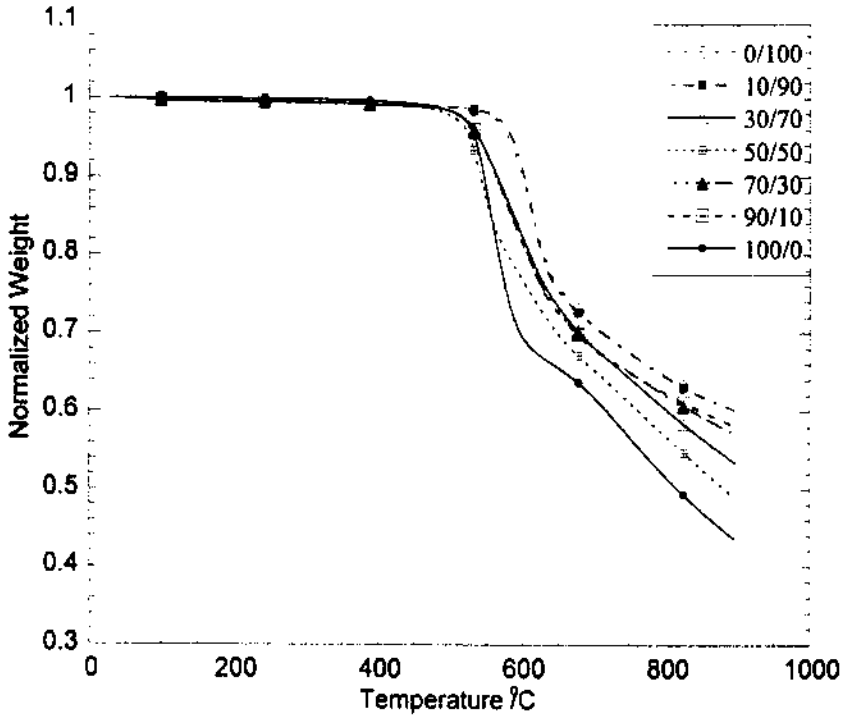

Figure 7. Weight loss as a function of temperature for the undried semicrystalline TPI + y PLC blends.

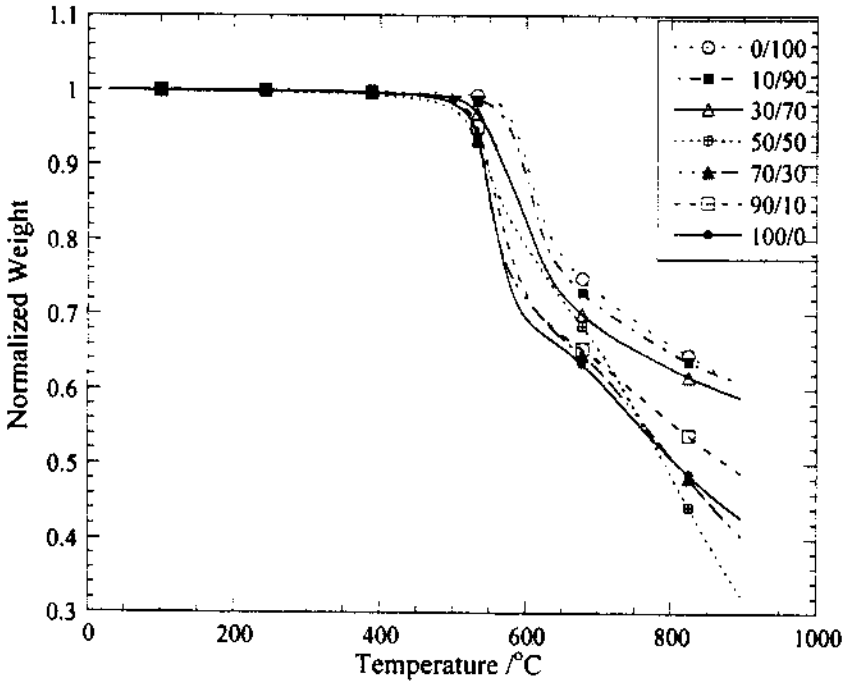

Figure 8. Weight loss as a function of temperature for the dried semicrystalline TPI + y PLC blends.

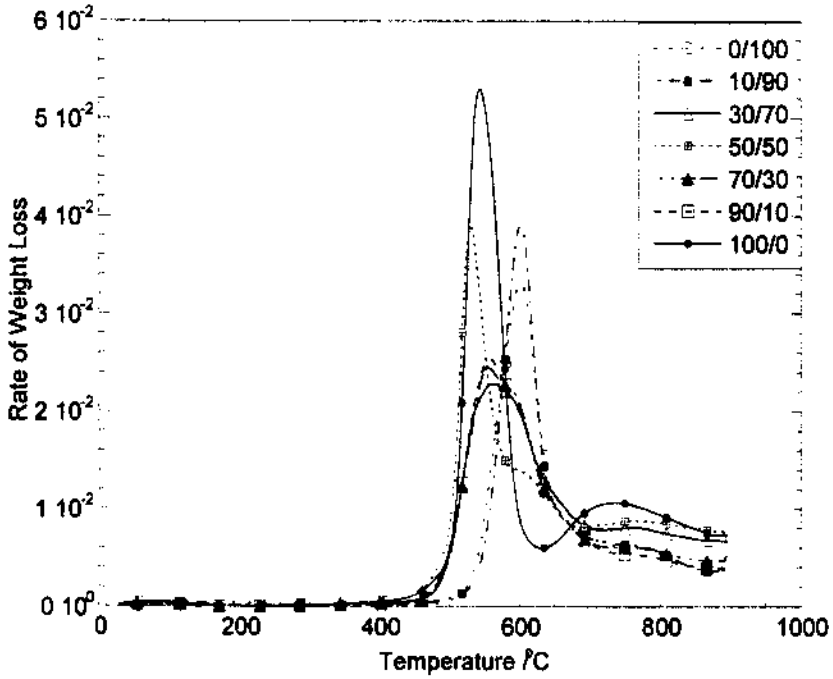

Figure 9. Rate of weight loss as a function of temperature for the undried semicrystalline TPI + y PLC blends.

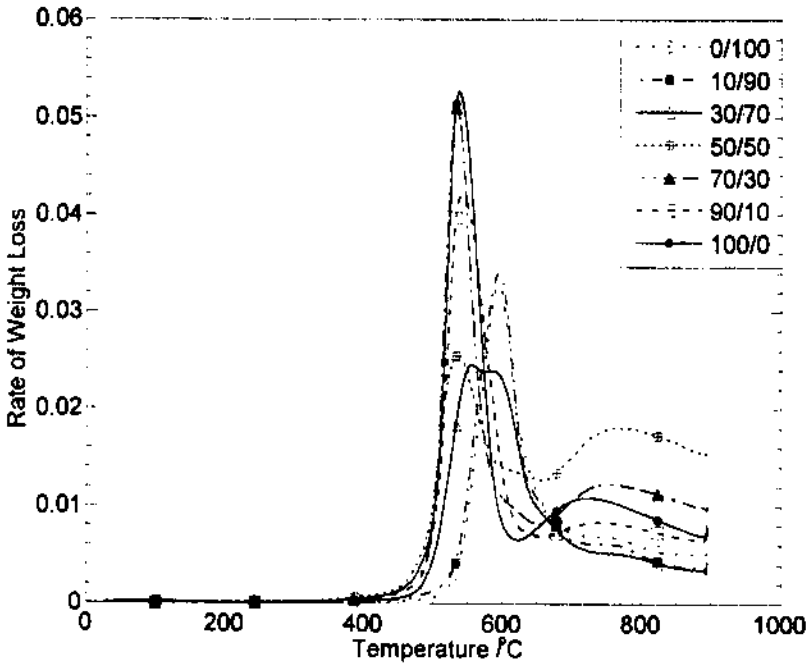

Figure 10. Rate of weight loss as a function of temperature for the dried semicrystalline TPI + y PLC blends.

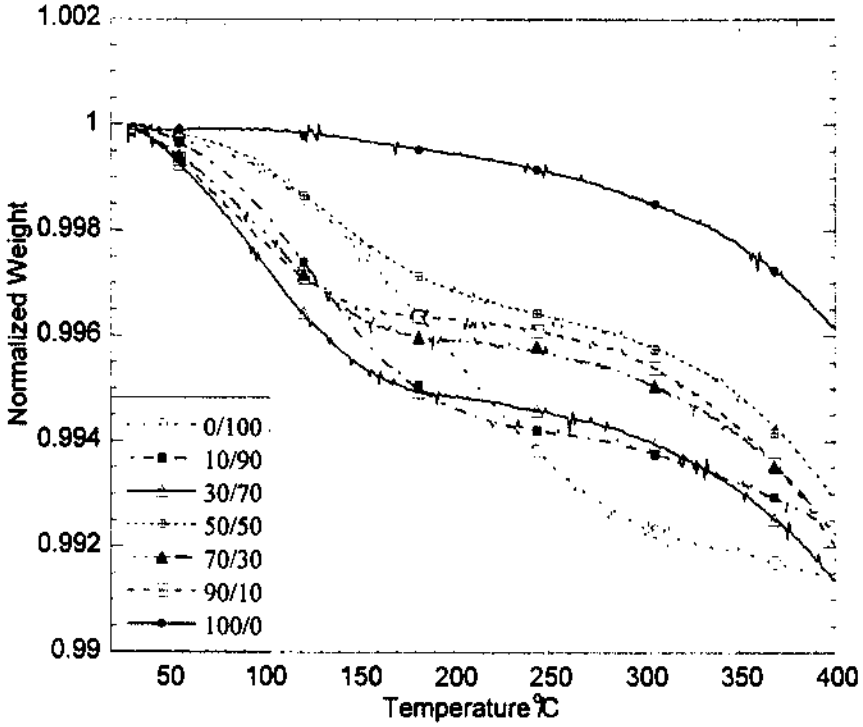

Figure 11. Moisture weight loss for the undried semicrystalline TPI + y PLC blends

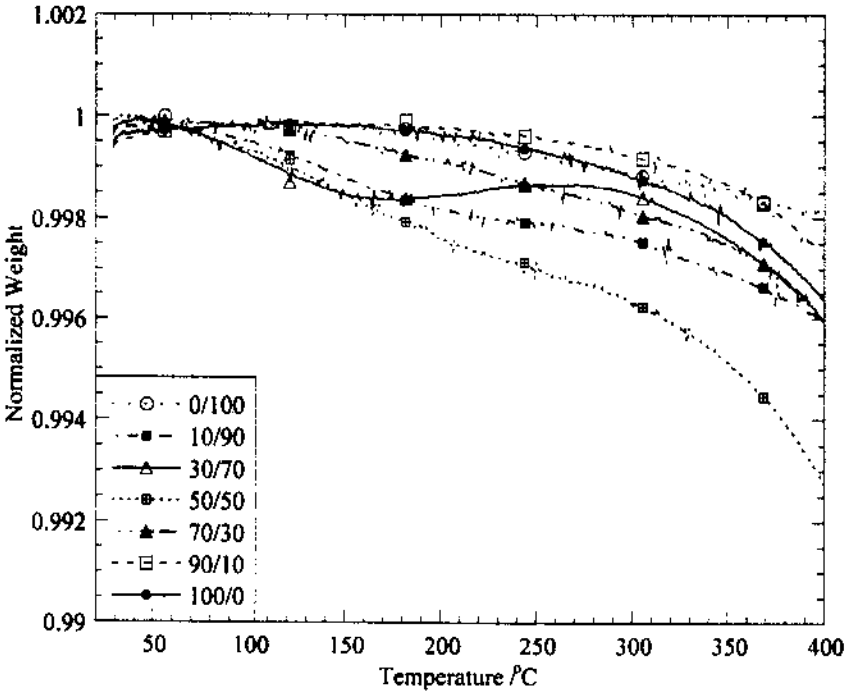

Figure 12. Moisture weight loss for the dried semicrystalline TPI + y PLC blends

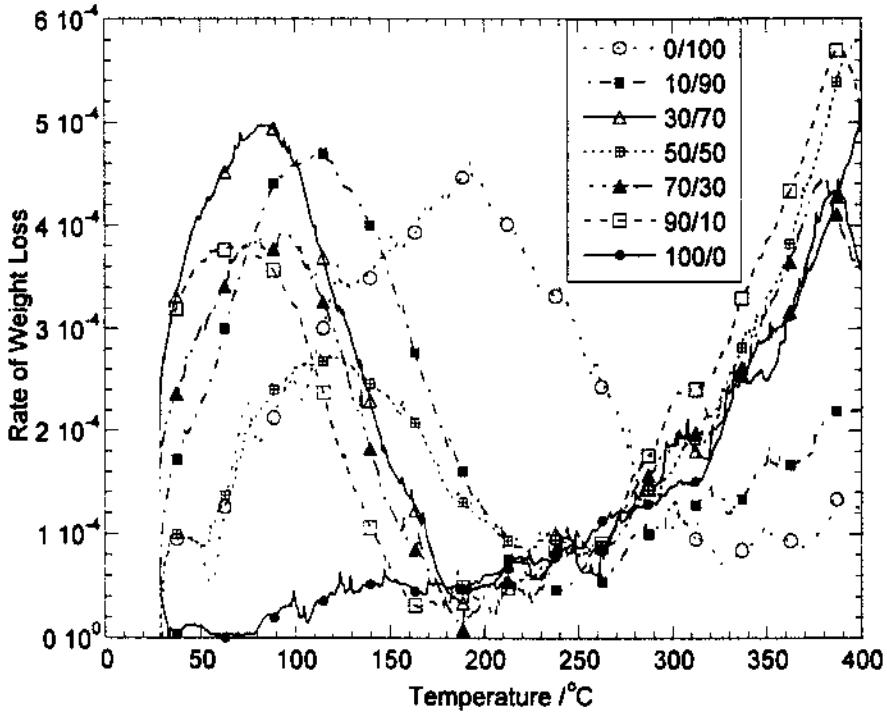

Figure 13. Rate of moisture loss as a function of temperature for the undried semicrystalline TPI + y PLC blends.

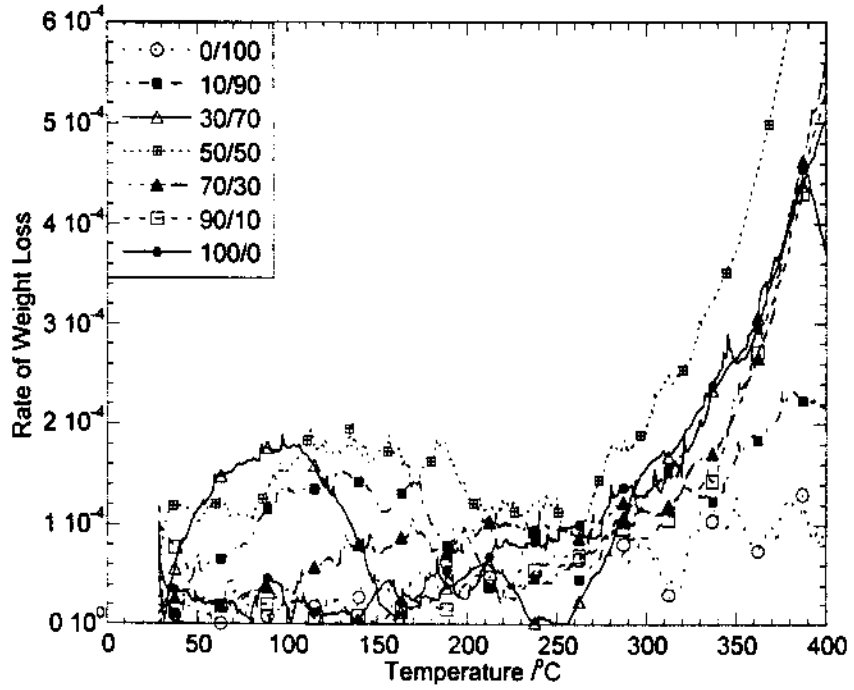

Figure 14. Rate of moisture loss as a function of temperature for the dried blends.

Figure 15 shows the trend of degradation onset temperature and the temperature at which maximum rate of degradation occurs, as a function of PI concentration in the system. Degradation onset temperature does not change appreciably until very high concentrations of the PI. Moisture does not significantly affect the degradation onset temperature. A similar trend is observed for the temperature at maximum rate of weight loss T_{max}. On the other hand, the absorbed moisture (Figure 16) does increase with the concentration of PI for the undried samples. The 50/50 sample retained more moisture than other samples after drying. In other words, the moisture absorbed in that sample was released only at temperatures higher than 150 °C.

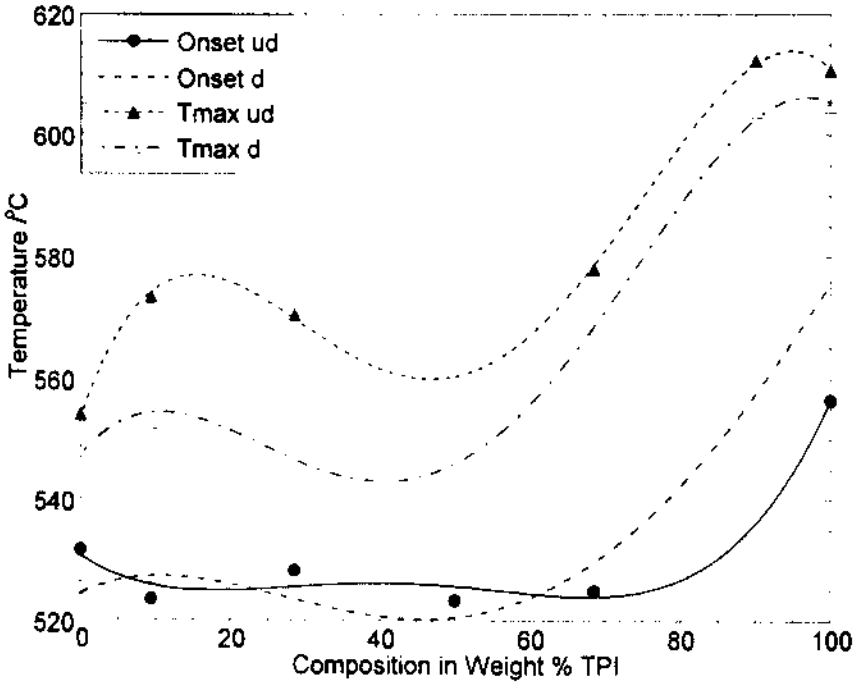

Figure 15. Degradation onset and peak temperatures as a function of composition for the semicrystalline TPI + y PLC blends.

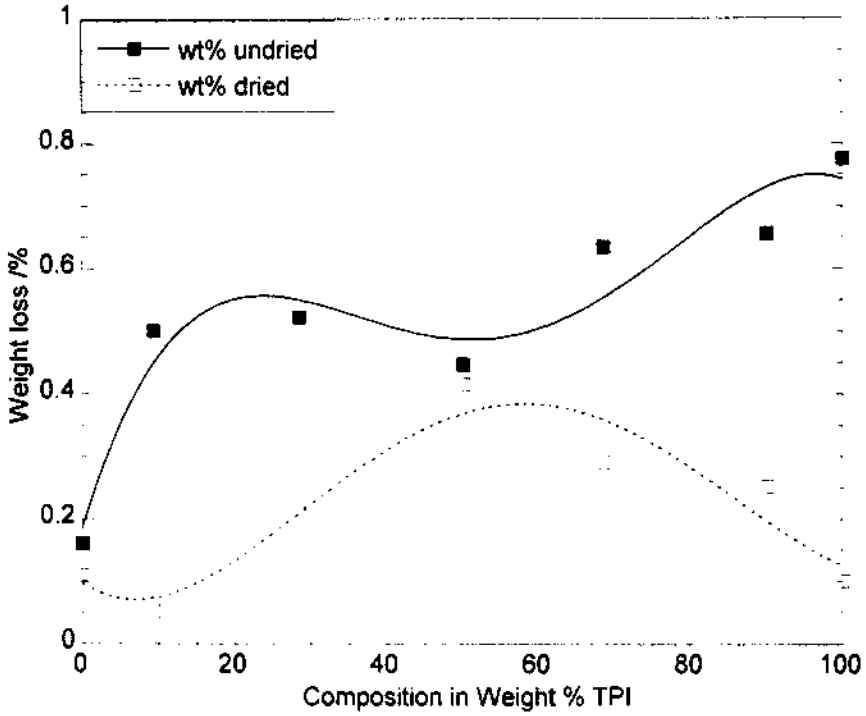

Figure 16. Moisture loss as a function of composition for the semicrystalline TPI + y PLC blends.

4.5 The Phase Diagram

The data obtained from the DSC and TGA experiments were used to construct the phase diagram shown in Figure 17. To analyze the diagram, we begin with the lowest temperature region - that is the glassy state. Variations of the T_g with the composition are negligible as seen from the second heating run (Figure 6), testifying to the lack of miscibility between the components. Above the glass transition one usually talks about the formerly amorphous fraction, of the semicrystalline TPI, becoming a liquid. However, in the presence of a PLC, this fraction results in the formation of the quasi-liquid (q-l) phase [37], with the mobility lower than that of an ordinary melt. The LC sequences constitute obstacles to the flow, as do the crystalline regions still present. At

the same time, we have the amorphous fraction of the TPI forming an ordinary melt phase, particularly at higher TPI concentrations, hence the co-existence of three phases. Phase diagrams with the co-existence of four phases inside one region have been reported [37, 17].

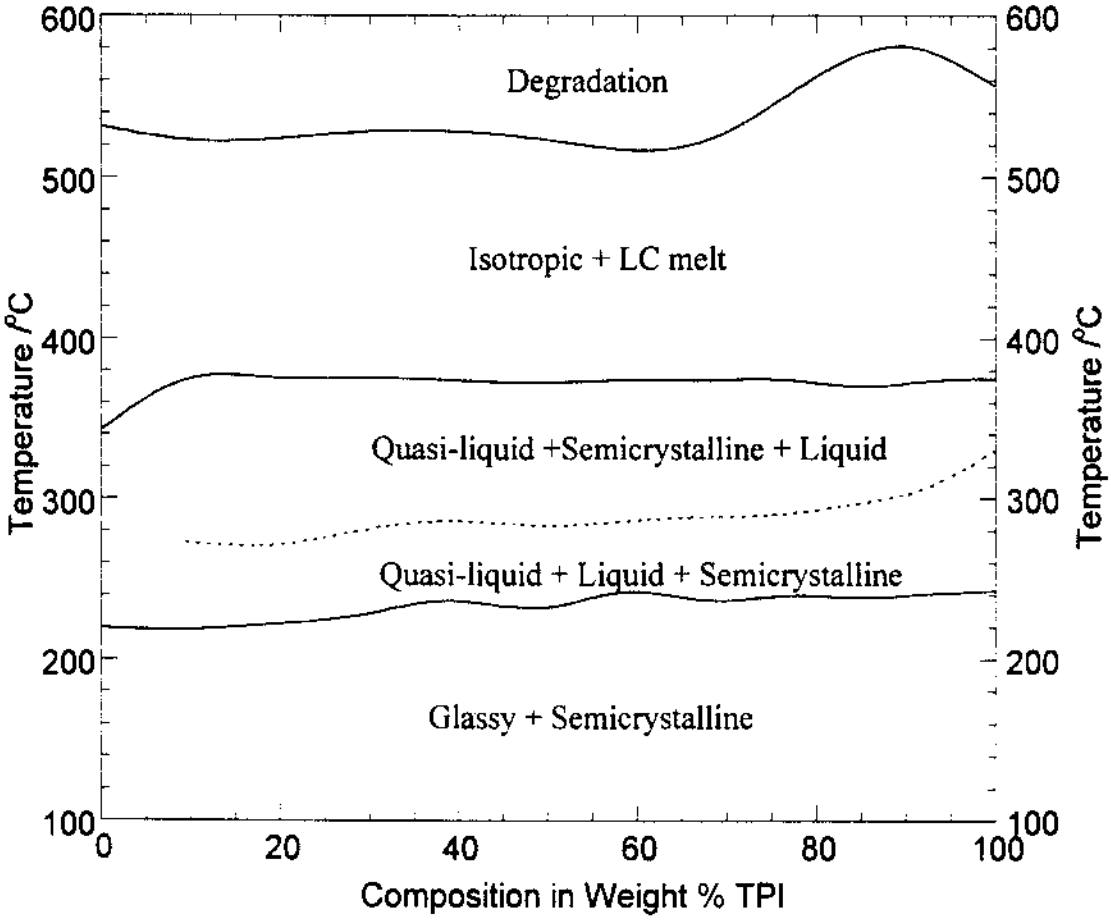

Figure 17. Phase diagram for the semicrystalline TPI + y PLC blends.

Continuing to go upward with the temperature, we have the next line around 300°C. This is not exactly a line at which a transition takes place; the line represents the maximum of cold crystallization and that process takes place also above and below the line. This line is similar to the maximum cold crystallization line in the phase diagrams

of PET/xPHB copolymers as a function of x [37]. Reasons for the cold crystallization are also similar. The quasi-liquid phase contains the formerly glassy material, which now with its increased mobility can aggregate around the LC sequences and crystallize. We have already discussed in Section 4.3, the channeling effect created by the LC sequences. Thus, the cold crystallization line does not separate the phase regions, but it runs inside a phase region. However, since the amount of crystalline phase is higher above that line, we have listed the phases present above and below the line in different order. The amount of the q-l phase will be higher on the left hand side (l.h.s.) and lower on the right hand side (r.h.s.) of the phase diagram.

The next transition is the melting line corresponding to the crystalline fraction of the TPI. Since we have one LC component, above that transition we have isotropic melt produced by TPI and at least one LC phase coming from the PLC. The evaluation of the exact type of the LC phase is made difficult by the temperature, which is of the order of 500°C. It is possible that the degradation the onset of which is represented by the top line in the diagram occurs before the full conversion of the melt to an isotropic phase particularly so in the l.h.s. of the diagram. The existence of the smectic E and smectic B phases in PET/xPHB copolymer for high x values, at temperatures some 200 K higher than the melting line, is noted [38, 37].

PLCs have hierarchical structures. According to Rule 4 of formation of such structures [39], "smaller entities (such as molecules) determine sizes, shapes and structures of larger entities (such as phases)". Understanding the hierarchical structures facilitates

property manipulation. Blending of high temperature PLCs with high temperature TPIs provides additional maneuverability.

4.6 References

1 S. Esaki, *Adv. Mater. & Proc.*, **5**, 37 (1995).

2 H. Ishida and K. Kelley, *Polymer*, **32**, 1585 (1991).

3 W. H. Tsai, F. J. Boerio and K. M. Jackson, *Langmuir*. **8**, 1443 (1992).

4 H. Ishida and M. T. Huang, *Spectrochim. Acta*, **51**, 319 (1995).

5 H. Ishida and M. T. Huang, *J. Polymer Sci., Phys.*, **32**, 2271 (1994).

6 J. B. Friler and P. Cebe, *Polymer Eng. and Sci.* **33**, 587 (1993).

7 B. S. Hsiao, B. B. Sauer and A. Biswas, *J. Polymer Sci., Phys.*, **32**, 737 (1994).

8 C. R. Gautreaux, J. R. Pratt and T. L. St. Clair, *J. Polymer Sci., Phys.*, **30**, 71 (1992).

9 W. Brostow, *Kunststoffe*, **78**, 411, (1988).

10 W. Brostow, *Polymer*, **31**, 979, (1990).

11. W. Brostow, *Physical Properties of Polymers Handbook*, Ed.: J. E. Mark, American Institute of Physics Press, Woodbury, NY, Chapter 33 (1996).

12 A. Siegmann, A. Dagan and S. Kenig, *Polymer*, **26**, 1325 (1985).

13 G. Kiss, *Polymer Eng. and Sci.*, **27**, 410, (1987).

14 W. Brostow, T.S. Dziemianowicz, J. Romanski and W. Werber, *Polymer Eng. and Sci.*, **28**, 785 (1988).

15 G. Groeninckx and G. Crevecoeur, *Polymer Eng. and Sci.*, **30**, 532 (1990).

16 K. Engberg, M. Ekblad, P-E. Werner and U. W. Gedde, *Polymer Eng. and Sci.* **34**, 1346 (1994).

17 W. Brostow, M. Hess, B. L. López and T. Sterzynski, *Polymer,* **37**, 1551 (1996).

18 W. Brostow, T. Sterzynski and S. Triouleyre, *Polymer,* **37**, 1561 (1996).

19 L. S. Rubin, K. Jayaraj and J. M. Burnett, *International Electronics Packaging Conference*, 664 (1994).

20 R. D. Jester, *SAMPE International Electronics Conference*, 428 (1992).

21 T. E. Noll, K. Blizard, K. Jayaraj and L. S. Rubin, NASA-CR-189338.

22 S. Tamai, Y. Ookawa, A. Yamaguchi, *SAMPE Internat.Conf.* (1995).

23 Y. Aihara and P. Cebe, *Polymer Eng. and Sci.*, **34**, 1275 (1993).

24 L. Torre, A. Maffezzoli and J. M. Kenny *J. Appl. Polymer Sci.*, **56**, 985 (1995).

25 T. H. Hou and R. M. Reddy *SAMPE Quart.*, **22**, 38 (1991).

26 P. P. Huo, J. B. Friler and P. Cebe, *Polymer,* **34**, 4387 (1993).

27. W. Brostow, N. A. D'Souza and B. Gopalanarayanan, *Polymer Eng. and Sci.*, **38**, 204 (1998).

28 J. A. Hinkely and J. J. Yeu, *J. Appl. Polymer Sci.*, **57**, 1539 (1995).

29 P. J. Flory, *Proc. Royal Soc.* **A 234**, 60,73 (1956).

30 P. J. Flory, *Macromol.* **11**, 1141 (1978).

31 S. Blonski, W. Brostow, D. A. Jonah and M. Hess, *Macromol.* **26**, 84 (1993).

32. V. A. Bershtein and V. M. Egorov, *Differential Scanning Calorimetry of Polymers: Physics, Chemistry, Analysis, Technology*, Ellis Horwood, New York City (1994).

33. T. G. Fox, *Bull. Am. Phys. Soc.*, **1**, 123 (1956).

34. N. A. D'Souza, Ph.D. Thesis, Texas A&M University, College Station, Texas (1994).

35. O. Olabisi, L. M. Robeson and M. T. Shaw, *Polymer-Polymer Miscibility*, Academic Press, New York City (1979).

36. P. R. Couchman, *Macromol.*, **11**, 1156 (1978)

37 W. Brostow, M. Hess and B. L. López, *Macromol.* **27**, 2262 (1994).

38 D. Y. Yoon, N. Masciocci, L. E. Depero, C. Viney and W. Parrish, *Macromol.*, **23**, 1793 (1990).

39 W. Brostow and M. Hess, *Mater. Res. Soc. Symp.*, **255**, 57 (1992).

CHAPTER 5

ANALYSIS OF AMORPHOUS THERMOPLASTIC POLYIMIDE + POLYMER LIQUID CRYSTAL BLENDS

5.1 Introduction

In Chapter 3, the characterization of semicrystalline and amorphous TPIs is presented. The DSC evaluation of the semicrystalline TPI shows that cold crystallization begins at about 300°C. In Chapter 4, we have seen that the addition of PLC reduces the cold crystallization onset temperature depending on the concentration of PLC [1]. This considerably narrows the operating temperature window. Apart from this, the development of such crystallinity is not desirable from the adhesion standpoint [2, 3].

We can see, from the results and discussions in Chapter 3, that the amorphous TPI exhibits sub-T_g relaxations just as semicrystalline TPI. These sub-T_g relaxations, by virtue of absorption and dissipation of energy improve the mechanical properties [4, 5, 6]. The cooperative nature of the sub-T_g relaxation in amorphous TPI will absorb and dissipate more energy than the semicrystalline counterpart. This is also evident from the higher activation energy reported for the sub-T_g relaxation of amorphous TPI as compared to the semicrystalline TPI. In fact, such nondestructive energy dissipation is preferred over the destructive fracture mechanisms, which comes from the "chain relaxation capability" (CRC) theory proposed by Brostow [7, 8]. For the above-mentioned reasons, we determined that amorphous TPI is better suited for applications where the

development of crystallinity in the operating temperature range is undesirable. The amorphous TPI will exhibit higher damping than the semicrystalline TPI, by virtue of stronger sub-T_g relaxation.

Another interesting result from the analysis of semicrystalline TPI + PLC blends, is that PLC concentration above 30 wt. % does not significantly change the blend properties. For this reason, our evaluation of amorphous TPI blends will be limited to 30 wt. % PLC concentrations. To obtain better homogeneity of the blend, PLC without macroscopic glass fiber reinforcement is used.

Thermal conductivity evaluation is important in determining the applicability and processing optimization of a material. The knowledge of thermal conductivity also aids in the design aspect of an end product for applications requiring heat dissipation. One of the potential applications of the TPI + PLC blends is in the microelectronics industry. During the operation of microelectronic devices, heat is generated. The potential for heat dissipation of these materials has to be evaluated.

TPIs, due to their high thermal stability, are found in many high performance applications. In many of these applications, expansivity is one of the critical property requirements. There are various methods for meeting the expansivity requirements. One of these methods is the incorporation of PLCs to control the expansivity. Tamai e. a. [9] co-reacted polyimide precursors with monomer liquid crystals (MLCs) to make PLCs with polyimide segments in their chains. Blending of PLCs offers an attractive alternative to the copolymerization route. Blends of TPIs with PLCs are also currently

being reviewed for printed wiring board applications [10, 11, 12]. Aihara and Cebe [13] investigated blends of a commercial PLC called Xydar® with the semicrystalline TPI by zone drawing. In this chapter, the blends of amorphous TPI and PLC are evaluated.

5.2 Sample Preparation

The amorphous thermoplastic polyimide was Aurum PL 500 obtained from Mitsui Toatsu Chemical Co./ MTC America, New York City. The amorphous TPI is based on pyromellitic dianhydride and (4,4' bis(3-aminophenoxy))biphenyl. The polymer liquid crystal was Zenite 7100, from E. I. du Pont de Nemours & Co., Wilmington, DE, without glass fiber reinforcement. Zenite 7100 is described by the manufacturer as a "wholly aromatic polyester". As mentioned in Section 4.2, it is presumed to be longitudinal PLC [14, 15, 16] - with the LC sequences in the main chain and oriented along the chain backbone.

The amorphous TPI was obtained in pellet form. Prior to extrusion compounding, dry blending was performed. The compounding was carried out in a Randcastle (RCP0500), ½" Single Screw Extruder with a vertical screw design. The feed zone was maintained at 310°C, the compression region at 330°C and the metering region at 350°C. The blends were pelletized using a Randcastle micropelletizer. These blend pellets were subsequently used for making films using a flexible lip die. The samples' the nomenclature is as follows: 05/95 is the blend with 05 wt. % PLC + 95 wt. % amorphous TPI, 10/90 is the blend with 10 wt. % PLC + 90 wt. % amorphous TPI and 30/70 is the blend with 30 wt. % PLC + 70 wt. % amorphous TPI. Circular sections were cut from the films using a hole punch for the DSC, TGA and thermal conductivity evaluations.

For the TMA investigations, rectangular specimens were cut from the films.

5.3 Differential Scanning Calorimetry

The DSC was performed using a Perkin-Elmer DSC-7. A description of this DSC apparatus is provided in Section 2.1. The extruded films were dried for 24 hours at 100° C prior to testing. To provide a similar thermal history for the amorphous TPI blends as the semicrystalline TPI blends, the same temperature program was used. All samples were heated to 410 °C, annealed for 20 minutes, subsequently cooled at 10 K/min to 30°C and then heated to 400 °C at 10 K/min. Data from the first and second heating runs were analyzed.

Figure 1 shows the first heating DSC thermogram of the sample, whereas Figure 2 shows the second heating ramp. The first heating and the subsequent annealing, above the T_g, remove the effect of previous thermal history. Values of the glass transition temperatures are shown in Figure 5. The TPI has the T_g = 240°C, while the PLC exhibits the T_g = 220°C. The amorphous TPI undergoes molecular reorganization similar to the cold crystallization of the semicrystalline TPI during the first heating ramp. As shown in Section 3.3, after the annealing procedure, this event disappears [17]. This behavior is not observed for the blends even at concentrations of PLC as low as 5 %. In Section 4.4, the presence of PLC reduced the crystallization temperature. This reduction was explained by *channeling* [18, 19, 20]. This phenomenon also affects the reorientation process here.

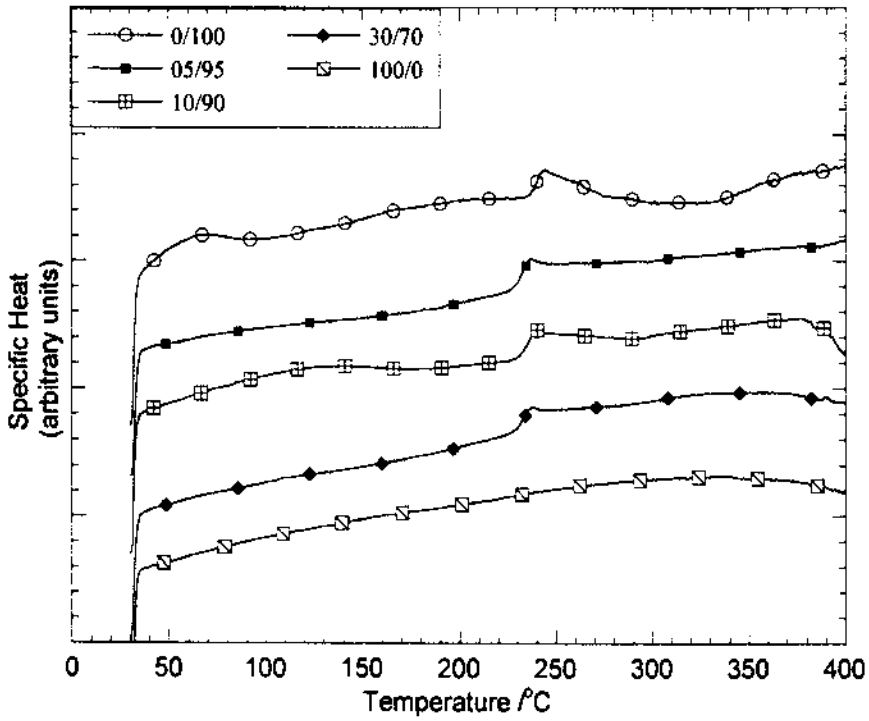

Figure 1. Heat capacities of amorphous TPI + y PLC blends, from the first heating ramp.

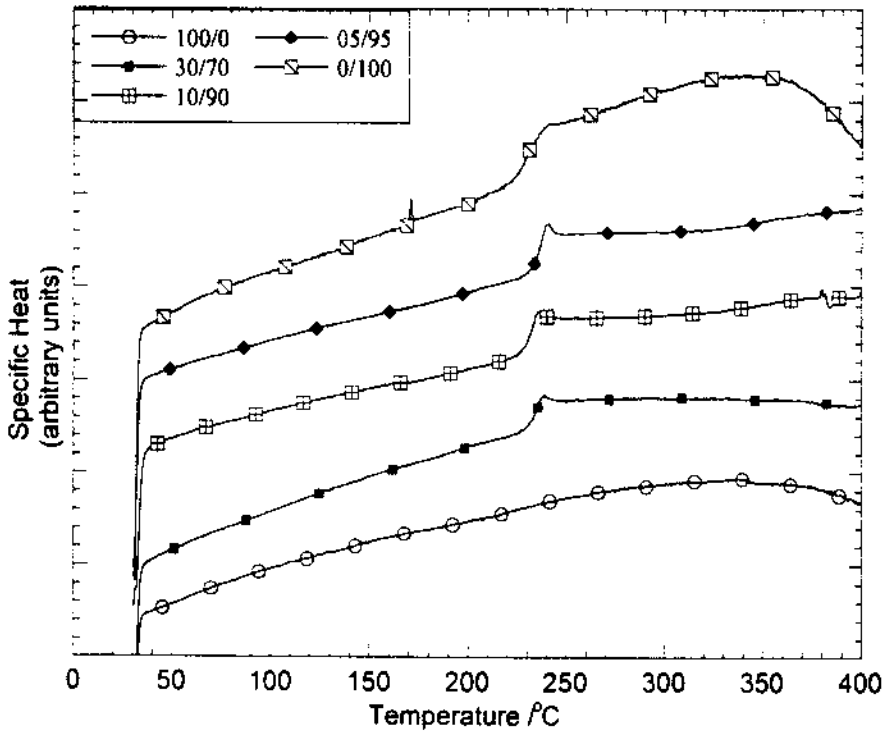

Figure 2. Heat capacities of amorphous TPI + y PLC blends, from the second heating ramp.

Figure 3 shows the change in heat capacity at the T_g as a function of composition of the blends. The change in heat capacity associated with the glass transition can be viewed as the change in restrictions imposed on the mobility of the chain [21]. The lower ΔC_p and the broad glass transition region are indicative of highly restricted mobility, which is evidence for the rigid rod structure. The ΔC_p vs. composition for the second heating ramp is smaller than the one observed prior to the annealing. This effect was also observed in the semicrystalline TPI + PLC blends. This reduction shows the additional restrictions imposed on the mobile chains as a result of the annealing. Similar to the semicrystalline TPI, the introduction of PLC significantly reduces the ΔC_p which again is a result of *channeling*. As a result of such a process the mobility of the chains become restricted, lowering ΔC_p.

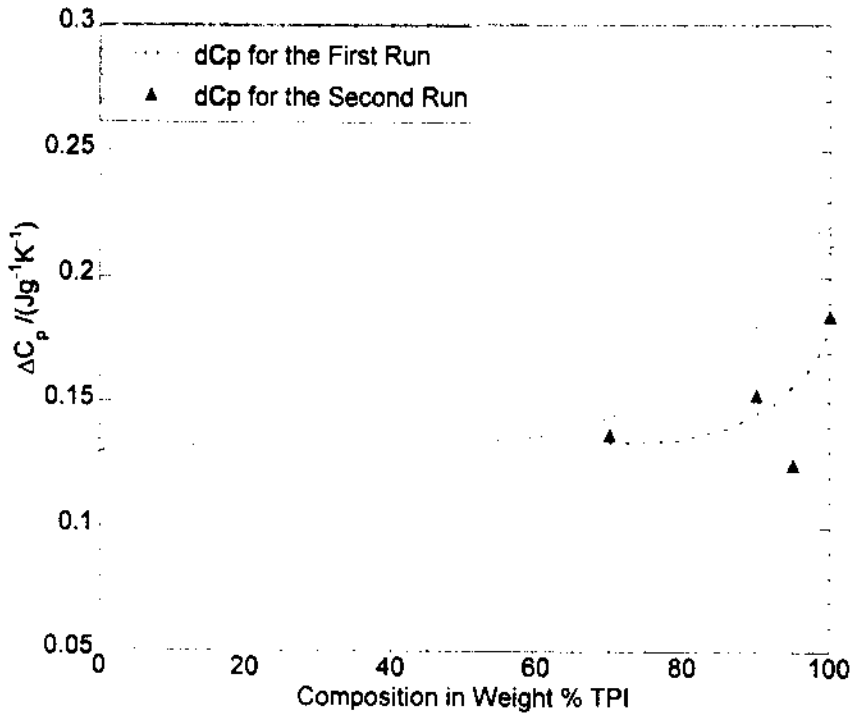

Figure 3. Heat capacity change at the T_g as a function of composition for the amorphous TPI + y PLC blends.

Miscible polymer blends can be described by the Fox Equation [22, 23, 24] :

$$\frac{1}{T_g} = \frac{w_1}{T_{g1}} + \frac{w_2}{T_{g2}} \tag{1}$$

where w and T_g are the weight fractions and glass transition temperature and the subscripts 1 and 2 correspond to the TPI and PLC respectively.

This equation has been shown to be effective for many miscible polymer blends where the component polymers have comparable ΔC_p associated with the glass transition. Couchman's equation [25] :

$$\ln(T_g) = \frac{w_1 \Delta C_{p1} \ln(T_{g1}) + w_2 \Delta C_{p2} \ln(T_{g2})}{w_1 \Delta C_{p1} + w_2 \Delta C_{p2}} \tag{2}$$

on the other hand, incorporates the entropic contribution via ΔC_p. Evaluation of both equations and the T_g of the blends are shown in Figure 4. Neither equation provides a good fit for the T_g of the blends which indicates that the PLC and the amorphous TPI do not show any thermodynamic miscibility in the composition range studied. The T_gs remain relatively unaffected by the annealing process. This indicates that the orientation, as a result of *channeling*, is thermodynamically stable. It is noted that despite such orientation, there is no development of crystallinity from the absence of a melting transition.

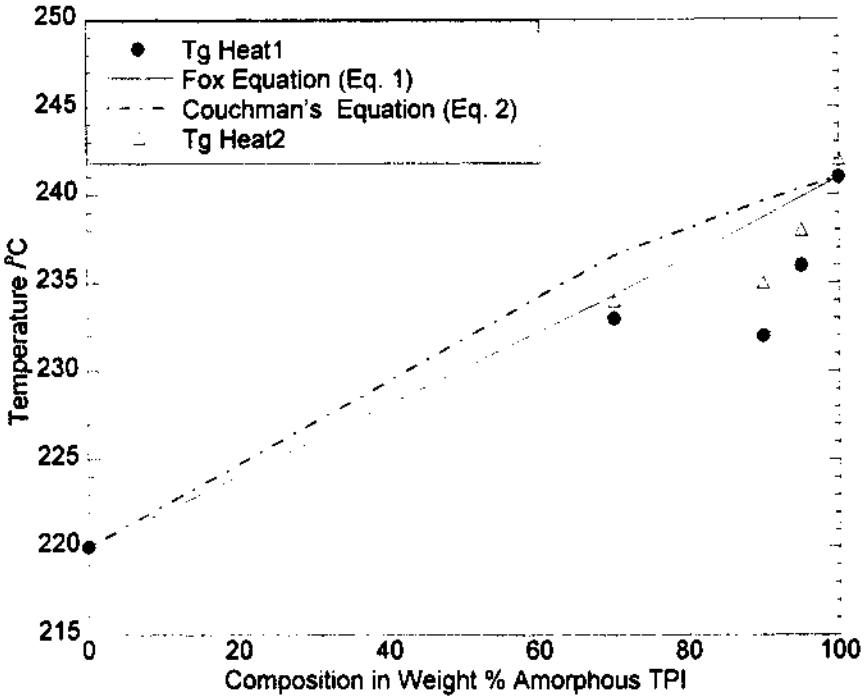

Figure 4. T_gs as a function of the composition for the amorphous TPI + y PLC blends.

5.4 Thermogravimetry

A Perkin-Elmer TGA-7 apparatus operating on a UNIX platform was used for the non-isothermal thermogravimetry of the samples under a N_2 atmosphere. A heating rate of 10 K/min was employed for all samples. Sample weight was in the range of 7.5 - 8.5 mg. Thermogravimetry (TG) curves for the blends are shown in Figure 5. The amorphous TPI blends show a higher extent of degradation than their analogous semicrystalline TPI blends, but the degradation onset does not significantly change. This high degradation onset temperature is attributed to the imide linkages. The higher extent of degradation of amorphous TPI blends, relative to the semicrystalline TPI blends, is due to the lack of crystalline regions.

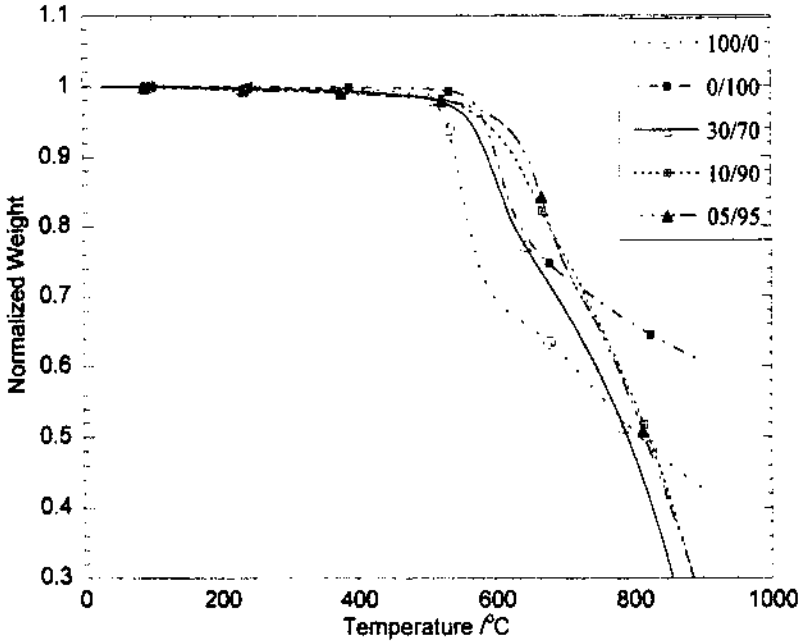

Figure 5. Weight loss as a function of composition for the amorphous TPI + y PLC blends.

5.5 Thermal Conductivity

A Perkin-Elmer DSC-7 was used. The experimental setup is shown in Figure 6. Two identical pieces (of known geometry) were cut from the extruded film for each sample. The planarity of the sample surfaces was ensured. One piece was placed in the reference pan and the other was placed in the sample pan. An aluminum disk, of 0.1 mm, with the premelted indium was placed on the specimen in the sample pan and an empty aluminum disk was placed on the sample in the reference pan. The endothermic Indium melting peak was obtained. For all thermal conductivity measurements, a heating rate of 10 K/min was utilized. Samples of various thicknesses were evaluated. This method, known as the standard melting method, is shown to be within 10% of the thermal conductivity measured by traditional steady state methods [21,26].

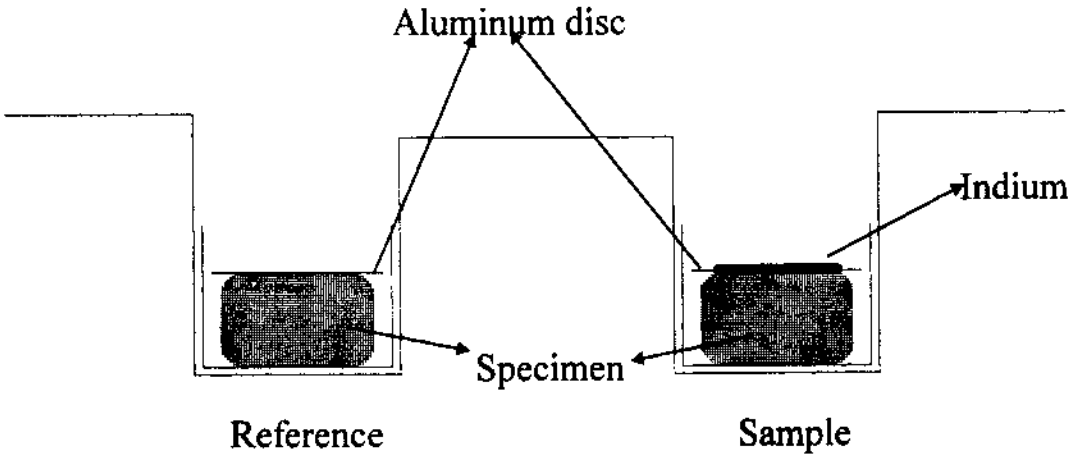

Figure 6. Experimental setup for the thermal conductivity measurement.

Figures 7 - 9 show the endothermic Indium melting peaks for samples of increasing thickness. As the thickness of the sample increases, the front slope of the melting endotherm decreases. Figure 10 shows the increase in cotangent of the slope angle (inverse of the slope). This increase corresponds to the fact that the thermal resistance increases due to the presence of an insulating material, such as a polymer, between the DSC furnace and Indium. Thermal conductivity is calculated as [21, 26,27] :

$$\lambda = \frac{x}{\left[\left(\cos\varphi - \cos\varphi_0\right) * A\right]} \tag{3}$$

where, x is the thickness of the sample, A is the surface area of the sample in contact with the aluminum disk and cot φ is the thermal resistance measured as the inverse of the front slope of the Indium melting endotherm.

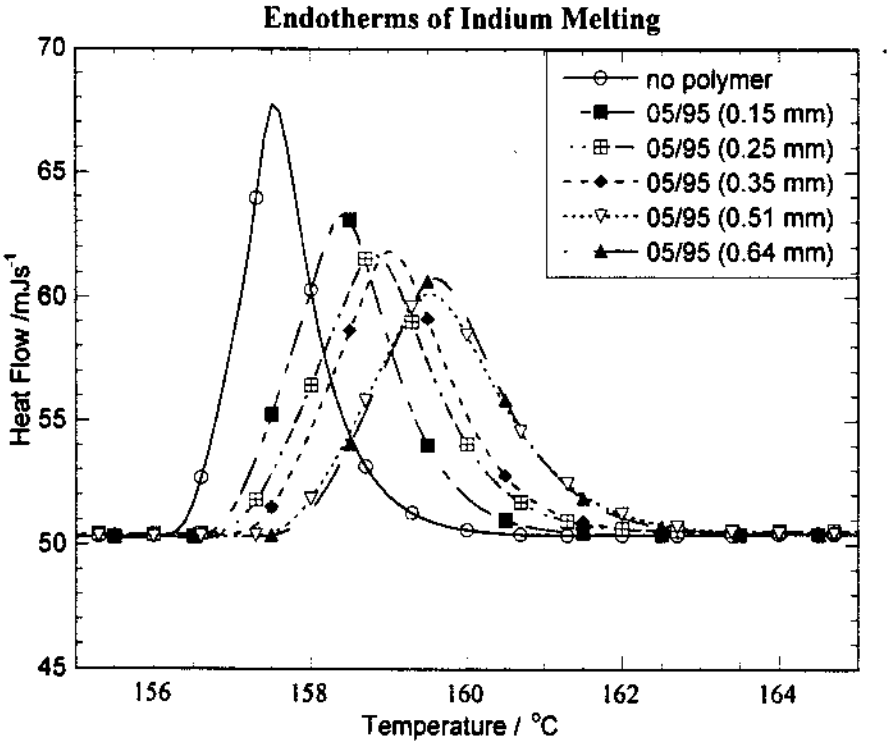

Figure 7. Indium fusion endotherm for the blend 9505.

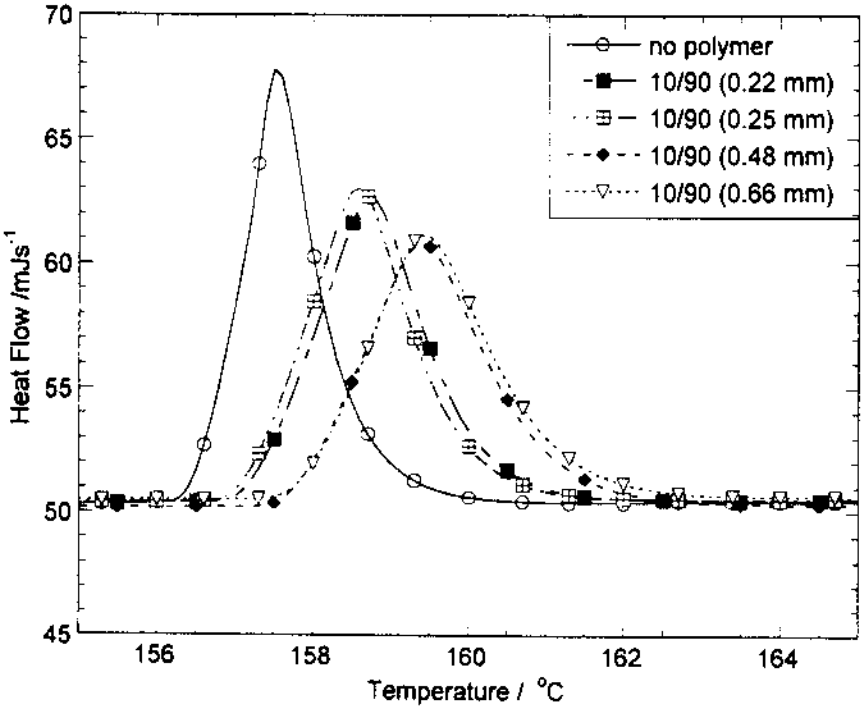

Figure 8. Indium fusion endotherm for the blend 9010.

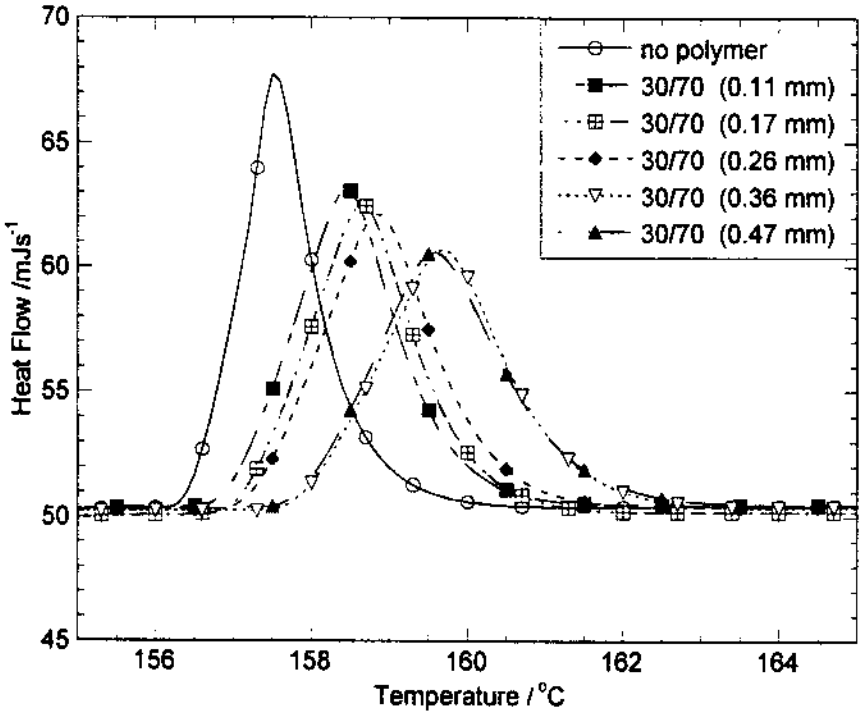

Figure 9. Indium fusion endotherm for the blend 7030.

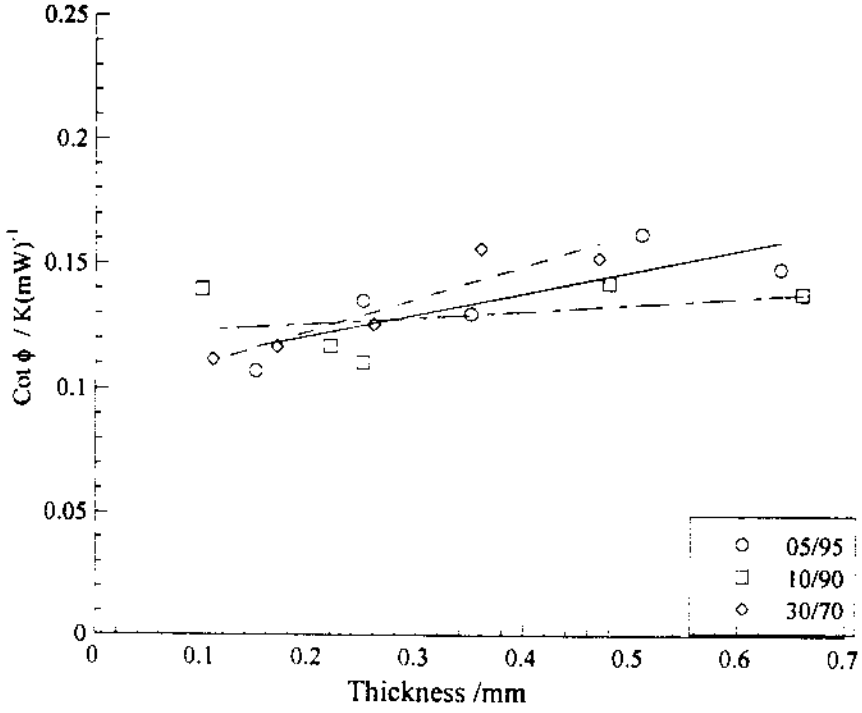

Figure 10. Cotangent of the front slope of indium melting endotherm.

Figure 11 shows the thermal conductivity of the blends as a function of PLC concentration. Thermal conductivity of the blends decreases with the increasing concentration of the PLC. The low thermal conductivity of the TPI is attributed to its complex chemical structure. Many polymers have been shown to exhibit anisotropy in thermal conductivity in directions parallel and perpendicular to the orientation direction[28]. This is true for even amorphous polymers such as poly(methyl methacrylate) and polystyrene [29, 30].

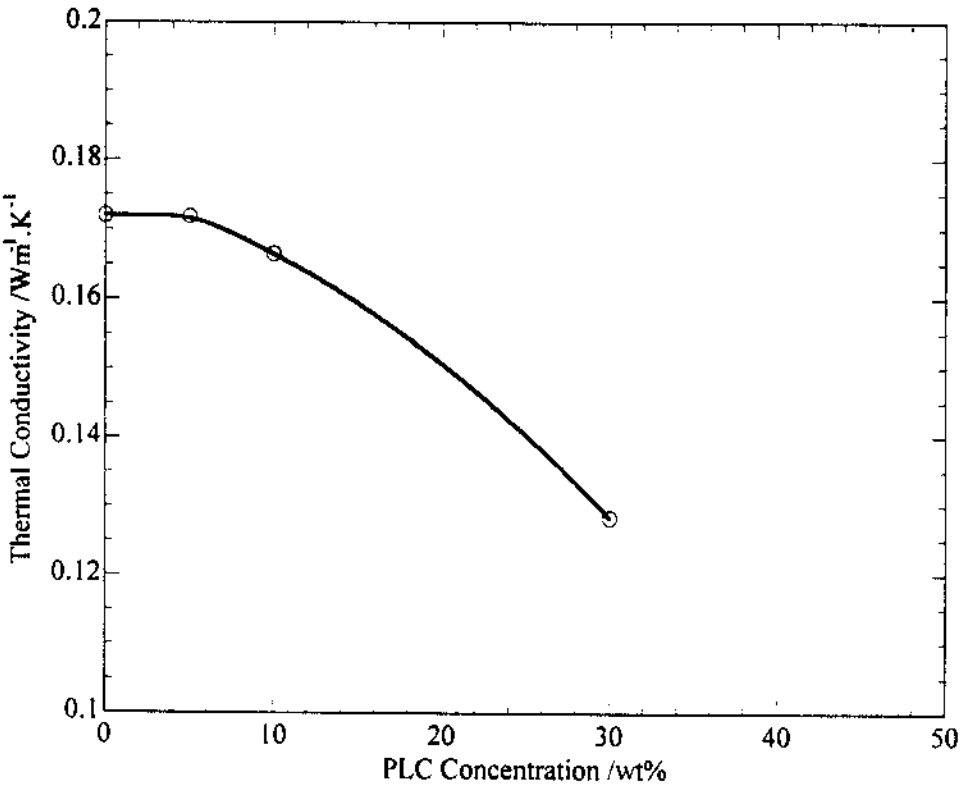

Figure 11. Thermal conductivity of the blends as a function of PLC concentration.

Thermal conductivity, like most other thermal properties, is determined by the phonon interaction in the material. As a result of development of orientation, the mean

free path for phonons parallel to the direction of orientation is larger than for that in the perpendicular direction. In the transverse direction phonons encounter more scattering centers by virtue of the orientation of the polymer chains. Therefore, the thermal conductivity in the transverse direction is smaller than that in longitudinal direction.

For amorphous polymers typically the ratio of the thermal conductivities parallel to and perpendicular to the orientation direction, the anisotropy coefficient, does not exceed 2 even at high orientations. On the other hand, for semicrystalline polymers this anisotropy coefficient can be as high as 50 [31], while values of $3 \cdot 10^3$ are even reported for polyethylene (PE) [32] at very high draw ratios. The reason for this high anisotropy is the orientation of the crystallites in the drawing direction. PE's simple chemical structure is reported to be the reason for such high anisotropy. Despite their complex chemical structure, many PLCs also exhibit strong anisotropy in thermal conductivity [33]. PLCs do not show much sensitivity to the draw ratio. This insensitivity can be explained by the achievement of high orientations by virtue of their rigid rod components. The PLC used in our studies is said to be rigid rod in nature, which was substantiated by the small ΔC_p from the DSC characterization, and is expected to be even less sensitive to the draw ratio. As discussed in Section 4.3 and 5.3, the *channeling* phenomenon, induces orientation of the TPI, thereby resulting in macroscopic orientation of the polymer chains. This orientation will cause anisotropy in thermal conductivity. The thermal conductivity reported here pertains to the transverse to orientation direction.

5.6 Thermal Expansivity

A Perkin Elmer TMA -7 apparatus was used for thermomechanical evaluation. A description is provided in Section 2.5. Thermomechanical testing was performed on the rectangular samples obtained from the films of the three TPI + PLC blends. TMA of the TPIs and PLCs was performed on the samples made from the pellets. The temperature range studied was from 30°C to 250°C at a 5 K/min heating rate.

Thermomechanical analysis of the amorphous TPI + PLC blends was performed in three directions with respect to the PLC orientation, as shown in Figure 12. The directions D1 and D3 are perpendicular to the orientation direction and D2 is along the orientation direction. Thermal expansion of the amorphous TPI is shown in Figure 13.

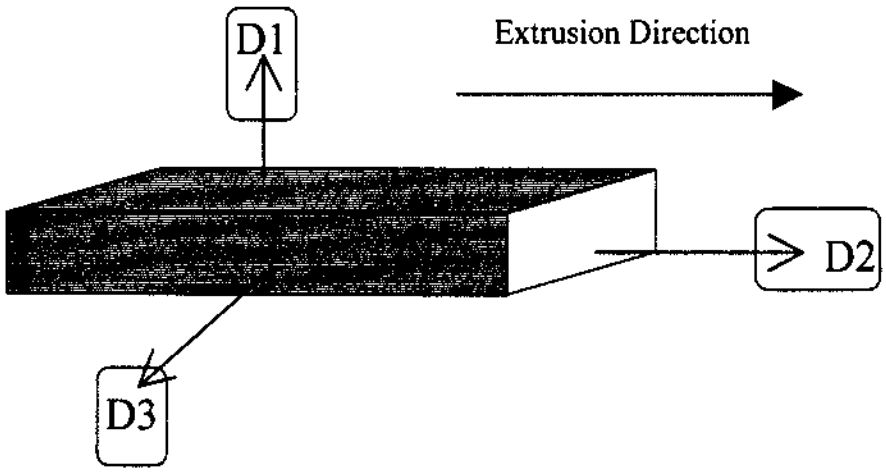

Figure 12. Thermal expansivity measurement directions.

The amorphous TPI does not show any anisotropy. The semicrystalline TPI does indicate slight anisotropy in the extrusion direction shown in Figure 14. This is a result of the crystalline orientation development due to the extrusion process. The PLC shows strong

anisotropy (Figure 15) in the orientation direction , D2, as expected. Figures 16 - 18 show the thermal expansion for the three blends. It can be seen from the figures that even an addition of 5 % PLC results in a development of anisotropy. The anisotropy is magnified with increasing concentration of the PLC. The expansivities for the D1, D2 and D3 directions are shown in Figures 19 - 21, respectively. It can be seen from the figures that the expansivity does not vary linearly with temperature. Thus, the conventional representation of expansivity over a temperature range could be misleading.

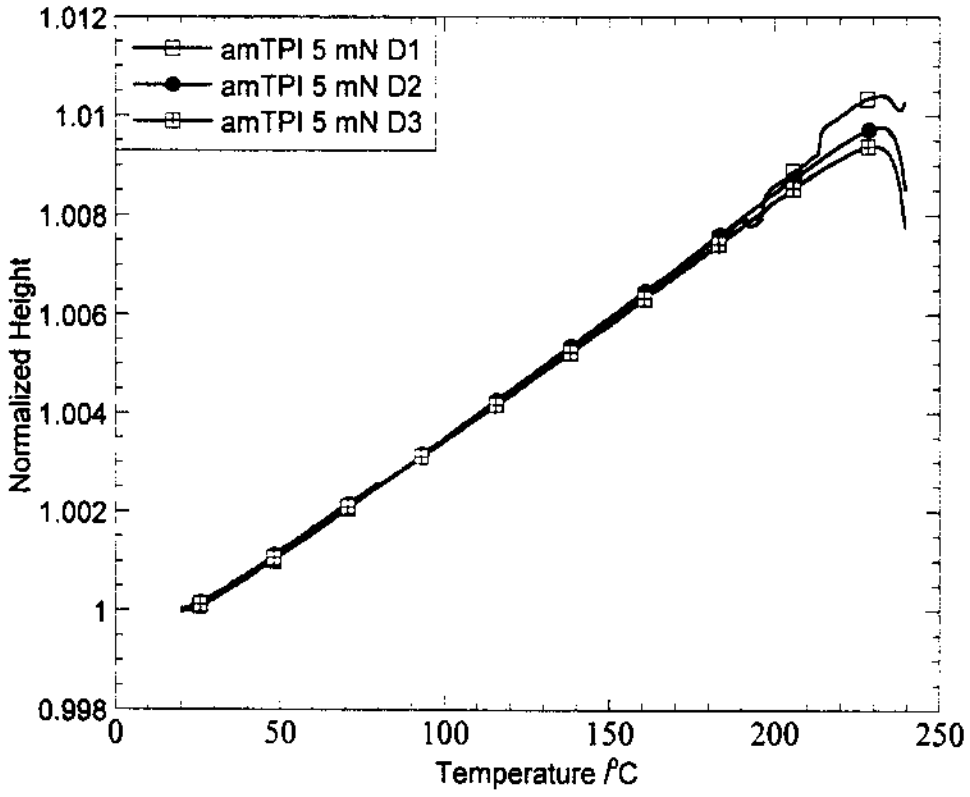

Figure 13. Thermal expansion of the amorphous TPI.

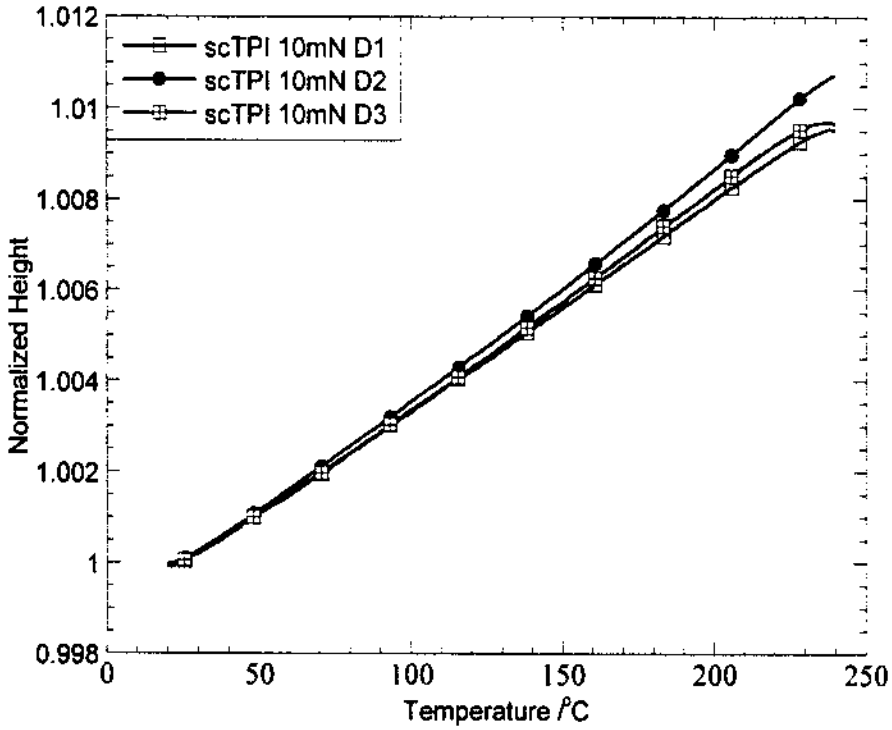

Figure 14. Thermal expansion of the semicrystalline TPI.

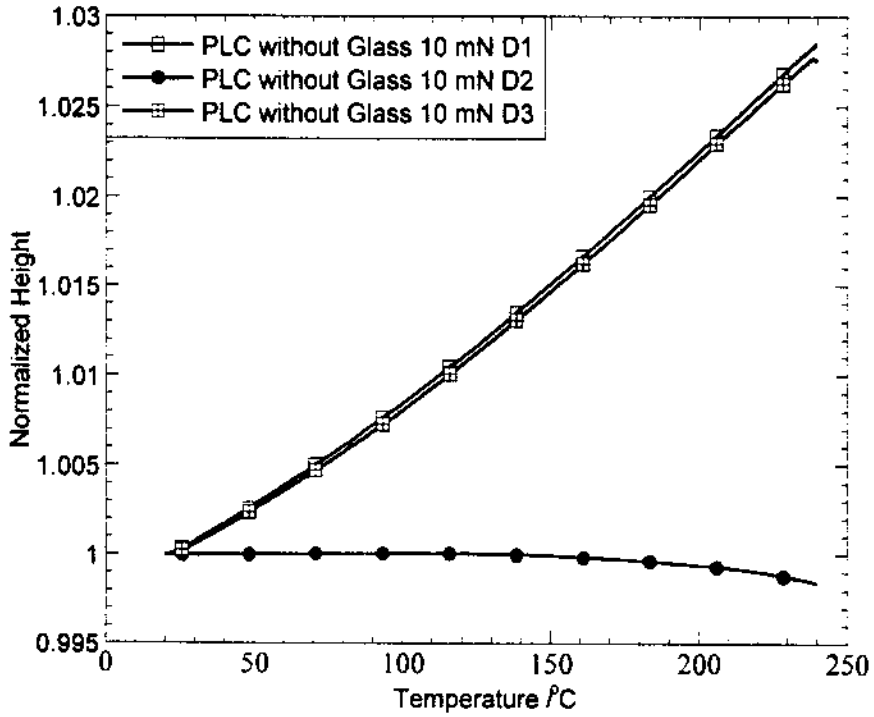

Figure 15. Thermal expansion of the PLC.

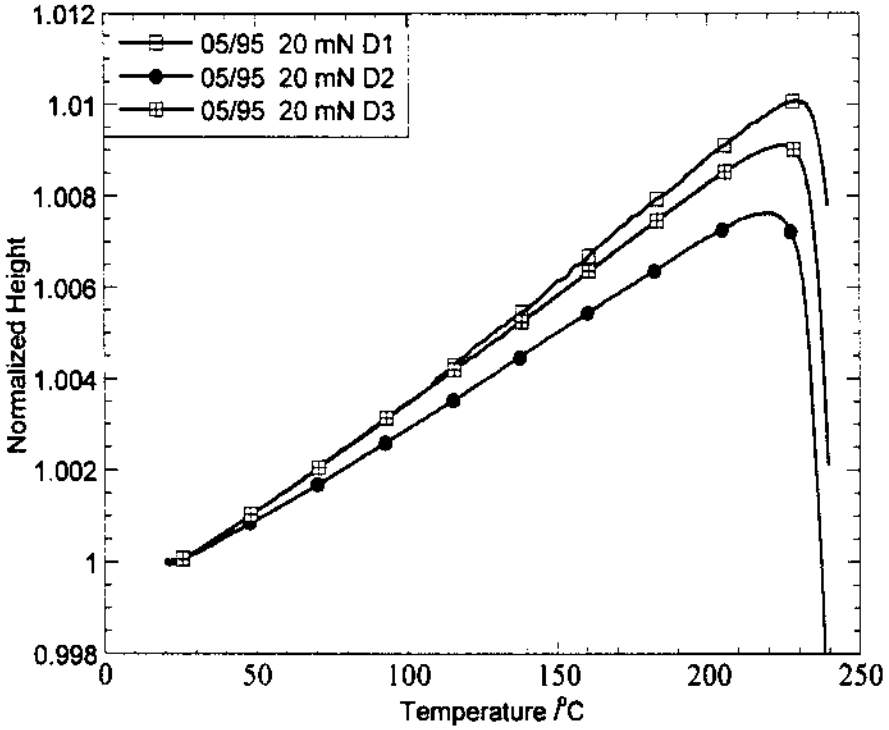

Figure 16. Thermal expansion of the amorphous TPI + 05 wt. % PLC blend.

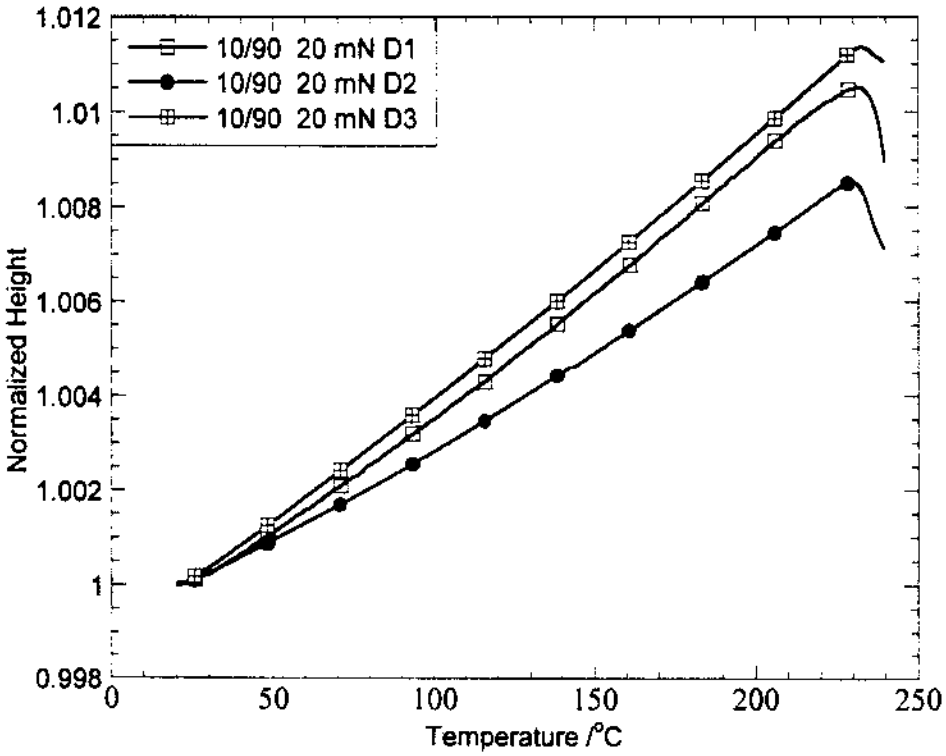

Figure 17. Thermal expansion of the amorphous TPI + 10 wt. % PLC blend.

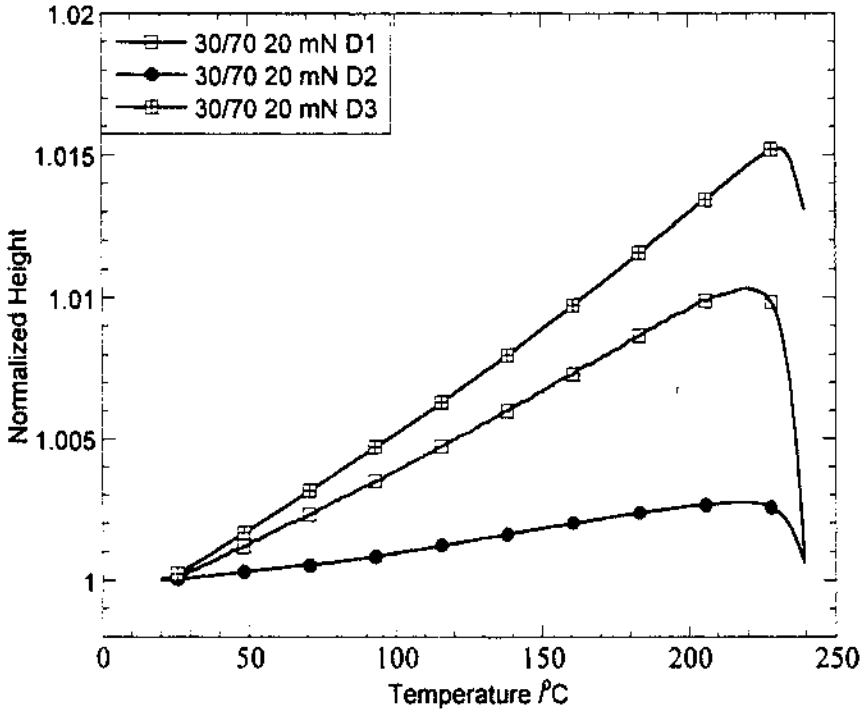

Figure 18. Thermal expansion of the amorphous TPI + 30 wt. % PLC blend.

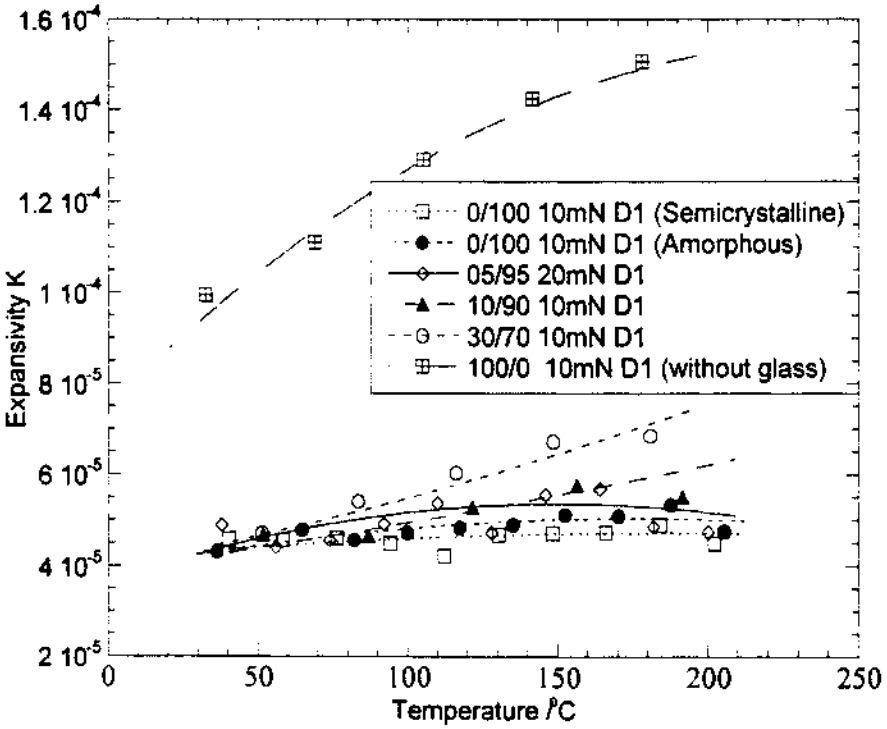

Figure 19. Thermal expansivity as a function of temperature for the direction D1.

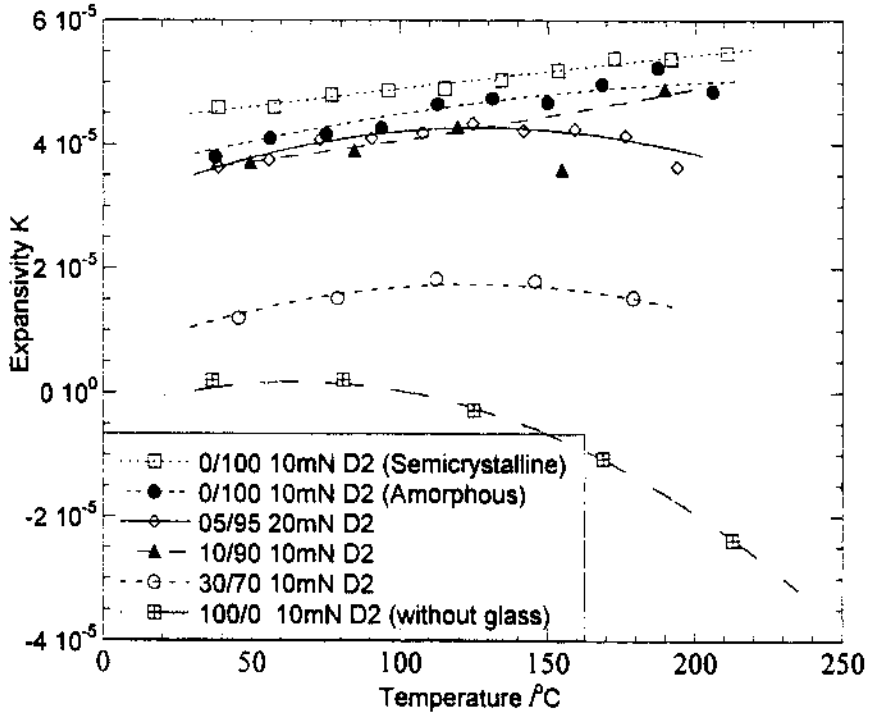

Figure 20. Thermal expansivity as a function of temperature for the direction D2.

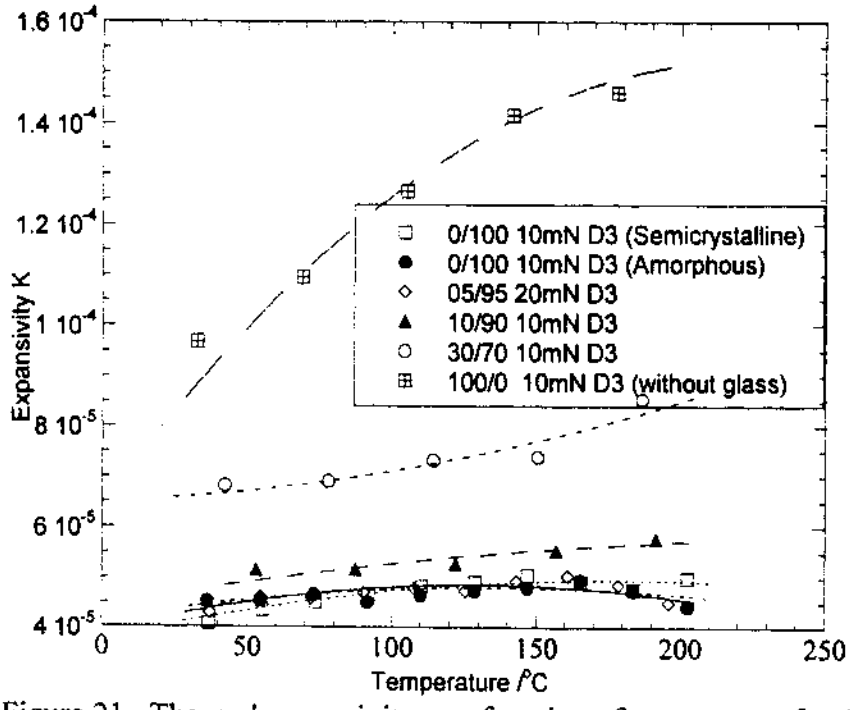

Figure 21. Thermal expansivity as a function of temperature for the direction D3.

Thermal expansivity occurs due to the anharmonic vibration of the polymer chains. It has been shown for many polymers that the expansivity of their crystals along their chain axis is negative. Such behavior is also shown to be only a weak function of the chemical structure [28]. The absence of such negative expansivity along their macroscopic orientation direction is usually indicative of the absence of long range order, that is, a lack of order of the crystalline domains. For the semicrystalline TPI, the lack of such negative expansivity and the absence of anisotropy indicate the random orientation of the crystalline regions in the matrix. On the other hand, the PLC shows significant anisotropy between the directions parallel and perpendicular to the macroscopic orientation direction. This anisotropy indicates the presence of long range order, after processing. However, there is no endothermic melting observed from the DSC confirming the lack of crystallinity. During the processing operation, other than the extrusion - induced orientation , no additional orientation was performed on the PLC or the blends. As shown in Sections 4.3 and 5.3, the small change in heat capacity at the glass transition, indicates relatively low flexibility of the molecular chains. These facts put together reaffirm the claim of this PLC to be rigid rod structure.

Looking at the blends of amorphous TPI + PLC, we see the development of anisotropic expansivity with the addition PLC even at concentrations as low as 5 %. The negative deviation of ΔC_p from linearity (Figure 4), indicates a larger restriction to flexibility of TPI than expected. This phenomenon was explained on the basis of *channeling*. These two facts indicate the development of macroscopic orientation, even

with the amorphous TPI. The high flexibility of TPI and the rigid rod nature of the PLC magnify this *channeling* process, which explains the negative deviation from linearity. It should be noted that such a process does not develop crystallinity, which is seen from the absence of a melting endotherm. This indicates that the blends posses the macroscopic anisotropy without the crystallinity.

5.7 Conclusions

From the DSC evaluations clearly the amorphous TPI + PLC do not show any thermodynamic miscibility. The negative deviation from linearity of the ΔC_p indicates the increased restriction imposed on the polyimide chains by the PLC as a result of *channeling*. The amorphous TPI blends show degradation onset temperatures of over 520°C. The thermal conductivity in the transverse direction decreases with the addition of PLC. This reduction is possibly a result of increased orientation through the addition of PLC. The expansivity of the blends exhibits strong anisotropy with PLC concentrations as low as 5 %. The DSC evaluation reveals that the orientation resulting from the addition of PLC is unaffected by annealing indicating the thermodynamic stability of such orientation. Addition of PLC improved the ease of processing, which was noted from the reduction in the motor current during processing. Such a phenomenon of reduction of melt viscosity as a result of addition of PLC has been reported by many authors [16, 34, 35]. The blends show good film formability.

5.8 References

1. W. Brostow, N. A. D'Souza and B. Gopalanarayanan, *Polymer Eng. and Sci.*, **38**, 204 (1998).
2. W. Brostow, N. A. D'Souza, H. Galina and A. C. Ramamurthy, *Polymer Eng. and Sci.*, **36**, 1101 (1996).
3. E. Jacobs, Personal communication.
4. R. F. Boyer, *Polymer Eng. and Sci.*, **8**, 161 (1968).
5. E. Sacher, *J. Appl. Polymer Sci.*, **19**, 1421 (1975).
6. E. Sacher, *J. Macromol. Sci. B*, **15**, 171 (1978).
7. W. Brostow, *Makromol. Chem. Macromol. Symp.*, **41**, 119 (1991).
8. W. Brostow, Failure of Plastics, Eds.: W. Brostow and R. D. Corneliussen, Hanser Publishers, New York, Chap. 10 (1986).
9 S. Tamai, Y. Ookawa, A. Yamaguchi, *SAMPE Internat.Conf.* (1995).
10 L. S. Rubin, K. Jayaraj and J. M. Burnett, *International Electronics Packaging Conference*, 664 (1994).
11 R. D. Jester, *SAMPE International Electronics Conference*, 428 (1992).
12 T. E. Noll, K. Blizard, K. Jayaraj and L. S. Rubin, NASA-CR-189338.
13 Y. Aihara and P. Cebe, *Polymer Eng. and Sci.*, **34**, 1275 (1993).
14. W. Brostow, *Kunststoffe*, **78**, 411 (1988).

15. W. Brostow, *Polymer*, **31**, 979 (1990).

16. W. Brostow, Physical Properties of Polymers Handbook, Ed.: J. E. Mark, American Institute of Physics Press, Woodbury, NY, Chap. 33 (1996).

17. W. Brostow, N. A. D'Souza and B. Gopalanarayanan, *POLYCHAR-6,* Denton, TX, Jan (1998).

18. P. J. Flory, *Proc. Royal Soc.*, **A 234**, 60,73 (1956).

19. P. J. Flory, *Macromol.*, **11**, 1141 (1978).

20. S. Blonski, W. Brostow, D. A. Jonah and M. Hess, *Macromol.* **26**, 84 (1993).

21. V. A. Bershtein and V. M. Egorov, Differential Scanning Calorimetry of Polymers: Physics, Chemistry, Analysis, Technology, Ellis Horwood, New York City (1994).

22. T. G. Fox, *Bull. Am. Phys. Soc.*, 1, 123 (1956).

23. N. A. D'Souza, Ph.D. Thesis, Texas A&M University, College Station, Texas (1994).

24. O. Olabisi, L. M. Robeson and M. T. Shaw, Polymer-Polymer Miscibility, Academic Press, New York City (1979).

25. P. R. Couchman, *Macromol.*, **11**, 1156 (1978)

26. G. Hakvroot, L. L. van Reijen, *Thermochim. Acta*, **93**, 317 (1985).

27. W. Brostow, N. A. D'Souza and B. Gopalanarayanan, *Proc. Annual Tech. Conf. Soc. Plast. Eng.*, **57**, 1842 (1997).

28. Y. Godovsky, Thermophysical Properties of Polymers, Springer-Verlag Berlin, New York (1994).

29. W. Knappe, *Adv. Polymer Sci.*, **7**, 477 (1971).

30. C. L. Choy, E. L. Ong and F. Chen, *J. Appl. Polymer Sci.*, **25,** 2325 (1981).

31. S. Burgess and D. Greig, *J. Phys. D,* **8,** 1637 (1975).

32. C. L. Choy, S. P. Wang and K. Young, *J. Polymer Sci. Phys.*, **23,** 1495 (1985).

33. C. L. Choy, Y. W. Wong, K. W. E. Lau, G. Yang and A. F. Lee, *J. Polymer Sci. Phys.*, **33,** 2055 (1995).

34. W. Brostow, *Kunststoffe,* **78**, 411 (1988).

35. W. Brostow, *Polymer,* **31**, 979 (1990).

CHAPTER 6

SUMMARY AND FUTURE WORK

6.1 Summary

The amorphous and semicrystalline TPIs show T_gs of 240°C and 249°C, from the DSC evaluations. The TSD and TMDSC evaluation show the presence of sub-T_g relaxations. The chain relaxation capability theory (CRC) tells us that these relaxations improve the mechanical properties. The α relaxation shows cooperative nature. The semicrystalline TPI shows thermo-irreversible cold crystallization. The addition of PLC lowers the cold crystallization temperature. The PLC, due to its high T_g of 230°C, does not limit the upper use temperature. The DSC evaluations show no effect of PLC on the T_g and T_m indicating the absence of thermodynamic miscibility. The presence of PLC induces a *channeling* phenomenon in the blends, resulting in a smaller change in heat capacity at the glass transition. The semicrystalline TPI, PLC and their blends show degradation onset temperatures above 520°C. Moisture absorption does not show an effect on the degradation phenomenon. Moisture absorption also decreased with the addition of the PLC.

The DSC evaluations show that the amorphous TPI + PLC blends do not exhibit thermodynamic miscibility. The negative deviation from linearity of the ΔC_p indicates the increased restriction imposed on the polyimide chains by the PLC as a result of

channeling. The amorphous TPI blends show degradation onset temperatures of over 520°C. The thermal conductivity in the transverse direction decreases with the addition of PLC. The expansivity of the blends exhibits strong anisotropy even with PLC concentrations as low as 5 %. The TMA evaluations reveal that the orientation resulting from the addition of PLC is unaffected by annealing indicating the thermodynamic stability of such orientation. Addition of PLC improved the ease of processing. The blends show good film formability.

6.2 Suggestions for Future Work

1. To study the liquid crystalline phase of the PLC.
2. To quantify the viscosity reduction with the PLC addition to both the amorphous and semicrystalline TPI.
3. To evaluate the effect of PLC on the thermal conductivity in the parallel direction to the orientation.
4. To evaluate the use of electric and magnetic fields in the control of orientation of the PLC and thereby the expansivity.
5. To characterize the effect of addition of PLC on the adhesion of TPI to metals.

CHAPTER 7

REFERENCES

Z. Adonyl and G. Korosi, Thermochim. Acta, 60, 23 (1983).

N. A. Adrova, M. I. Bessonov, L. A. Laius and A. P. Ruakov, *Polyimides - New Class of Thermally Stable Polymers*, Technomic Publishing, Lancaster, PA (1970).

Y. Aihara and P. Cebe, *Polymer Eng. and Sci.*, **34**, 1275 (1993).

W. M. Alvino and L. E. Edelman, *J. Appl. Polymer Sci.*, **19**, 2961 (1975).

W. M. Alvino, *Plastics for Electronics: Materials, Properties and Design Applications*, McGraw-Hill, New York (1995).

J. Barandiarán, J. J. Del Val, C. Lacabanne, D. Chatain, J. Millán and G. Martínez, *J. Macromol. Sci. Phys.*, **B22**, 645 (1983).

H. J. Barber and W. R. Wragg, *Nature*, **158**, 514 (1946).

J. Bayard, J. Grenet, C. Cabot and E. Dargent, *IEE Proc. Sci. Measur. Technol.*, **144**, 168 (1997).

A. Bernes, D. Chatain and C. Lacabanne, *IEEE Trans. Electrical Insul.*, **27**, 464 (1992).

A. Bernes, D. Chatain and C. Lacabanne, *Thermochim. Acta*, **204**, 69 (1992).

V. A. Bershtein and V. M. Egorov, *Differential Scanning Calorimetry of Polymers: Physics, Chemistry, Analysis, Technology*, Ellis Horwood, New York City (1994).

M. I. Bessonov, M. M. Koton, V. V. Kudryavtsev and L. A. Laius, *Polyimides - Thermally Stable Polymers*, Plenum, New York (1987).

N. Bicak and G. Koza, *Angew. Makromol. Chemie*, **217**, 71 (1994).

D. M. Bigg, *Adv. Polymer Sci.*, 119, 1 (1995).

S. Blonski, W. Brostow, D. A. Jonah and M. Hess, *Macromol.* **26**, 84 (1993).

S. Blonski, W. Brostow and J. Kubat, *Makromol. Chem, Macromol. Symp.*, **65**, 109

(1993).

S. Blonski, W. Brostow and J. Kubat, *Phys. Rev. B,* **49,** 6494 (1994).

S. L. Boersma, *J. Am. Ceramic Soc.*, **38**, 281 (1955).

T. M. Bogert, R. R. Renshaw, *J. Am. Chem. Soc.*, **30**, 1135 (1908).

L. Bohlin and J. Kubát, *J. Solid State Commun,* **20,** 211 (1976).

A. Boller, Y. Jin and B. Wunderlich, *J. Thermal Anal.*, **42**, 307 (1994).

R. F. Boyer and R. S. Spencer, *J. Appl. Phys.*, **15**, 398 (1944).

R. F. Boyer and R. S. Spencer, *J. Appl. Phys.*, **16**, 594 (1945).

R. F. Boyer, *Polymer Eng. and Sci.,* **8,** 161 (1968).

W. Brostow and M. Hess, *Mater. Res. Soc. Symp.*, **255**, 57 (1992).

W. Brostow, B. K. Kaushik, S. B. Mall and I. M. Talwar, *Polymer*, 33, 4687 (1992).

W. Brostow, *Failure of Plastics*, Eds.: W. Brostow and R. D. Corneliussen, Hanser Publishers, New York, Chap. 10 (1986).

W. Brostow, J. Kubat and M. J. Kubat, *Mat. Res. Soc. Symp. Proc.,* **321,** 99 (1994).

W. Brostow, J. Kubat and M. J. Kubat, *Mechanics of Compo. Mater.,* **321,** 99 (1994).

W. Brostow, *Kunststoffe,* **78**, 411 (1988).

W. Brostow, *Liquid Crystal Polymers: From Structures to Applications*, Ed.: A. A. Collyer, Elsevier Applied Science, London and New York, Chapter 1 (1992).

W. Brostow, M. Hess, B. L. López and T. Sterzynski, *Polymer,* **37**, 1551 (1996).

W. Brostow, M. Hess and B. L. López, *Macromol.* **27**, 2262 (1994).

W. Brostow, *Makromol. Chem. Macromol. Symp.*, **41**, 119 (1991).

W. Brostow, N. A. D'Souza, H. Galina and A. C. Ramamurthy, *Polymer Eng. and Sci.,* **36,** 1101 (1996).

W. Brostow, N. A. D'Souza and B. Gopalanarayanan, *POLYCHAR-6,* Denton, TX (1998).

W. Brostow, N. A. D'Souza and B. Gopalanarayanan, *Proc. Annual Tech. Conf. Soc. Plast. Eng.,* **55**, 1499 (1997).

W. Brostow, N. A. D'Souza and B. Gopalanarayanan, *Polymer Eng. and Sci.*, **38**, 204 (1998).

W. Brostow, *Physical Properties of Polymers Handbook*, Ed.: J. E. Mark, American Institute of Physics Press, Woodbury, NY, Chapter 33 (1996).

W. Brostow, *Polymer*, **31**, 979 (1990).

W. Brostow, T. Sterzynski and S. Triouleyre, *Polymer*, **37**, 1561 (1996).

W. Brostow, T.S. Dziemianowicz, J. Romanski and W. Werber, *Polymer Eng. and Sci.*, **28**, 785 (1988).

C. Bucci and R. Fieschi, *Phys. Rev. Lett.*, **12**, 16 (1964).

C. Bucci, R. Fieschi and Guidi, *Phys. Rev.*, **148**, 816 (1966).

A. B. Buhri and R. P. Singh, *J. Food Sci.*, **58**, 1145 (1993).

S. Burgess and D. Greig, *J. Phys. D*, **8**, 1637 (1975).

L. Cahn and H. Schultz, *Anal. Chem.*, **35**, 1729 (1963).

P. E. Cassidy Thermally Stable Polymers, Mercel Decker, New York (1980).

J. A. Cella, *Polyimides Fundamentals and Applications*, Eds.: M. K. Ghosh and K. L. Mittal, Mercel Decker Inc., New York, Chap. 13 (1996).

R. Chen, *J. Appl. Phys.*, **40**, 570 (1969).

S. Chen, *J. Mater. Sci.*, **28**, 3823 (1993).

F. C. Chen, Y. M. Poon and C. L. Choy, *Polymer*, **18**, 129 (1977).

S. Z. D. Cheng, F. E. Arnold Jr., A. Zhang, S. L. C. Hsu and F. W. Harris, *Macromol.*, **24**, 5856 (1991).

S. Z. D. Cheng, T. M. Chalmers, Y. Gu. Y. Yoon, F. W. Haris, *Macromol. Chem. and Phys.*, **196**, 1439 (1995).

P. Chevenard, X. Wache and R. De La Tullaye, *Bull. Soc. Chem. Fr.*, **11**, 41 (1954).

B. Chowdhury, *New Characterization Techniques for Thin Polymer Films*, Eds.: H. Tong and L. T. Nguyen, Wiley, New York, Chapter 10 (1990).

C. L. Choy, E. L. Ong and F. Chen, *J. Appl. Polymer Sci.*, **25**, 2325 (1981).

C. L. Choy, S. P. Wang and K. Young, *J. Polymer Sci. Phys.*, **23**, 1495 (1985).

C. L. Choy, W. P. Leung and Y. K. Ng, *J. Polymer Sci. Phys.*, **25**, 1779 (1987).

C. L. Choy, Y. W. Wong, K. W. E. Lau, Guangwu Yang and A. F. Lee, *J. Appl. Polymer Sci.*, 33, 2055 (1995).

C. L. Choy, Y. W. Wong, K. W. E. Lau, G. Yang and A. F. Lee, *J. Polymer Sci. Phys.*, **33,** 2055 (1995).

F. N. Cogswell, B. P. Griffin and J. B. Rose, U. S. Patent 4, 386, 174 (1983).

F. N. Cogswell, B. P. Griffin and J. B. Rose, U. S. Patent 4, 460, 735 (1984).

P. J. Collings, Liquid Crystals: Nature`s Delicate State of Matter, University Press, Princeton, NJ (1990).

G. Collins and B. Long, *J. Appl. Polymer Sci.*, **53**, 587 (1994).

J. Colmenero, Alegria, J. M. Alberdi, J. J. del Val and G. Ucar, *Phys. Rev. B,* **35**, 3995 (1987).

P. R. Couchman, *Macromol.*, **11**, 1156 (1978)

T. J. Coutts and N. M. Pearsall, *Appl. Phys. Lett.*, **44,** 134 (1984).

N. A. D'Souza, *PLC book series*, Ed.: W. Brostow, Thomson Science, London, Vol. 4, Chapter 4 (1998).

N. A. D'Souza, Ph.D. Thesis, Texas A&M University, College Station, Texas (1994).

L. David, C. Girard, R. Dolmazon, M. Albrand and S. Etienne, *Macromol.*, **29**, 8343 (1996).

J. J. del Val, A. Alegría, J. Colmenero and C. Lacabanne, *J. Appl. Phys.*, **59**, 3829 (1986).

J. J. del Val, A. Alegría, J. Colmenero and J. M. Barandiarán, *Polymer*, **27**, 1771 (1986).

J. J. del Val, J. Colmenero and C. Lacabanne, *Solid State Commun.*, **69,** 707 (1989).

A. M. Donald and A. H. Windle, *Liquid Crystalline Polymers*, University Press, Cambridge, UK (1992).

A. Dufresne, C. Lavergne and C. Lacabanne, *Solid State Commun.*, **88,** 753 (1993).

J. Economy, W. Volksen, C. Viney, R. Geiss, R. Seimens and T. Karis, *Macromol.*, **21,** 2777 (1988).

M. Eguchi, *Jap. J. Phys.*, 1, 10 (1922).

M. Eguchi, *Phil. Mag.*, **49**, 178 (1925).

D. D. Eley, *J. Polymer Sci. C*, **17**, 73 (1967).

K. Engberg, M. Ekblad, P-E. Werner and U. W. Gedde, *Polymer Eng. and Sci.* **34**, 1346 (1994).

L. Erdey, F. Paulik and J. Paulik, *Acta Chim. Acad. Hung.*, **10**, 61 (1956).

S. Esaki, *Adv. Mater. & Proc.*, **5**, 37 (1995).

P. J. Flory, *Macromol.*, **11**, 1141 (1978).

P. J. Flory, *Proc. Royal Soc.* **A 234**, 60, 73 (1956).

J. H. Flynn and D. M. Levin, *Thermochim. Acta*, **126**, 93 (1988).

T. G. Fox, *Bull. Am. Phys. Soc.*, **1**, 123 (1956).

H. Frei and G. Groetzinger, *Physik Z.*, **37**, 720 (1936).

M.G. Friedel, *Ann. Physique*, **18**, 273 (1922).

J. B. Friler and P. Cebe, *Polymer Eng. and Sci.* **33**, 587 (1993).

M. F. Froix, U. S. Patent 4,460,735 (1984).

P. K. Gallagher, *Thermal Characterization of Polymeric Materials*, Vol. 1, Ed.: E. A. Turi, Academic Press, New York, Chapter 1 (1997).

P. D. Garn, C. R. Geith and S. De Balla, *Rev. Sci. Instru.*, **33**, 293 (1962).

C. R. Gautreaux, J. R. Pratt and T. L. St. Clair, *J. Polymer Sci. Phys.*, **30**, 71 (1992).

A. V. Gerashchenko, Ya. S. Vygodskii, G. L. Slonimskii, A. A. Klimova, F. B. Sherman and V. V. Korshak, *Polymer Sci. USSR*, **15**, 1927 (1973).

P. S. Gill, S. R. Sauerbrunn and M. Reading, *J. Thermal Anal.*, **40**, 931 (1993).

S. Glasstone, K. J. Laidler and H. Eyring, *The Theory of Rate Processes*, McGraw Hill, New York (1941).

Y. Godovsky, *Thermophysical Properties of Polymers*, Springer-Verlag Berlin, New York (1994).

G. Groeninckx and G. Crevecoeur, *Polymer Eng. and Sci.*, **30**, 532 (1990).

B. Gross, *J. Electrochem. Soc.*, **115**, 376 (1968).

M. Grunze and R. N. Lamb, *Surface Sci.*, **204**, 183 (1988).

G. Hakvroot and L. L. van Reijen, *Thermochim. Acta*, **93**, 317 (1985).

F. W. Harris and L. H. Lenier, *Structure - Solubility Relationships in Polymers*, Eds.: F. W. Harris and R. B. Seymour, Academic Press, New York, p. 183 (1977).

F. W. Harris, S. L. C. Hsu and C. C. Tso, *High Perf. Polymers*, **1**, 1 (1989).

F. W. Harris, S. O. Norris, *J. Polymer Sci. Chem.*, **11**, 2143 (1973).

T. Hatakeyama and F. X. Quinn, *Thermal Analysis: Fundamentals and Applications to Polymer Science*, John Wiley & Sons, New York (1994).

A. Hensel, J. Dobbertin, J. E. K. Schawe, A. Boller and C. Schick, *J. Thermal Anal.*, **46**, 935 (1996).

J. A. Hinkely and J. J. Yeu, *J. Appl. Polymer Sci.*, **57**, 1539 (1995).

J. D. Hoffman, G. Williams and E. Passaglia, *J. Polymer Sci. C*, **14**, 173 (1966).

Ch. Hogfors, J. Kubát and M. Rigdahl, *Phys. Status Solidi B*, **107**, 147 (1981).

L. Horvath, *Thermochim. Acta*, **85**, 193 (1985).

T. H. Hou and R. M. Reddy *SAMPE Quart.*, **22**, 38 (1991).

B. S. Hsiao, B. B. Sauer and A. Biswas, *J. Polymer Sci. Phys.*, **32**, 737 (1994).

S. H. Hsiao, C. P. Yang and K. Y. Chu, *Macromol.*, **30**, 165 (1997).

B. S. Hsiao, M. T. Shaw and E. T. Samulski, *Macromol.*, **21**, 543 (1988).

P. P. Huo, J. B. Friler and P. Cebe, *Polymer*, **34**, 4387 (1993).

P. Huo, P. Cebe, *Polymer*, **34**, 696 (1993).

J. M. Hutchinson and S. Montserrat, *Thermochim. Acta*, **286**, 263 (1996).

M. Hutnik, A. S. Argon and U. W. Suter, *Macromol.*, **24**, 5970 (1991).

J. P. Ibar, A. Matthiesen, R. McIntyre and J. R. Saffell, *6th Nat. Conf. Rheol.*, Clayton (1992).

J. P. Ibar, *Polymer Eng. & Sci.*, **31**, 1467 (1991).

M. Iijima and Y. Takahashi, *Macromol.*, **29**, 2944 (1989).

M. Iijima, Y. Takahashi, K. Inagawa and A. Itoh, *J. Vac. Soc. Jpn.*, **28**, 437 (1985).

Y. Imai, *J. Polymer Sci. B*, **8**, 555 (1970).

H. Ishida and K. Kelley, *Polymer*, **32**, 1585 (1991).

H. Ishida and M. T. Huang, *J. Polymer Sci. Phys.*, **32**, 2271 (1994).

H. Ishida and M. T. Huang, *Spectrochim. Acta*, **51**, 319 (1995).

W. J. Jackson Jr., *Brit. Polymer J.*, **12**, 154 (1980).

E. Jacobs, Personal communication.

E. T. Jensen and C. A. Beevers, *Trans. Faraday Soc.*, **34**, 1478 (1938).

R. D. Jester, *SAMPE International Electronics Conference*, 428 (1992).

M. Kakimoto, R. Akiyama, S. Negi and Y. Imai, *J. Polymer Sci. Chem.*, **26**, 99 (1988).

V. A. Kargin and G. V. Slonimskii, *Dokl. Akad. Nauk SSSR*, **62**, 239 (1948).

W. Kast, *Angew. Chemie*, **67**, 592 (1955).

G. Kemeny and B. Rosenberg, *Nature*, **243**, 400 (1973).

J-H. Kim and J. A. Moore, *Macromol.*, **26**, 3510 (1993).

G. Kiss, *Polymer Eng. and Sci.*, **27**, 410, (1987).

W. Knappe, *Adv. Polymer Sci.*, **7**, 477 (1971).

S. Kobayashi, *Mol. Cryst. Liq. Cryst.*, **165**, 1 (1988).

R. R. Krug, W. G. Hunter and R. A. Grieger, *J. Phys. Chem* **80**, 2341 (1976).

J. Kubat and M. Rigdahl, *Failure of Plastics*, Eds.: W. Brostow and R. D. Corneliussen, Hanser Publishers, New York, Chap. 4 (1986).

J. Kubat, L. A. Nilsson and W. Rychwalski, *Res Mechanica*, **5**, 309 (1982).

J. Kubát, *Nature*, **204**, 378 (1965).

J. Kubat, *Phys. Status Solidi,* **111,** 599 (1982).

D. Kumar, *J. Polymer Sci. Chem.,* **22,** 3439 (1984).

F. P. La Mantia, (Ed.) *Thermotropic Liquid Crystal Polymer Blends*, Technomic Publishing Company Inc., Lancaster, PA (1993).

C. Lacabanne, A. Lamure, G. Teyssedre, A. Bernes, M. Mourgues, *J. Non-Cryst. Solids*, **172-174**, 884 (1994).

C. Lacabanne, D. Chatain and J. C. Monpagens, *J. Macromol. Sci. Phys.,* **B13**, 537 (1977).

C. Lacabanne, D. Chatain, J. C. Mopagens, A. Hiltner and E. Baer, *Solid State Commun.,* **27**, 1055 (1978).

C. Lacabanne, Ph. D. Thesis, University of Toulouse, France (1974).

J. E. S. D. Ladbury, B. R. Currell, J. R. Horder, J. R. Parsonage and E. A. Vidgeon, *Thermochim. Acta*, **169**, 39 (1990).

C. Lavergne and C. Lacabanne, *IEEE Electr. Insul. Mag.*, **9**, 5 (1993).

S. X. Lu, P. Cebe, and M. Capel, *J. Appl. Polymer Sci,* 57, 1359 (1995).

A. C. Lunn and I. V. Yannas, *J. Polymer Sci. Phys.*, **10**, 2189 (1972).

R. W. Lusignea, W. S. Stevenson J. F. McCoy, III, U. S. Patent 4,966,806 (1990).

S. M. Marcus and R. L. Blaine, *Thermochim. Acta*, **243**, 231 (1994).

Y. Y. Maruo, Y. Andoh and S. Sasaki, *Vac. Sci. Technol. A,* **11**, 2590 (1993).

M. Masui, H. Nagasaka and K. Yahagi, *Jap. J. Appl. Phys.,* **16,** 177 (1977).

J. Maxwell, *Plastics in High Temperature Applications*, Pergamon Press, Oxford-New York (1992).

F. McIntyre, C. Hasson, A. Matthiesen, and J. P. Ibar, *Thermochim. Acta,* **226,** 133 (1993).

I. C. McNeill and S. Basan, *Polymer Degradat. Stabil.*, **39**, 145 (1993).

J. C. Monpagens, D. Chatain and C. Lacabanne, *Electrostatics*, **3**, 87 (1977).

J. J. Moura Ramos, J. F. Mano and B. B. Sauer, *Polymer*, **38**, 1081 (1997).

M. Mourgues-Martin, A. Bernes, C. Lacabanne, O. Nouvel and G. Seytre, *IEEE Trans. Electrical Insul.*, **27**, 795 (!992).

S. Nakatsuka and A. L. Andrady, *J. Appl. Polymer Sci.*, **45**, 1881 (1992).

U. Natarajan and W. L. Mattice, *Macromol. Theory and Simul.*, **6**, 949 (1997).

C. M. Neag, *Thermomechanical Analysis in Materials Science: Materials Characterization by Thermomechanical Analysis*, Eds.: A. T. Riga and C. M. Neag, American Society for Testing and Materials, Philadelphia (1991).

W. Nernst and E. H. Riesenfeld, *Ber. Dtsch. Chem. Ges.*, **36**, 2086 (1903).

T. E. Noll, K. Blizard, K. Jayaraj and L. S. Rubin, NASA-CR-189338.

S. Numata, K. Fujisaka and N. Kinjo, *Polyimides: Synthesis, Characterization and Applications*, Ed.: K. L. Mittal, Plenum Press, New York, Vol. 1, 259 (1984).

O. Olabisi, L. M. Robeson and M. T. Shaw, *Polymer-Polymer Miscibility*, Academic Press, New York City (1979).

W. J. Parker, R. J. Jenkins, C. P. Butler and G. L. Abbot, *J. Appl. Phys.*, **32**, 1679 (1961).

V. P. Privalko and V. V. Novikov, *The Science of Heterogeneous Polymers: Structure and thermophysical properties*, John Wiley and Sons Ltd., West Sussex (1995).

G. Rabilloud and B. Sillion, *J. de Physique IV*, **3**, 1493 (1993).

M. Reading, A. Luget and R. Wilson, *Thermochim. Acta.*, **238**, 295 (1994).

M. Reading, B. K. Hahn and G. S. Crowe, U. S. Patent 5,224,775 (1993).

M. Reading, D. Elliott and V. Hill, *Proc. 21st North Am. Thermal Anal. Soc. Conf.*, 145 (1992).

M. Reading, D. Elliott and V. Hill, *J. Thermal Anal.*, **40**, 949 (1993).

M. Ree, K. Kim, S.H. Woo and H. Chang, *J. Appl. Phys.*, **81**, 698 (1997).

G. G. Roberts, *J. Phys. C*, **4**, 3167 (1971).

W. C. Roberts-Austin, *Metallographist*, **2**, 186 (1889).

D. Ronarc'h, P. Audren and J. L. Moura, *J. Appl. Phys.*, **58**, 466 (1985).

D. Ronarc'h, P. Audren and J. L. Moura, *J. Appl. Phys.*, **58**, 474 (1985).

B. Rosenberg, B. B. Bhowmik, H. C. Harder and E. Postow, *J. Chem. Phys.*, **49,** 4108 (1968).

L. S. Rubin and K. G. Blizard, U. S. Patent 5,529,741 (1996).

L. S. Rubin, K. Jayaraj and J. M. Burnett, *Internat. Electronics Packag. Conf.*, 664 (1994).

E. Sacher, *J. Appl. Polymer Sci.*, **19,** 1421 (1975).

E. Sacher, *J. Macromol. Sci. B*, **15,** 171 (1978).

J. R. Salem, F. O. Sequeda, J. Duran, W. Y. Lee and Y. M. Yang, *J. Vac. Sci. Technol. A*, **4,** 369 (1986).

E. T. Samulski, *Faraday Disc.*, **79**, 7 (1985).

G. Sawa, K. Kitagawa, and M. Ieda, *Jap. J. Appl. Phys.*, **11,** 416 (1972).

J. Schaefer, E. O. Stejskal, D. Perchak, J. Skolnick and R. Yaris, *Macromol.*, **18,** 368 (1985).

J. E. K. Schawe and E. Bergmann, *Thermochim. Acta*, **304-305**, 179 (1997).

J. E. K. Schawe and G. W. H. Höhne, *J. Thermal Anal.*, **46**, 893 (1996).

J. E. K. Schawe and G. W. H. Höhne, *Thermochim. Acta*, **287**, 213 (1996).

J. E. K. Schawe and M. Margulies, U. S. Patent 5,549,387 (1996).

J. E. K. Schawe, *Thermochim. Acta*, **260**, 1 (1995).

J. E. K. Schawe, *Thermochim. Acta*, **261**, 183 (1995).

J. E. K. Schawe, *Thermochim. Acta*, **271**, 127 (1996).

H. Shimizu, T. Kitano and K. Nakayama, *Jpn. J. Appl. Phys.*, **35,** L231 (1996).

A. Siegmann, A. Dagan and S. Kenig, *Polymer*, **26**, 1325 (1985).

E. Sommer and H. J. Keuzer, *Phys. Rev. Lett.*, **49,** 61 (1982).

E. Sommer and H. J. Keuzer, *Surface Sci.*, **119,** L331 (1982).

R. S. Spencer and R. F. Boyer, *J. Appl. Phys.*, **17**, 398 (1946).

F. S. Spring and J. C. Woods, *Nature*, **158,** 754 (1946).

C. E. Sroog, *Prog. Polymer Sci.*, **16**, 561 (1991).

A. K. St. Clair, D. M. Stoaldey and B. R. Emerson, *NASA Tech Briefs*, **Feb.**, 59 (1994).

T. L. St. Clair, K. S. Whitney and J. R. Pratt, *NASA Tech Briefs*, **Feb.**, 58 (1994).

T. L. St. Clair, *Polyimides*, Eds. D. Wilson, H. D. Stenzenberger and P. M. Hergenrother, Chapman and Hall, New York (1985).

R. C. Steere, *J. Appl. Phys.*, **37**, 3338 (1966).

H. D. Stenzenberger, *Adv. Polymer Sci.*, **117**, 165 (1994).

J. K. Stille, F. W. Harris, H. Mukamal, R. O. Rakutis, C. L. Schilling, G. K. Noren and J. A. Reeds, *Adv. Chem. Series.* **91**, 628 (1969).

D. M. Stoakley, A. K. St. Clair and R. M. Baucom, *SAMPE Quart.*, **20**, 3 (1989).

R. L. Stone, *Bull.-Ohio State Univ. Eng. Exp. Stn.*, **146**, 1 (1951).

P. Sullivan and G. Seidel, *Phys. Rev.*, **173**, 679 (1968).

T. Takekoshi, J. G. Wirth, D. R. Heath, J. E. Kochanowski, J. S. Manello and M. J. Webber, *J. Polymer Sci., Chem.*, **18**, 3069 (1980).

T. Takekoshi, *Polyimides Fundamentals and Applications*, Eds.: M. K. Ghosh and K. L. Mittal, Mercel Decker Inc., New York, Chap. 2 (1996).

T. Takekoshi, U. S. Patent 4,024,110 (1977).

S. Tamai, A. Yamaguchi and M. Ohta, *Polymer*, **37**, 3683 (1996).

S. Tamai, Y. Ookawa, A. Yamaguchi, *SAMPE Internat.Conf.* (1995).

G. Tessèdre and C. Lacabanne, *J. Phys.D. Appl. Phys.*, **28**, 1478 (1995).

G. Tessèdre, P. Demont and C. Lacabanne, *J. Appl. Phys.D*, **79**, 9261 (1996).

L. Torre, A. Maffezzoli and J. M. Kenny *J. Appl. Polymer Sci.*, **56**, 985 (1995).

W. H. Tsai, F. J. Boerio and K. M. Jackson, *Langmuir*, **8**, 1443 (1992).

J. van Turnhout, *Thermally Stimulated Discharge of Polymer Electrets*, Elsevier, Amsterdam (1975).

J. van Turnout, *Polymer J.*, **2**, 173 (1971).

J. Vanderschueren and J. Gasiot, *Thermally Stimulated Relaxation in Solids*, Ed.: P. Bräunlich, Springer-Verlag, New York, Chapter 4 (1979).

W. Volksen, *Adv. Polymer Sci.*, **117**, 111 (1994).

E. S. Watson, M. J. O'Neill, J. Justin and N. Brenner, *Anal. Chem.*, **36**, 1233 (1964).

W. W. Wendlandt, *Thermal Analysis*, Wiley, New York (1986).

F. E. Wiley, *Ind. Eng. Chem.*, **34**, 1052 (1942).

F. J. Williams and P. E. Donahue, *J. Organic Chem.*, **42**, 3414 (1977).

F. J. Williams, U. S. Patent 3,847,869 (1974).

J. G. Wirth and D. R. Heath, U. S. Patent 3,787,364 (1974).

J. G. Wirth, *High Performance Polymers: Their Origin and Development*, Eds.: R. B. Seymour and G. S. Krishenbaum, Elsevier, Amsterdam (1986).

B. Wunderlich, *Thermal Analysis*, Academic Press, San Diego (1990).

B. Wunderlich, Y. Jin and A. Boller, *Thermochim. Acta*, **238**, 277 (1994).

N. Yamazaki, F. Higashi and J. Kawabata, *J. Polymer Sci. Chem.*, **12**, 2149 (1974).

N. Yamazaki, M. Matsumoto and F. Higashi, *J. Polymer Sci. Chem.*, **13**, 1373 (1974).

D. Y. Yoon, N. Masciocci, L. E. Depero, C. Viney and W. Parrish, *Macromol.*, **23**, 1793 (1990).